Title

Fatigue Performance of Asphalt Concrete Mixes and Its Relationship to Asphalt Concrete Pavement Performance in California

Authors

Harvey, John T.
Deacon, John A.
Tsai, Bor-Wen
et al.

Publication Date

1995-10-01

FATIGUE PERFORMANCE OF ASPHALT CONCRETE MIXES AND ITS RELATIONSHIP TO ASPHALT CONCRETE PAVEMENT PERFORMANCE IN CALIFORNIA

Report Prepared for
CALIFORNIA DEPARTMENT OF TRANSPORTATION

by
John T. Harvey
Assistant Research Engineer
Institute of Transportation Studies
University of California at Berkeley

John A. Deacon
Professor of Civil Engineering Emeritus
University of Kentucky, Lexington

Bor-Wen Tsai
Graduate Student Researcher
Institute of Transportation Studies
University of California at Berkeley

Carl L. Monismith
Robert Horonjeff Professor of Civil Engineering and
Research Engineer
Institute of Transportation Studies
University of California at Berkeley

October 1995
Asphalt Research Program, CAL/APT Program
Institute of Transportation Studies
University of California, Berkeley

Technical Report Documentation Page

1. Report No. RTA-65W485-2	2. Government Accession No.	3. Recipient's Catalog No.	
4. Title and Subtitle Fatigue Performance of Asphalt Concrete Mixes and Its Relationship to Asphalt Concrete Pavement Performance in California		5. Report Date October 1995 6. Performing Organization Code	
7. Authors John T. Harvey, John A. Deacon, Bor-Wen Tsai, Carl L. Monismith		8. Performing Organization Report No.	
9. Performing Organization Name and Address Asphalt Research Program: CAL/APT Program Institute of Transportation Studies University of California at Berkeley Berkeley, CA 94720		10. Work Unit No. 11. Contract or Grant No. RTA-65W485	
12. Sponsoring Agency Name and Address Division of New Technology and Research California Department of Transportation Sacramento, CA 94273-0001		13. Type of Report and Period Covered Technical Task Report, July 94-Sept 95 14. Sponsoring Agency Code	
15. Supplementary Notes This 5 year project is being performed in cooperation with the U.S. Department of Transportation, Federal Highway Administration.			
16. Abstract In California, fatigue cracking is considered to be the most important type of distress affecting the performance of asphalt concrete pavements on major state highways. This report describes the results of a laboratory study of the fatigue response of a typical California asphalt concrete mix to define the effects of degree of compaction (as measured by air-void content), asphalt content, and aging on this performance parameter. The test results are then used in analytical simulations to estimate the effects of asphalt and air-void contents (with and without long-term-aging) on pavement performance. These simulations demonstrate that accurate construction control of air void content is more important than accurate control of asphalt content relative to the design target values. For example, a mixture targeted at 5-percent asphalt and 5-percent air voids will suffer a 30-percent reduction in fatigue life if the air-void content exceeds its target by 1-percent but only a 12-percent reduction if the asphalt content is shy of its target by 1 percent. Complicating this matter, however, is the likelihood that smaller-than-specified asphalt contents will result in increased air-void contents. A mix design and analysis system for fatigue is presented; this system was initially developed as a part of the Strategic Highway Research Program (SHRP) Project A-003A. Its most attractive features include the ability to consider not only laboratory fatigue test results but also the anticipated environment and the ability to make risk assessments about design choices. Refinements to the original SHRP developed methodology are described, including improved procedures for computing pavement temperature profiles as well as calibrations which reflect uniquely California conditions. Analyses of "rich-bottom" pavements (pavements with larger asphalt content in the bottom lift) suggest added potential for improved pavement performance. Finally, a series of recommendations are presented for enhancing the fatigue performance of California pavements which include changes to current construction specifications and/or construction quality assurance procedures.			
17. Key Words Asphalt concrete, fatigue performance, air void content, degree of compaction, asphalt content, aging, mix design and analysis, shift factor, temperature conversion factor, rich-bottom pavements		18. Distribution Statement No restrictions. This document is available to the public through the National Technical Information Service, Springfield, VA 22161	
19. Secunty Classif. (of this report) Unclassified	20. Secunty Classif. (of this page) Unclassified	21. No. of Pages	22. Price

DISCLAIMER

The contents of this report reflect the views of the authors who are responsible for the information and the accuracy of the data presented herein. The contents do not necessarily reflect the official views or policies of the California Department of Transportation or the Federal Highway Administration. This report does not constitute a standard, specification, or regulation.

FINANCIAL DISCLOSURE STATEMENT

This research has been funded by the Division of New Technology and Research of the State of California Department of Transportation (contract No. RTA-65W485). The total contract amount for the five year period (1 July 1994 through 30 June 1999) is $5,751,159. The purpose of the study included in this report was to evaluate the effects of asphalt content and air-void content on the fatigue response of a typical California asphalt concrete mix and to develop recommendations for improving the fatigue performance of asphalt concrete pavements in California.

IMPLEMENTATION STATEMENT

The information presented herein offers considerable potential for enhancing the fatigue performance of California pavements. It is recommended that the Caltrans staff use the proposed mix design and analysis system to mitigate fatigue distress on a trial basis. Moreover, means should be explored for more closely integrating the processes of mix design with those of structural design. The analysis presented herein relative to “rich-bottom” pavements suggests

that construction and evaluation of one or more experimental sections with this type of construction should be undertaken as soon as practicable. Finally, one of the most important activities to be implemented early on is to change construction specifications and/or quality assurance procedures for asphalt concrete mixes to reduce maximum limits for the in-situ air-void contents.

ACKNOWLEDGEMENTS

Financial support for this project was provided by the State of California Department of Transportation as part of the CAL/APT Project. Mr. Wesley Lum of the Division of New Technology and Research is the CAL/APT Project Manager and Mr. William Nokes, Office of Project Planning and Design, is the Contract Monitor for the University of California, Berkeley contract.

Contents

List of Figures

List of Tables

EXECUTIVE SUMMARY

The primary purpose of the project reported herein was to evaluate the effects of asphalt content and air-void content on the fatigue response of a typical California asphalt concrete mix and to develop recommendations for improving the fatigue performance of asphalt concrete pavements in California. In addition, the project was to begin demonstration and adaptation of the testing and analysis procedures developed as a part of the SHRP A-003A project for use in the design and analysis of California asphalt concrete mixes and asphalt concrete pavements for improved fatigue performance.

The design for the laboratory experiment (Chapter 2) to study the effects of air-void content and asphalt content was a balanced full factorial with three air-void contents, five asphalt contents, two strain levels, and three duplicates resulting in a nominal total of 90 tests (actually a total of 97 tests were performed). The mix consisted of an AR-4000 California Valley asphalt cement and a Watsonville granite. The aggregate gradation passed between the middle limits of Caltrans 3/4 medium and coarse gradations and can be considered representative of California mixes.

Test specimens were sawed from slabs of the mixes prepared to the target air-void contents by rolling wheel compaction. Controlled-strain flexural fatigue tests were performed using the SHRP-developed fatigue test equipment and procedure. The tests were conducted at a temperature of 19±1°C (67±2°F) and at a frequency of loading of 10 Hz.

The long term aging experiment employed a full factorial design as well, with three aging periods, two air-void contents, four asphalt contents, two strain levels, and two replicates for a nominal total of 96 tests (actually 114 tests were performed). Aging was conducted using long term oven aging on the specimens after they had been sawed from the compacted slabs.

An analysis of the fatigue test data (Chapter 3) produced the following:

- For controlled-strain testing, an increase in asphalt content results in an increase in laboratory fatigue life and a decrease in mix stiffness.
- For controlled-strain testing, an increase in air-void content results in a decrease in laboratory fatigue life and a decrease in mix stiffness.
- For the materials tested, the effects of asphalt and air-void contents on laboratory fatigue performance can be modeled as follows:

$$N = 2.2953*10^{-10}\, e^{0.594AC-0.164AV}\varepsilon_t^{-3.730} \qquad (R^2=0.916) \qquad (1)$$

and

$$S_o(\text{MPa})=4.5524*10^{5}\, e^{-0.171AC-0.076AV} \qquad (R^2=0.685) \qquad (2)$$

Where:

N = number of strain repetitions to failure

ε_t = applied tensile strain

AC = asphalt content, percent by weight of aggregate

AV = air void content, percent

S_o = initial mix stiffness, MPa

Main effects in these models are statistically significant at a level of significance in excess of 99 percent. Interactive effects of the independent variables are not included in the models because they are not statistically significant.

- Voids filled with bitumen (VFB) apparently captures some, but not all, of the effects of asphalt and air-void contents on fatigue life. An increase in voids filled with bitumen results in an increase in laboratory fatigue life which can be modeled as follows:

$$N = 7.9442 * 10^{-11}\ e^{0.044 VFB} \varepsilon_t^{-3.742} \qquad (R^2 = 0.875) \quad (3)$$

The advantage of including voids filled with bitumen in comprehensive fatigue models is that, unlike asphalt and air-void contents, voids filled with bitumen is not highly correlated with flexural stiffness. Because of this relatively weak correlation, both variables can be simultaneously incorporated into fatigue models as indicated below:

$$N = 2.5875 * 10^{-8}\ e^{0.053 VFB} S_o^{-0.726} \varepsilon_t^{-3.761} \qquad (R^2 = 0.885) \quad (4)$$

Such a model is one of the more promising types for generally describing the effects on fatigue life of a wide range of mix characteristics, including not only asphalt and air-void contents but also asphalt type and possibly aggregate type and gradation as well. At the same time, users of such models must recognize the

imprecision with which they capture mix-proportion effects and must not use them for detailed mix-design purposes.

Determination of the effects of asphalt and air-void contents on laboratory fatigue life and flexural stiffness is a necessary first step in determining their effects on in-situ pavement performance. However, because mix proportions significantly affect flexural stiffness (and hence, strains induced in the pavement as a result of traffic loads) as well as fatigue life, the linkage between fatigue performance in the laboratory and that in situ is not necessarily direct. As a result it is necessary to combine analytical simulations of in-situ strains with laboratory fatigue models to predict in-situ performance.

In order to evaluate the effects of asphalt and air-void contents on in-situ fatigue performance, 18 pavement designs were developed using established California Department of Transportation procedures, one design for each combination of traffic index (three levels), subgrade R-value (three levels), and base type (two levels). For each design, 15 mixes were evaluated representing those tested herein (five asphalt contents and three air-void contents). Then for each of the 270 resulting combinations, the maximum principal tensile strain at the bottom of the asphalt concrete layer was computed using a multilayer elastic computer code (ELSYM5) and stiffness as determined from equation (2). The assumed truck loading consisted of a 50 kN (9,000 lb) single half axle with dual tires spaced 335 mm (13.2 in.) center-to-center and a tire pressure of 758 kPa (110 psi). Finally, the simulated in-situ fatigue life was then estimated using equation (1).

A major result from this study was the demonstration of the importance of construction control. With respect to fatigue performance, accurate control of air-void content is more important than accurate control of asphalt content. For example, a mix targeted at 5 percent asphalt and 5 percent air voids will suffer a 30 percent reduction in fatigue life if the air-void content exceeds its target by 1 percent but only a 12 percent reduction if the asphalt content is shy of its target by 1 percent. Complicating this matter, however, is the likelihood that smaller-than-specified asphalt contents will result in increased air-void contents.

Results of the aging study suggested that the basic effects of asphalt and air-void contents on laboratory fatigue life and stiffness are not affected by long-term aging. Nevertheless, long term aging increases mix stiffness but has little, if any, effect on laboratory fatigue life. Limited in-situ simulations suggest that long-term aging may benefit pavement fatigue performance slightly but only as a result of increase in mix stiffness. Conditioning laboratory fatigue specimens by long-term oven aging does not appear to be necessary for purposes of mix design and analysis. These findings of the effects of long-term aging are tentative pending completion of testing and analysis—currently underway—of a second, more aging-susceptible mix.

The mix design and analysis system presented herein (Chapter 4) was originally developed as a part of SHRP Project A-003A. Its most attractive features include the ability to consider not only laboratory measurements but also the anticipated in-situ environment and the ability to make risk assessments about design choices. The current project enabled important refinements to be made, most notably in the procedures for computing pavement temperature profiles, as well as calibrations which reflect uniquely California conditions. Although more refinements will doubtlessly be necessary in the future, the system is sufficiently mature to

warrant its trial use. Experience is necessary to identify its weaknesses and to suggest areas for possible improvement.

Although the shift factors proposed herein, relating laboratory estimates of fatigue life to service estimates of ESALs represent an effective point of beginning, future adjustments are inevitable. The recommended design relationship at this time is:

$$\textit{Design shift factor} = 2.7639 * 10^{-5} \varepsilon^{-1.3586} \qquad \textit{for } \varepsilon \geq 0.000040 \tag{5}$$

in which ε = simulated strain produced by a standard wheel load at the underside of the asphalt-concrete layer. Ultimately, shift factors are expected to depend not only on strain level but also on the extent of permissible cracking and possibly such added factors as the nature and thickness of the structural section, the rate of accumulation of traffic loading, mode of loading, and perhaps mix properties as well.

It is important to emphasize that for given mix constituents, maximum asphalt content and minimum air-void content are limited not only by economics but also by other distress mechanisms, specifically pavement rutting, instability, and bleeding. Fatigue analysis is necessary to assure that the mix will perform satisfactorily at these limits or, if not, to design a better performing alternative. Flexural beam testing and related analysis provide a powerful, easy-to-use, and efficient tool for evaluating fatigue life and stiffness.

Chapter 5 explores possible implications of this project for California design and construction practice. It includes a discussion of the consistency of California structural design practice with respect to fatigue distress; an evaluation of issues related to mix design, construction specifications, and quality assurance; examination of the merits of rich-bottom designs which replace the bottom few inches of the asphalt-concrete surface with a richer and

more dense layer; and a mix-design example illustrating use of the UC-Berkeley mix design and analysis system for designing fatigue-resistant mixes.

From an evaluation of the information presented in Chapter 5 as well as that described above it appears that developments of this project offer considerable potential for enhancing the fatigue performance of California pavements. Specific recommendations are presented in Chapter 6 and include the following:

1) For mixes for new and overlay pavement design:

- Use the mix design and analysis system on a trial basis;
- Avoid specifying very low design asphalt contents or, if that is not possible, compensate by increasing layer thickness as necessary to prevent premature fatigue cracking;
- Evaluate the current structural design system to identify any conditions for which typical California mixes might be particularly susceptible to fatigue distress; and
- Explore means for more closely integrating the processes of mix design with those of structural design.

2) Relative to construction:

- Consider establishing maximum limits for in-situ air-void contents by changing construction specifications and/or construction quality assurance procedures;
- Consider construction and evaluation of one or more experimental rich-bottom pavement sections; The use of accelerated pavement testing with the Heavy Vehicle Simulator provides an excellent opportunity to evaluate this recommendation.

1.0 Introduction

The fatigue resistance of an asphalt concrete mix is its ability to withstand repeated loading without fracture. Fatigue in asphalt concrete pavements appears as cracking at the surface of the pavement. In California and perhaps other states as well, fatigue cracking is recognized historically as the most important type of distress afflicting asphalt concrete pavements on major state highways. The recently completed Strategic Highway Research Program (SHRP) Project A-003A made significant advancements in testing and evaluating the fatigue resistance of asphalt concrete mixes. Using SHRP testing and analysis procedures, the project reported herein evaluated the effects of mix variables, construction practices, and pavement design alternatives on the fatigue performance of asphalt concrete pavements in California.

1.1 Purpose

The primary purpose of this project was to evaluate the effects of asphalt content and air-void content on the fatigue response of a typical California asphalt concrete mix to develop recommendations for extending service life through improved fatigue performance of asphalt concrete pavements in California. The secondary purpose of the project was to begin demonstration and adaptation of the testing and analysis procedures developed as part of SHRP

A-003A for use in the design and analysis of California asphalt concrete mixes and pavements to achieve this improved fatigue performance.

1.2 Background

1.2.1 California Mix Design, Pavement Design and Compaction Specification Practices

Asphalt concrete mix design by the California Department of Transportation (Caltrans) is currently based on standard specifications for aggregate texture, durability, and aggregate gradation; Hveem Stabilometer test results including the effects of moisture vapor; swell characteristics; and visual examination for "flushing" of laboratory compacted specimens. The mix design procedure is primarily intended to eliminate mixes that might be susceptible to rutting; fatigue performance is not directly evaluated in the mix design process.[1] This process has been successful in meeting its objective, and rutting is not commonly observed in dense-graded, conventional asphalt mixes for which Caltrans is responsible.

The current pavement thickness design procedure is intended to provide an adequate structure to accommodate the equivalent single axle loads (ESALs) expected during the design life of the pavement. It is an empirical procedure that implicitly considers not only rutting but also fatigue cracking. However, thickness design does not explicitly consider mix properties and

[1]Indirectly, fatigue performance is included if the basic philosophy of mix design is followed; i.e., as much asphalt as possible is included for good durability and fatigue performance but no so much that the load carrying capability is reduced below some minimum desirable level (as defined by the Hveem Stabilometer) dependent on traffic.

construction practice and, hence, provides no quantitative means for addressing the relative merits of different mixes.

Field compaction of asphalt concrete is currently specified in terms of relative compaction, that is, the ratio of in-situ density to the density of laboratory specimens compacted at the design asphalt content and denoted as test maximum density (TMD). The Triaxial Institute kneading compactor is used for laboratory compaction, and typical specifications require 95-percent relative compaction. The relative compaction specification allows quite large, in-situ air-void contents. For example, even with maximum laboratory compaction (corresponding to the 4.0-percent minimum air-void content allowed by the mix design procedure), 95 percent relative compaction allows for an in-situ air-void content of 8.8 percent (100-0.96*0.95*100). Similarly, 5.0 percent air voids at the design asphalt content would result in almost 10 percent air voids in the pavement section.

These current procedures for mix design, pavement thickness design, and compaction specification were specifically addressed in the experiment design and analysis of fatigue performance included in this report.

1.2.2 SHRP A-003A Products and Limitations

The objectives of SHRP Project A-003A were to develop accelerated performance-related laboratory tests for the most important types of distress affecting asphalt-aggregate mixes and to develop mix design and analysis methods to predict related pavement performance.

The scope of A-003A included fatigue cracking, and its principal products related thereto included:

Flexural Beam Test for Fatigue and Stiffness - this equipment provides a means for accelerated laboratory testing of asphalt concrete for both flexural stiffness and fatigue

life under controlled-strain conditions with computerized control and data acquisition; and

Mix Design and Analysis System - this system provides an effective method for analysis of laboratory fatigue measurements and prediction of pavement fatigue cracking performance. The system not only incorporates mix testing but also allows consideration of traffic (repetitions, wheel loads, and tire pressures), environmental conditions (temperature), and the pavement cross-section design. The system also allows evaluation of the effects of both mix design and construction compaction.

These products were used for this project and were evaluated in terms of California experience as part of the process of adapting it for use in the state.

Laboratory tests previously conducted by SHRP A-003A were insufficient in number and scope to conclusively establish the influence of asphalt and air-void contents on flexural stiffness and fatigue behavior. The results presented in this report are intended in part to augment earlier work as well as to examine other factors including effects of long-term aging. An important extension reported herein is a simulation of the effects of asphalt and air-void contents on the in-situ performance of a variety of representative California pavements.

1.2.3 Hypothesized Effects of Asphalt and Air-Void Contents

Based on SHRP testing and prior experience, the working hypothesis for the present project was that, within practical ranges, increased asphalt content and decreased air-void content result in increased pavement fatigue life. The following discussion suggests a plausible rationale.

Increased asphalt content means increased thickness of the binder film between aggregate particles and an increased proportion of asphalt over a cross-section normal to the direction of tensile stress. Because bending strains are concentrated in the asphalt binder (the binder is much

more compliant than the stiffer aggregate particles), thicker films result in smaller binder strain if the overall mixture strain is not altered by the added asphalt. Moreover, because tensile stresses must ultimately be transferred through the asphalt, more asphalt means more asphalt area in cross-section and, hence, less stress in the asphalt. The effects are complicated, however, by the related effects of asphalt content on mix stiffness and, as a result, on the stresses and strains that must be resisted in situ.

A smaller air-void content has at least two effects that likely contribute to longer fatigue life. First, because air transmits little or no stress, replacing some of its volume with asphalt and aggregate reduces the stress level in these components. Second, a smaller air-void content creates a more homogenous asphalt-aggregate structure--one with fewer, smaller, and more uniformly distributed voids--which results in less stress concentration at critical solid-air interfaces.

Reduced porosity has been found to increase stiffness and ultimate strength of most solid engineering materials. For asphalt concrete the concept of improved performance with reduced porosity has often been expressed in terms of voids filled with bitumen (VFB), as in the surrogate fatigue expression developed from regression of flexural beam test results during SHRP A-003A:

$$N_f = 2.738 \times 10^5 \ \exp^{0.077\ VFB} \ \varepsilon_t^{\ -3.624} \ LS_o^{-2.720} \qquad (1.1)$$

in which N_f = fatigue life (repetitions of tensile strain to failure), e = exponent, Naperian base, VFB = percent voids filled with bitumen, ε_t = tensile strain, and LS_0 = initial loss stiffness, psi. In other A-003A calibrations, the effects of reduced porosity were expressed directly in terms of air-void content instead of VFB.

Finally, the combination of increased asphalt content and decreased air-void content should result in a material in which thick asphalt films between the aggregate particles transmit

tensile stresses throughout the solid, with reduced stress concentrations due to voids and at locations where aggregate particles are in direct contact. The microcracks that begin to develop under repetitive loading should grow more slowly and take longer to interconnect because of the reduced number and smaller size of air voids, which tend to concentrate stresses and eventually to allow cracks to extend from one location to another.

1.3 Organization of Report

The next section of this report explains the experiment design for the laboratory testing phases of this work, describes the materials that were tested, and the procedures that were followed. The primary experiment concentrated on measuring effects of asphalt and air-void contents while a secondary experiment considered long-term aging as well. Test results are presented next, and they are joined with analytical simulations to estimate the effects of asphalt and air-void contents (with and without long-term aging) on pavement performance. Attention then turns to the UC-Berkeley mix design and analysis system. Following a brief description of the overall system, refinements and recalibrations which reflect California conditions and incorporate some of the contributions of this project are explained. Implications of the results of this project on design and construction practice are then investigated, and the report is concluded with a summary of conclusions and recommendations.

2.0 Experiment Design, Materials, and Test Procedure

The primary laboratory experiment for this project was designed to provide data regarding the effects of asphalt content and air-void content on mixture fatigue performance and flexural stiffness including the variance in test measurements. A secondary experiment was performed to ascertain the likely effects of long-term oven aging (LTOA) on these properties. Descriptions of the experiment design, materials, and test procedures are presented in this section.

2.1 Experiment Design

The experiment design of the main experiment was a balanced full factorial with three air-void contents, five asphalt contents, two strain levels, and three replicates, resulting in a nominal total of 90 (3*5*2*3) tests, Table 2.1. Because of extra replicates in some cells, a total of 97 tests were performed.

The air-void contents included in the experiment design (1 to 3 percent, 4 to 6 percent, and 7 to 9 percent) were selected to span the range typically obtained in California with current specifications as well as to provide data for the evaluation of more stringent compaction standards. Testing at larger air-void contents is impractical because of the difficulty in obtaining competent test specimens with air voids exceeding 9 percent. At such levels, they often disintegrate as they are cut or sawed from a larger compacted mass.

The five asphalt contents included in the experiment design were approximately centered about the optimum binder content as determined by the Hveem stabilometer procedure (minimum stability of 35). The optimum Hveem binder content was found during the SHRP A-003A project to be 4.9 percent, by weight of aggregate. For the current project, binder contents were 4.0, 4.5, 5.0, 5.5 and 6.0 percent, by weight of aggregate.

The laboratory-compaction air-void content corresponding to the optimum, 4.9-percent asphalt content is 5.4 percent. Current Caltrans asphalt concrete specifications typically require 95 percent relative compaction [field density divided by density (TMD) obtained from standard compaction effort using the Triaxial Institute kneading compactor] (Caltrans Test Method 304). This would result in a maximum allowable air-void content of about 10 percent. Reduction of the design asphalt content usually results in a higher allowable air-void content.

High and low strain levels were selected, based on past experience, to result in average fatigue lives of approximately 50,000 and 500,000 repetitions, respectively. The strain levels chosen were 300 and 150 microstrain. There is some slight variability in strain during each fatigue test, usually within ± 5 percent.

2.2 Materials

The aggregate and asphalt for the experiment are typical of the southern end of the San Francisco Bay Area and were also included in SHRP A-003A and other SHRP projects. The asphalt cement was a California Valley AR-4000 (SHRP Materials Reference Library [MRL] asphalt AAG-1) (Table 2.2). The aggregate was Watsonville granite (SHRP-MRL aggregate RB). Watsonville granite is composed of quartz, feldspar, and chlorite (Folliard and Trejo,

1991). It was completely crushed, with the larger particles having angular shape and rough surface texture.

The selected aggregate gradation was termed medium gradation No. 2 which had been used in SHRP A-003A research (Table 2.3). The gradation passes approximately between the Caltrans 3/4 inch coarse and medium gradations (California Department of Transportation, 1994), as can be seen in Figure 2.1, and can therefore be considered typical of Caltrans mixes. The SuperPave Level I "restricted zone" for 19 mm (3/4 in.) maximum size aggregate is also shown in Figure 2.1. Both Caltrans gradations and the gradation used for this project pass through the restricted zone and, therefore, do not meet SuperPave specifications (McGennis et al., 1994).

2.3 Specimen Preparation

Specimen preparation procedures followed those used in SHRP A-003A research performed at UC-Berkeley (Harvey, 1991).

Aggregate was screened into 10 sizes and then recombined to create the desired gradation. The batched aggregate was regularly checked by wet and dry sieve tests (ASTM C117 and C136). At least two hours prior to mixing, the aggregate was put into steel pans and placed into a pre-heated 138°C (280°F) forced-draft oven. Asphalt was heated for 1.5 to 3 hours at the same temperature before mixing. The asphalt was stirred several times during heating. Mixing, at 138°C (280°F), was performed for four minutes using a rotating bowl equipped with a counter-rotating paddle in the middle.

After mixing, the uncompacted, loose mix was placed back into steel pans in approximately 7 kg (14.4 lb) batches and was subjected to four hours of short-term oven aging at

135°C (275°F) in a forced-draft oven. This procedure essentially duplicates the short-term oven aging (STOA) procedure recommended by SHRP A-003A researchers as duplicating the combined aging effects of both construction and several years of aging thereafter (Bell, Wieder, and Fellin, 1994). The mix was compacted using a small steel-wheel roller at 116°C (240°F). The slabs prepared by this method produced two to seven fatigue beams per compaction, depending on the size of the mold.

After compaction, the slabs were cut into fatigue beams using a wet saw. Fatigue beam dimensions were 380 mm length, 64 mm width, and 51 mm height (15 in., 2.5 in., and 2.0 in., respectively).

Air-void contents were computed using the bulk specific gravity of the beam when wrapped in Parafilm™ and the maximum effective specific gravity (ASTM D 2041) (Del Valle, 1985, and Harvey et al., 1994).

2.4 Test Procedure

All tests were performed in a controlled-temperature room at 19 ± 1°C (67 ± 2°F). The test apparatus, developed as part of SHRP A-003A and described in SHRP Report A-404 and other references (Tayebali et al., 1994a and 1994b), subjects beam specimens to third-point, controlled-strain flexure. It was fabricated by James Cox and Sons, Inc. and incorporates several significant changes from original equipment developed at UC-Berkeley in the 1960s (Deacon, 1965, and Epps, 1969) that greatly reduce testing time, testing difficulty, and variance in test results.

For this project, a 10 Hz haversine wave was used, with the deformation of the beam centroid calculated to produce the desired tensile strain in the extreme fiber at the bottom of the

beam. The haversine wave had a mean value equal to one half the desired deformation, resulting in no deformation at one peak and the desired maximum deformation at the other. The ATS control and acquisition software collects load and deformation data at predefined cycles spaced at logarithmic intervals. Failure is assumed to occur when the stiffness reaches half of its initial value, taken at the 50th cycle. The initial stiffness is determined from the load at approximately 50 repetitions; the test is terminated manually when this load has diminished by 50 percent. Maximum stress, strain, and stiffness are determined as follows:

$$\sigma = \frac{3aP}{wh^2} \tag{2.1}$$

$$\varepsilon = \frac{12h\delta}{3L^2 - 4a^2} \tag{2.2}$$

$$S = \frac{\sigma}{\varepsilon} \tag{2.3}$$

in which σ = peak-to-peak stress, ε = peak-to-peak strain, P = applied peak-to-peak load, S= stiffness, L = beam span, w = beam width, h = beam height, δ = beam deflection at neutral axis, and a = L/3. A detailed description of the test method is included herein as Appendix A.

2.5 Long-Term Aging Experiment

The long-term aging experiment employed a full-factorial experiment design with three LTOA periods, two air-void contents, four asphalt contents, two strain levels, and two replicates, resulting in a nominal total of 96 (3*2*4*2*2) tests. Because of additional replicates, primarily in the cells with no LTOA, 114 tests were actually performed.

LTOA periods used for this experiment were zero, three, and six days. For dense mixes, LTOA is performed on compacted specimens at 85□C (185□F). Based on field validation data,

SHRP A-003A researchers at Oregon State University have been able to associate eight days of LTOA with about nine years of in-situ aging in a dry-freeze environment and about 18 years of in-situ aging in a wet-no freeze environment. A less conclusive estimate was made that two days of LTOA is associated with about two to six years of aging (Bell, Wieder, and Fellin, 1994).

The two air-void-content levels[2] were 4 to 6 percent and 7 to 9 percent, and the four asphalt contents were 4.0, 4.5, 5.0, and 5.5 percent, by weight of aggregate. The two strain levels were 300 and 150 microstrain. As with the primary experiment, the California Valley AR-4000 asphalt cement and Watsonville granite (UC-Berkeley medium gradation No. 2) were used.

The Valley asphalt has been found to be relatively unsusceptible to aging (Bell, Wieder, and Fellin, 1994). It ranked 15th among 16 asphalts in its viscosity ratio, the ratio of the viscosity at 60°C (140°F) after and before the thin film oven test (TFO) (Christenson and Anderson, 1992). Moreover in comparing the Valley asphalt with seven other MRL asphalts in mixes with four different aggregates, the long-term aging characteristics of the Valley asphalt were found to be less sensitive to aggregate characteristics than the other asphalts utilized (Bell and Sosnovske, 1994).[3]

[2]The 1 to 3 percent air void level was not included since little aging would take place in this range of air voids.

[3]These findings suggest that mixes with Valley asphalt and Watsonville granite are likely to have aging resistance which may not be representative of some combinations of asphalt and aggregate used in California. Relative to fatigue resistance, however, it is likely that increased stiffness resulting from poorer resistance to aging will have little influence in fatigue cracking in other than thin [~50 mm (26 in.)] asphalt-bound layers overlaying a less stiff layer.

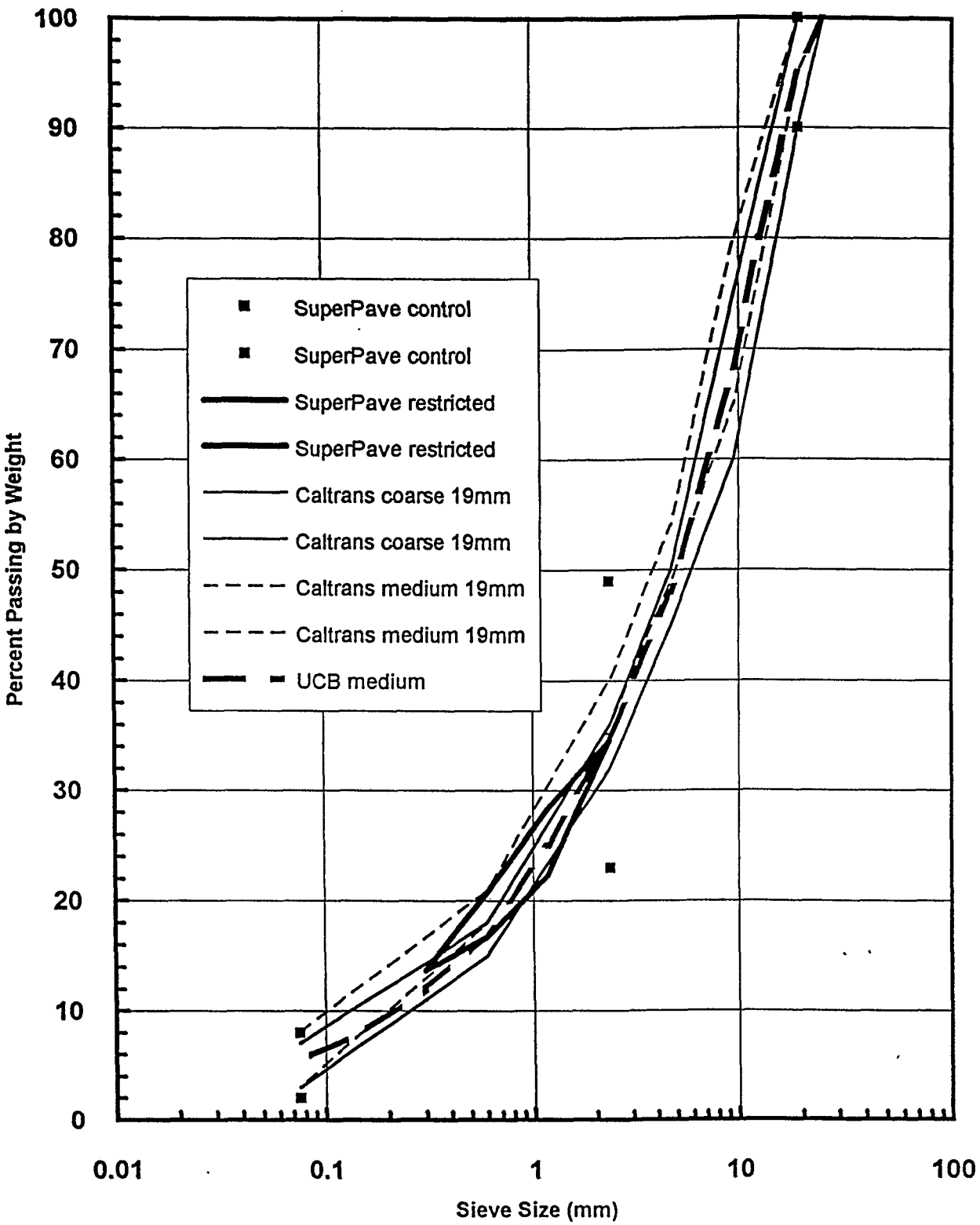

Figure 2.1 Project aggregate gradation compared with Caltrans and SuperPave Level I specifications

Table 2.1 Features of Main Fatigue Experiment

Number of Asphalts	1- MRL Asphalt, AAG-1
Number of Aggregates	1- MRL Aggregate, RB
Asphalt Contents	5- 4.0, 4.5, 5.0, 5.5, 6.0, percent (by weight of aggregate)
Air-Void Contents	3 - 2±1, 5±1, and 8±1 percent
Strain Levels	2 - 150 and 300×10^{-6} mm/mm (in/in)
Replicates	3 per strain level
Total Number of Specimens	97 (nominal total: 5*3*2*3=90)

Table 2.2 Properties of California Valley asphalt

SHRP code		AAG-1
Grade		AR-4000
Original viscosity	60°C (140°F)	1858 poise
	135°C (275°F)	247 cSt
Thin film oven viscosity	60°C (140°F)	3253 poise
	135°C (275°F)	304 cSt
Viscosity ratio [60□C (140□F), TFO/Original]		1.75
Penetration [0.1mm, 100 g, 5 sec, 25°C (77°F)]		53
Elemental analysis	Carbon	86.39%
	Hydrogen	10.33%
	Nitrogen	1.12%
	Sulphur	2.03%
	Vanadium	32ppm
	Nickel	71ppm

Table 2.3 Medium number 2 gradation

Sieve size (mm)	Sieve size (US)	Percent passing
25.4	1 in	100
19	3/4 in	95
12.5	1/2 in	80
9.5	3/8 in	68
4.75	No. 4	48
2.36	No. 8	35
1.18	No. 16	25
0.6	No. 30	17
0.3	No. 50	12
0.15	No. 100	8
0.075	No. 200	5.5

Table 2.4 Features of Long-Term Aging Experiment

Number of Asphalts	1- MRL Asphalt, AAG-1
Number of Aggregates	1- MRL Aggregate, RB
Asphalt Contents	4- 4.0, 4.5, 5.0, and 5.5 percent (by weight of aggregate)
Air-Void Contents	2- 5±1 and 8±1 percent
LTOA Periods	3- 0, 3, and 6 days
Strain Levels	2- 150 and 300×10^{-6} mm/mm (in/in)
Replicates	2 per Strain Level
Total Number of Specimens	114 (Nominal Total: 4*2*3*2*2=96)

3.0 Asphalt and Air-Void Contents

Asphalt mixes are predominantly three-phase systems comprised of asphalt, aggregate, and air. The relative proportions of these constituents--typically measured by asphalt content and air-void content--are among the mix characteristics most significantly affecting pavement performance. Asphalt content is selected during the mix design process: it must be sufficiently large to provide adequate fatigue resistance, durability, and workability while, at the same time, sufficiently small to minimize rutting, bleeding, and structural instability. Air-void content (and/or relative compaction) is considered both in mix design and construction specifications: it must be sufficiently small to avoid degradation in load resistance but not so much so as to promote structural instability and bleeding. This study was undertaken in part to extend existing knowledge about how asphalt-content selection and construction compaction affects fatigue performance and flexural stiffness. This section documents the laboratory testing program and describes effects of asphalt and air-void contents on simulated pavement performance.

3.1 Laboratory Results

The primary experiment investigated mixes with five asphalt contents ranging from 4 to 6 percent and air-void contents grouped into three intervals, 1 to 3 percent, 4 to 6 percent, and 7 to 9 percent. Each mix was tested at two nominal strain levels, 150 and 300 microstrain. Average

test results for the replicates are presented in Table 3.1, and individual data points together with logarithmic, best-fit lines are plotted on Figures 3.1-3.3.

Figures 3.1-3.2 provide visual confirmation of the a priori hypothesis that fatigue life is generally improved by increases in asphalt content and decreases in air-void content. The trends are similar for both the small flexural strain (Figure 3.1) and the larger one (Figure 3.2). Within the ranges of asphalt and air-void contents examined, the relationships appear to be monotonic.

The effects of asphalt and air-void contents on initial flexural stiffness are graphically depicted on Figure 3.3. Because, as demonstrated later (e.g. Table 3.3), strain level does not affect the relationships, data for both strain levels are plotted together. Figure 3.3 suggests that initial flexural stiffness is increased by decreases in both asphalt content and air-void content. Although the relationships appear to be monotonic, one particular anomaly deserves mention. Stiffness measurements for mixes with 4-percent asphalt and 1 to 3-percent air voids are smaller than expected. Perhaps this may be due to cracking of aggregate particles during compaction. Nevertheless these results seem to be of little practical significance because mix designs with a combination of such low asphalt and air-void contents are unlikely with aggregate gradations similar to that tested herein.

Routine statistical procedures were employed to quantify the correlations and relationships among the variables of interest and to determine their statistical significance. Treating asphalt content, air-void content, and strain level as categorical variables having five, three, and two levels, respectively, analysis of variance (ANOVA) was employed to establish the significance of both main effects and two-factor interactions on the two dependent variables, the logarithm of fatigue life (ln N) and the logarithm of initial flexural stiffness (ln S_o). Results, summarized in Table 3.2, are similar to those found in the SHRP A-003A fatigue studies

(Tayebali et al., 1994a, 1994b, and 1994c, and Harvey and Monismith, 1994). Tensile strain, asphalt content, and air-void content were found to significantly affect ln N, but all two-factor interactions were statistically insignificant. Asphalt content, air-void content, and their two-factor interaction significantly affected ln S_o, but tensile strain was statistically insignificant.

A Pearson correlation matrix was also constructed to demonstrate the strength of linear relationships among the variables (Table 3.3). Here all variables are treated as interval instead of categorical quantities, and three additional variables were considered including voids filled with bitumen (VFB), volume concentration of asphalt (V_{asp}), and volume concentration of aggregate (V_{agg}). Table 3.3 shows very small correlation among the primary independent variables, asphalt content, air-void content, and strain. This is a necessary condition for regression modelling and results from the way the current experiment was designed. If a "standard compaction" method had been used, e.g. Caltrans Method 304, asphalt content and air-void content would likely have been highly correlated, and independent effects of the design asphalt content and the effectiveness of construction compaction could not have been evaluated.

3.1.1 Fatigue Life Models

A number of multiple regression models for the natural logarithms of fatigue life and initial flexural stiffness were developed using results of this experiment (Table 3.4). Model 1, the basic fatigue life model, confirms the aforementioned effects of asphalt and air-void contents on fatigue life. No two-way interaction among the three independent variables was statistically significant. As evidenced by the adjusted R^2 of 0.916, the model is a reasonably accurate one.

Models 2 and 3 substitute other variables which measure or reflect the relative proportions of asphalt, aggregate, and air. The calibration of Model 2 demonstrates that the volume concentrations of aggregate and asphalt are as effective as asphalt and air-void contents

in describing the effects of mix proportions on fatigue life. Although not physically independent variables, V_{asp} and V_{agg} are not highly correlated in the statistical sense. For a given asphalt content, a decrease in air-void content will increase both V_{asp} and V_{agg}, but primarily V_{agg}. For a given air-void content, an increase in asphalt content will also increase both V_{asp} and V_{agg}, but primarily V_{asp}.

Voids filled with bitumen (VFB) is the percentage of the total voids (air and asphalt) in the mixture that are filled with asphalt. Following the hypothesis that reduced air-void content results in greater fatigue life because it reflects a more homogenous structure with better stress distribution, it is expected that a larger VFB would result in a larger fatigue life. This is confirmed by the positive coefficient on the VFB term of Model 3. Model 3 also demonstrates that VFB is not as effective a substitute for asphalt and air-void contents as is the combination of V_{asp} and V_{agg}.

Models 1 and 3 were further compared by calculating the fatigue lives of 15 hypothetical mixes spanning three levels of VFB (55, 60, and 75 percent). The five mixes at each VFB level had asphalt contents ranging from 4 to 6 percent: the air-void content of each was computed as required to yield the stipulated VFB level. As shown in Table 3.5, the general effects of Models 1 and 3 are similar. That is, fatigue life increases with more asphalt and with less air voids. At the same time there are two notable differences. First, Model 1 simulates effects of asphalt and air-void contents that are not fully captured by Model 3. Second, the simulations of Model 1 are more sensitive to asphalt and air-void contents than are the simulations of Model 3. Because of its larger adjusted R^2 and its more direct approach to capturing effects of asphalt and air-void contents, Model 1 is preferred. Model 3 is apparently less effective in fully capturing the effects of the three-phase (asphalt, air, and aggregate) mix.

Two traditional fatigue models are represented by Models 4 and 5. Model 4 includes flexural stiffness as an independent variable. For capturing effects of mixture proportions, Model 4 is considered to be an ineffective model because of the lower adjusted R^2 as well as the positive sign on the ln S_o coefficient. For controlled-strain testing, models of this type typically show that increased stiffness has a detrimental or negative effect on fatigue life. Adding voids filled with bitumen to the model reverses the sign of the ln S_o term and significantly increases the adjusted R^2 (Model 5). Certainly models similar to Model 5 offer considerable potential for use in investigations intended to capture multiple effects including not only mix proportions but also asphalt type and possibly aggregate type and gradation as well.

3.1.1 Stiffness Models

As confirmed by Figure 3.3, decreasing the air-void content (porosity) of asphalt mixes results in increased mix stiffness. Increased stiffness likely results from the larger volumetric proportion of asphalt and aggregate, mix components capable of bearing applied stresses. Figure 3.3 also suggests that decreasing the asphalt content will also increase mix stiffness. For a given air-void content, a smaller asphalt content means a larger relative presence of aggregate, a considerably stiffer material than asphalt except at quite cold temperatures.

Models 6-8 of Table 3.4 relate ln stiffness with the aforedescribed mix-proportion variables. The correlations are not quite as accurate as those for fatigue life, and, once again, volume concentrations of asphalt and aggregate are equally as effective as asphalt and air-void contents in capturing effects of mix proportions. Initial stiffness was not significantly affected by strain level, and two-factor interactions in Models 6 and 7 were not statistically significant. As demonstrated by Model 8, voids filled with bitumen is not a good indicator of flexural stiffness.

3.2 Simulated In-Situ Performance

Determination of the effects of asphalt and air-void contents on laboratory fatigue life and flexural stiffness is a necessary first step in determining their effects on in-situ pavement performance. However, because mix proportions significantly affect flexural stiffness (and, hence, strains induced in the pavement as a result of traffic loads) as well as fatigue life, the linkage between fatigue performance in the laboratory and that in situ is not necessarily direct. As a result it is necessary to combine analytical simulations of in-situ strains with laboratory fatigue models to predict in-situ performance.

In order to evaluate the effects of asphalt and air-void contents on in-situ fatigue performance, 18 pavement designs were developed using established California Department of Transportation procedures (Highway Design Manual, Chapter 600, 1990), one design for each combination of traffic index (three levels), subgrade R-value (three levels), and base type (two levels). For each design, 15 mixes were evaluated representing those tested herein (five asphalt contents and three air-void contents). Then for each of the 270 resulting combinations, the maximum principal tensile strain at the bottom of the asphalt concrete layer was computed using a multilayer elastic computer code (ELSYM5) and Model 6 (Table 3.4) stiffnesses. The assumed truck loading consisted of a 50 kN (9,000 lb) single half axle with dual tires spaced 335 mm (13.2 in) center-to-center, and a tire pressure of 758 kPa (110 psi). Finally, the simulated in-situ fatigue life was then estimated using Model 1 of Table 3.4.

3.2.1 Description of Hypothetical Pavement Structures

In order to accurately evaluate the effects of mix proportions on pavement fatigue, a wide range of hypothetical pavement structures was investigated. Hypothetical designs were produced

for three levels of traffic index (7, 11, and 15), three levels of subgrade R-value (5, 20, and 40), and two base types (Class B cement treated base and Class 2 aggregate base).[4]

The *traffic index* (TI) is used in the Caltrans design method as a measure of the number of equivalent single axle loads (ESALs) expected in the design period. The range in the number of ESALs corresponding to traffic indices of 7, 11, and 15 are 89,800 to 164,000, 4,500,000 to 6,600,000, and 64,300,000 to 84,700,000, respectively. The selected TI levels span the range of low, medium, and very high traffic loadings on state highway pavements.

The three *subgrade R-values* of 5, 20, and 40 span a similarly wide range in subgrade strength and load resistance. Elastic moduli were estimated to be 3,850, 12,200, and 23,400 psi for R-values of 5, 20, and 40, respectively (Kallas and Shook, 1977).

Base materials included Class B cement treated base and Class 2 aggregate base (Table 3.6). The Type II cement used in the Caltrans cement treated base acts principally to improve the engineering properties of those aggregate base materials which contain a large percentage of fines. Its percentage, limited to 2.5 percent by weight of aggregate, is insufficient to provide strong bonding with the aggregate particles. Class 2 aggregate base is commonly used in Caltrans pavement sections. Elastic moduli for base materials were estimated based on past experience of the authors as follows:

Asphalt concrete thickness	Class B cement treated base	Class 2 aggregate base
3.6 to 7.2 in	40,000 psi	30,000 psi
7.8 to 12.0 in	32,000 psi	25,000 psi
12.0 to 15.6 in	25,000 psi	20,000 psi

[4]Pavement structural sections did not include drainage layers (as is current Caltrans practice) to simplify the computations.

Layer thicknesses were designed by conventional Caltrans practice using the microcomputer program NEWCON90 to perform all calculations. Class 2 aggregate subbase (minimum R-value of 50) was selected for all pavements for which a subbase was included. The minimum thickness for all base layers was 150 mm (6 in). NEWCON90's default minimum thickness for aggregate subbase layers is 105 mm (4.2 in).

The default unit costs for materials in NEWCON90 were used to rank the alternative thickness designs, and the lowest cost design was selected for each case. If several thickness designs had the same lowest cost, the design with the thickest asphalt concrete layer was selected.

When the subgrade R-value was 40 and NEWCON90 designs included the minimum subbase thickness, the design was recalculated with the subbase eliminated. The rationale for this change was that the subgrade was of nearly equal strength as the eliminated subbase, and the added complications of constructing a very thin subbase layer would not be warranted in practice.

Table 3.7 identifies the 18 hypothetical pavements including the parameters used in ELSYM5's multilayered elastic analysis. As earlier noted, the flexural stiffness of the asphalt layer was computed by Model 6 of Table 3.4, and the fatigue life, by Model 1 of the same table. Pavement temperature was thus assumed to be 19□C and constant with depth.

3.3.3 Simulation Results

Typical results of the simulation are illustrated by Figure 3.4. The pavement structure for this particular simulation was designed with Class 2 aggregate base to resist traffic loading characterized by a TI of 11 when placed on an R-value 20 subgrade. When used within this structure, mixes with the best fatigue performance are those with the largest asphalt content and the smallest air-void content. The same pattern was repeated for each of the 17 other

hypothetical pavements. Thus, for a wide range of pavement structures (designed by California procedures) and traffic loads, simulated fatigue life was found to always increase as a result of increases in asphalt content and decreases in air-void content.

For each combination of asphalt mix and pavement structure, the simulated fatigue life was then normalized by computing the ratio of its fatigue life to that of a mixture with 5-percent asphalt and 5-percent air voids.[5] Normalized fatigue lives for the 270 mix-structure combinations are graphically depicted in Figure 3.5. For each given combination of asphalt content and air-void content, the normalized fatigue lives are remarkably similar among the 15 pavement structures: variability is seen to be largest at the extremes of low asphalt-low air voids and high asphalt-high air voids.

Regression analysis yields the following relationship:

$$Normalized\ \ fatigue\ \ life = 3.3465\, e^{0.1231\,AC\ -\ 0.3634\,AV} \qquad (R^2 = 0.993)$$

This statistical relationship quantifies the approximate, relative effects of asphalt and air-void contents on fatigue life for a range in pavement and traffic conditions. It can be used to determine, for example, the effects of failure to achieve targeted values for asphalt and air voids. For example assuming a targeted mixture of 5-percent asphalt and 5-percent air voids, off-target conditions result in the following:

A 1-percent decrease in asphalt results in a 12-percent decrease in fatigue life,

A 1-percent increase in air voids results in a 30-percent decrease in fatigue life, and

A 1-percent decrease in asphalt combined with a 1-percent increase in air voids results in a 39-percent decrease in fatigue life.

[5]The mix containing 5-percent asphalt and 5-percent air voids was considered to be a mix which had been well constructed and subjected to some traffic and would likely be resistant to rutting.

If quality control and assurance testing during construction permitted a 1-percent deficiency in asphalt and a 3-percent excess of air voids, the combined effect would be a quite significant 70-percent reduction in fatigue life. Examples such as this underscore the importance of careful attention to asphalt and air-void contents, both during the mix-design process as well as during construction.[6]

3.3 Long-Term Aging

The long-term aging experiment investigated mixes with four asphalt contents ranging from 4 to 5.5 percent and air-void contents grouped into two intervals, 4 to 6 percent and 7 to 9 percent. Each mix was subjected to long-term oven aging (LTOA) of 0, 3, and 6 days duration and tested at two nominal strain levels, 150 and 300 microstrain. Average test results are summarized in Table 3.8 and plotted, together with linear best-fit lines, on Figures 3.6-3.8.

These figures show that the basic effects of asphalt and air-void contents on laboratory fatigue life and initial stiffness are apparently unaffected by long-term aging. That is, with or without LTOA, 1) an increase in asphalt content results in an increase in laboratory fatigue life and a decrease in mix stiffness and 2) an increase in air-void content results in a decrease in laboratory fatigue life and a decrease in mix stiffness.

Routine statistical procedures were employed to quantify the correlations and relationships among the variables of interest and to determine their statistical significance.

---

[6]The need to carefully control both asphalt and air void contents during construction has been demonstrated over the years by analyses of the types described herein (e.g. Pell, 1975; and Lister and Powell, 1975). The state of Oregon has developed pay factors for construction control using fatigue data developed by Hicks et al (1982).

Accelerated pavement testing provides a unique opportunity to verify both the effect of compaction and asphalt content on pavement performance.

Treating asphalt content, air-void content, strain level, and LTOA as categorical variables having four, two, two, and three levels, respectively, analysis of variance (ANOVA) was employed to establish the significance of both main effects and two-factor interactions on the two dependent variables, the logarithm of fatigue life (ln N) and the logarithm of initial flexural stiffness (ln S_o). Results, summarized in Table 3.9, show that the significance of asphalt content, air-void content, and strain is essentially unchanged from that in the primary experiment (Table 3.2). LTOA appears to have a minor effect on ln N in terms of its two-factor interaction with tensile strain. LTOA has a more pronounced, statistically significant effect on ln S_o, however, both as a main effect and in its two-factor interaction with air-void content.

A Pearson correlation matrix was also constructed to demonstrate the strength of linear relationships among the variables (Table 3.10). Here all variables are treated as interval instead of categorical quantities. Table 3.10 shows very small correlation among the independent variables, asphalt content, air-void content, strain, and LTOA. This is a necessary condition for regression modelling and results from the way the current experiment was designed.

Regression modelling considered main effects of the four independent variables and all two-factor interactions among them. Final models in which only statistically significant terms are included are as follows:

$$N=6.1009*10^{-11}e^{0.489AC-0.152AV}\varepsilon_t^{-3.942-0.003\text{Days}} \qquad (R^2=0.907) \quad (3.1)$$

and

$$S_o(\text{MPa})=1.2301*10^{5}e^{-0.411AC-0.262AV+\text{Days}(0.010AV-0.023)+0.031AC*AV} \qquad (R^2=0.824) \quad (3.2)$$

These equations suggest that increases in LTOA result in decreases in fatigue life and increases in mix stiffness. The effect on fatigue life is very small, however, and it was necessary to reduce the significance level to 90 percent in order to justify including LTOA in the regression model

for fatigue life. In the stiffness model, the two-factor interaction of LTOA and air-void content suggests that the aging effect is intensified as air-void content increases. This is expected because increased porosity should allow greater aging by oxidation.

A brief analysis was also undertaken to ascertain the effects of LTOA on simulated in-situ fatigue life. Two pavement structures were evaluated, as follows:

	Thick	Thin
Asphalt Concrete	152 mm, E = variable v = 0.35	75 mm, E = variable v = 0.35
Aggregate Base	305 mm, E = 241 MPa v = 0.40	152 mm, E = 172 MPa v = 0.40
Subgrade	∞, E = 69 MPa v = 0.45	∞, E = 69 MPa v = 0.45

The initial stiffness of the asphalt concrete layer was calculated using Model 6 (Table 3.11) for each asphalt content (4.0, 4.5, 5.0 and 5.5 percent), air-void content (5 and 8 percent), and LTOA periods (0, 3 and 6 days).

Elastic layer theory (program ELSYM5) was used to estimate the maximum tensile strain at the bottom of the asphalt concrete layer for each structure, under a 40 kN axle load with dual tires spaced 33.5 mm apart and 690 kPa tire pressures. Beam fatigue life was calculated using the tensile strain and Model 1 (Table 3.11). A laboratory to field shift factor of 15 was applied to the beam fatigue life to obtain the predicted pavement fatigue life.

Because the results were for illustrative purposes only, a reliability level of 50 percent and a constant temperature of 19°C (67°F) were assumed.

The simulations showed that LTOA resulted in longer pavement fatigue life for both the thick and thin pavement structures, as can be seen in Figures 3.9 and 3.10, respectively. The simulations show that increases in mix stiffness from LTOA result in lower strains at the

underside of the asphalt concrete layer which, in combination with the negligible effect of LTOA on mix fatigue life, result in longer simulated fatigue life with more days of LTOA.

A more realistic assumption, that long-term aging would be more pronounced nearer to the surface of the asphalt concrete layer, was also simulated for the thick pavement structure. The asphalt concrete layer was divided into thirds, with the upper third assumed to have the stiffness and beam fatigue life relation associated with 6 days of LTOA, the middle third with 3 days of LTOA, and the bottom third with no LTOA.

The results of that simulation produced pavement fatigue lives similar to the 0 day of LTOA cases, as shown in Figure 3.9.

As stated in Section 2.5, the Valley asphalt-Watsonville aggregate mix evaluated herein is likely to have superior aging resistance. As a result, aging effects for other mixes may well be different from those of the Valley-Watsonville mix. Additional experimentation with a more aging-susceptible mix--currently underway--will help to establish the general validity of findings reported herein.

The primary significance of the long-term aging experiment for this work is that, for purposes of mix design and analysis, fatigue test specimens apparently do not require conditioning by long-term oven aging.

3.4 Conclusions

Conclusions based on the data and analyses presented herein are as follows:

1. For controlled-strain testing, an increase in asphalt content within the range tested results in an increase in laboratory fatigue life and a decrease in mix stiffness.

2. For controlled-strain testing, an increase in air-void content within the range tested results in a decrease in laboratory fatigue life and a decrease in mix stiffness.

3. For the materials tested, the effects of asphalt and air-void contents on laboratory fatigue performance can be modelled as follows (Table 3.4):

$$N = 2.2953*10^{-10}\, e^{0.594AC - 0.164AV}\varepsilon_t^{-3.730} \qquad (R^2=0.916) \quad (3.3)$$

and

$$S_o \text{ (MPa)} = 4.5524*10^{5}\, e^{-0.171AC - 0.076AV} \qquad (R^2=0.685) \quad (3.4)$$

Main effects in these models are statistically significant at a level of significance higher than 99 percent. Interactive effects of the independent variables are not included in the above models because they are not statistically significant.

4. Voids filled with bitumen apparently captures some, but not all, of the effects of asphalt and air-void contents on fatigue life. An increase in voids filled with bitumen results in an increase in laboratory fatigue life which can be modelled as follows:

$$N = 7.9442*10^{-11}\, e^{0.044VFB}\varepsilon_t^{-3.742} \qquad (R^2=0.875) \quad (3.5)$$

The advantage of including voids filled with bitumen in comprehensive fatigue models is that, unlike asphalt and air-void contents, voids filled with bitumen is not highly correlated with flexural stiffness. Because of this relatively weak correlation, both variables can be simultaneously incorporated into fatigue models (Table 3.4) as indicated below:

$$N = 2.5875*10^{-8}\, e^{0.053VFB} S_o^{-0.726}\varepsilon_t^{-3.761} \qquad (R^2=0.885) \quad (3.6)$$

Such a model is one of the more promising for generally describing the effects on fatigue life of a wide range of mix characteristics, including not only asphalt and air-void contents but also asphalt type and possibly aggregate type and gradation as well. At the

same time, users of such models must recognize the imprecision with which they capture mix-proportion effects and must not use them for detailed mix-design purposes.

5. Because asphalt and air-void contents affect not only fatigue life but also mix stiffness, simulation is required to estimate their effects on in-situ pavement performance. Simulation of the performance of a variety of pavement structures (compatible with current California design practice) and a variety of traffic loads verifies that fatigue performance is maximized by providing the maximum feasible asphalt content and the minimum feasible air-void content (limited by rutting and bleeding considerations).

6. The basic effects of asphalt and air-void contents on laboratory fatigue life and stiffness are not affected by long-term aging. Nevertheless, long-term aging increases mix stiffness but has little, if any, effect on laboratory fatigue life. Limited in-situ simulations suggest that long-term aging may benefit pavement fatigue performance slightly but only as a result of increases in mix stiffness. Conditioning laboratory fatigue specimens by long-term oven aging does not appear to be necessary for purposes of mix design and analysis. These findings of the effects of long-term aging are tentative pending completion of testing and analysis--currently underway--of a second, more aging-susceptible mix.

7. An important consideration in mix design is construction control. With respect to fatigue performance, the data presented herein indicate that accurate control of air-void content is more important than accurate control of asphalt content. For example, a mix targeted at 5-percent asphalt and 5-percent air voids will suffer a 30-percent reduction in fatigue life if the air-void content exceeds its target by 1 percent but only a 12-percent reduction if the asphalt content is shy of its target by 1 percent. Complicating this matter, however, is

the likelihood that smaller-than-specified asphalt contents will result in increased air-void contents due primarily to the increased compactive effort required to achieve the requisite degree of compaction.

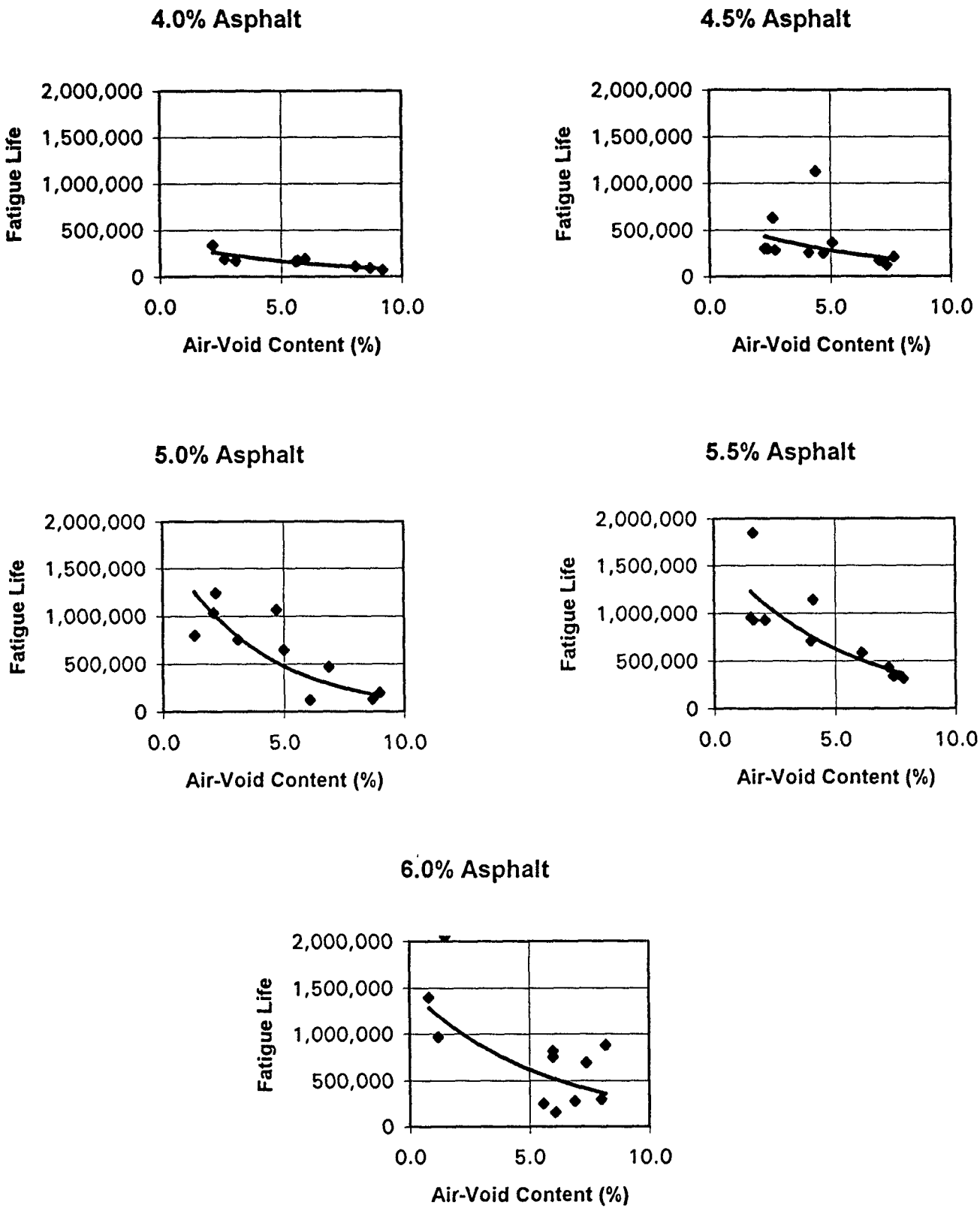

Figure 3.1 Effect of asphalt and air-void contents on laboratory fatigue life (150 microstrain)

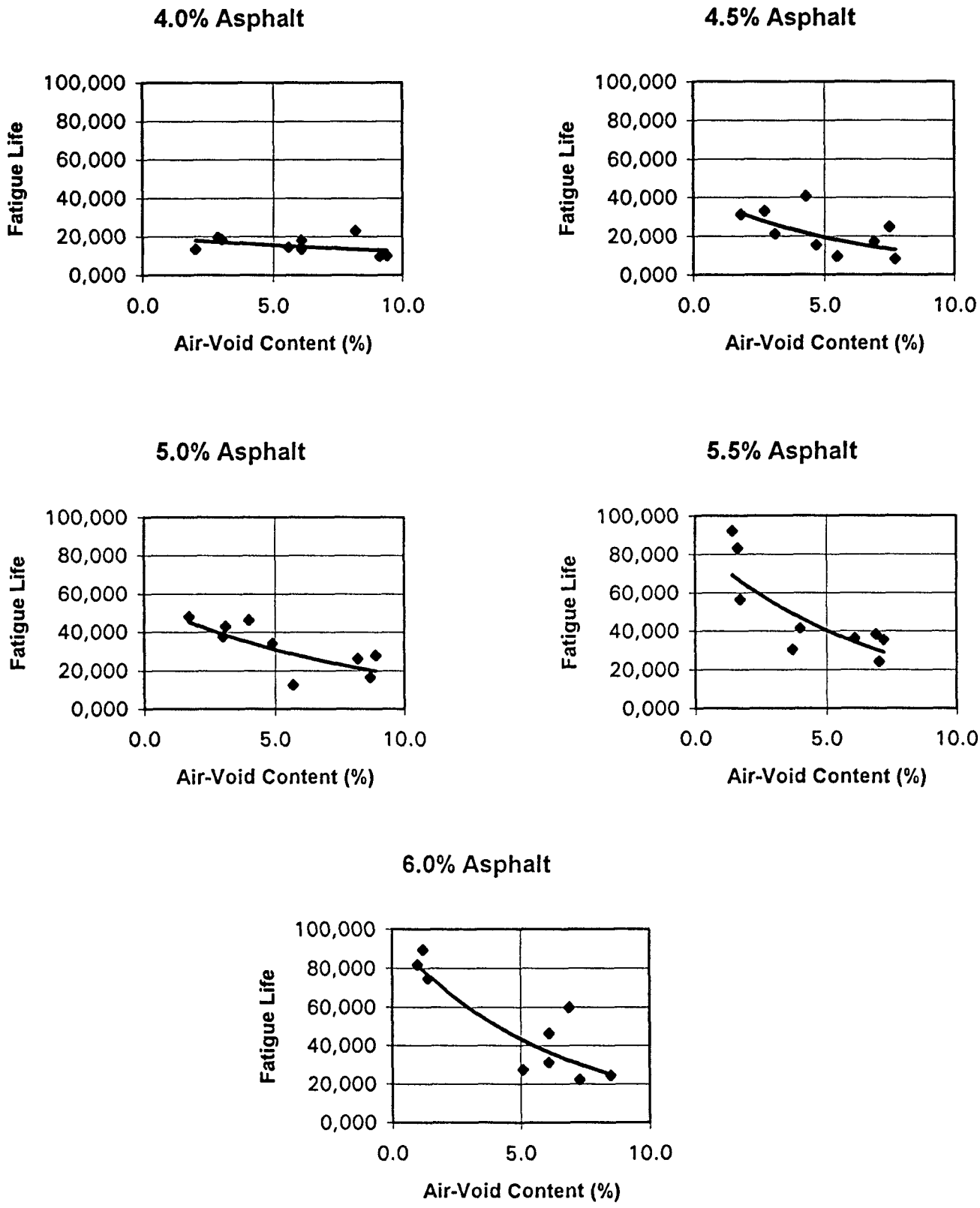

Figure 3.2 Effect of asphalt and air-void contents on laboratory fatigue life (300 microstrain)

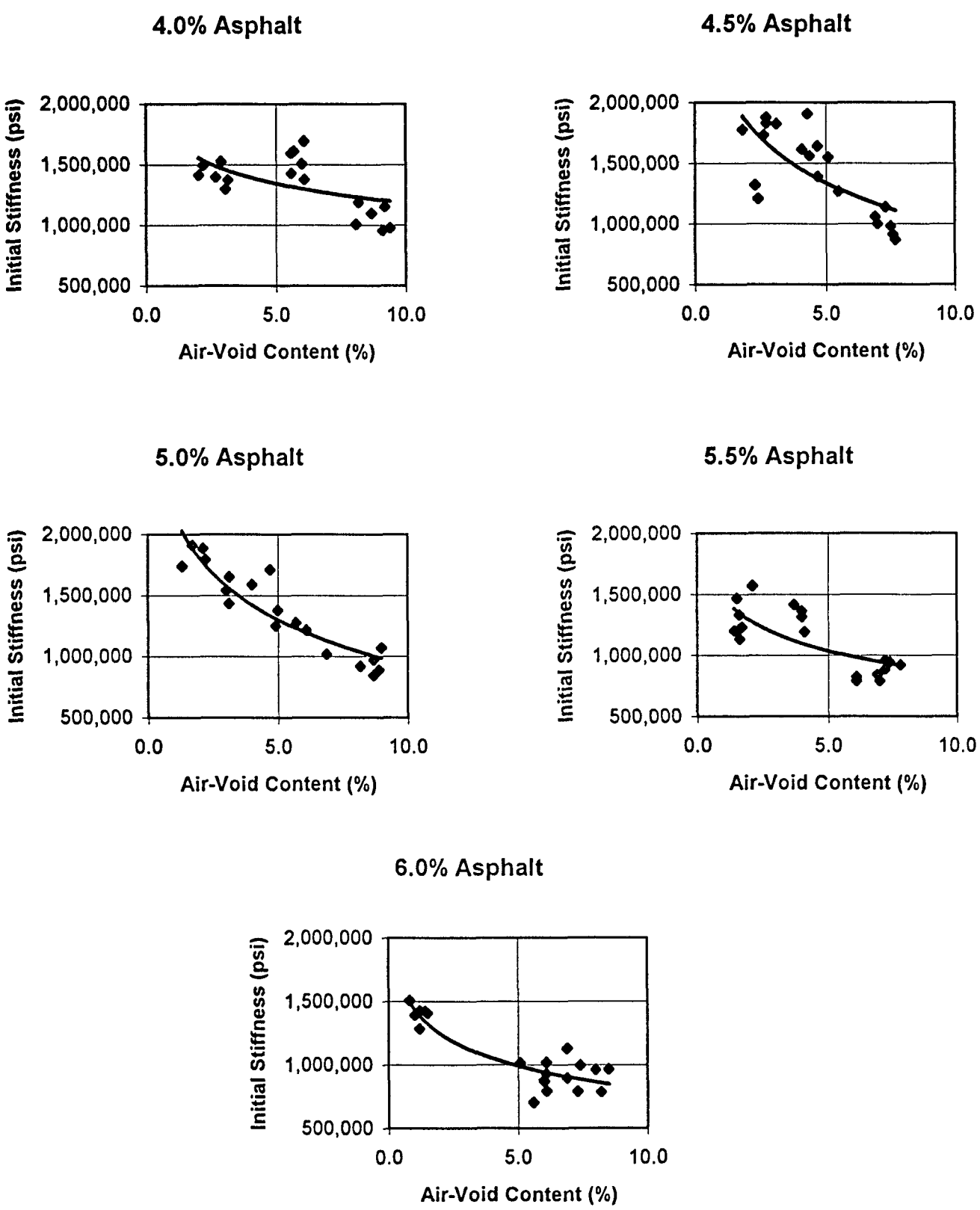

1 psi=6.89 kPa

Figure 3.3 Effect of asphalt and air-void contents on laboratory initial stiffness

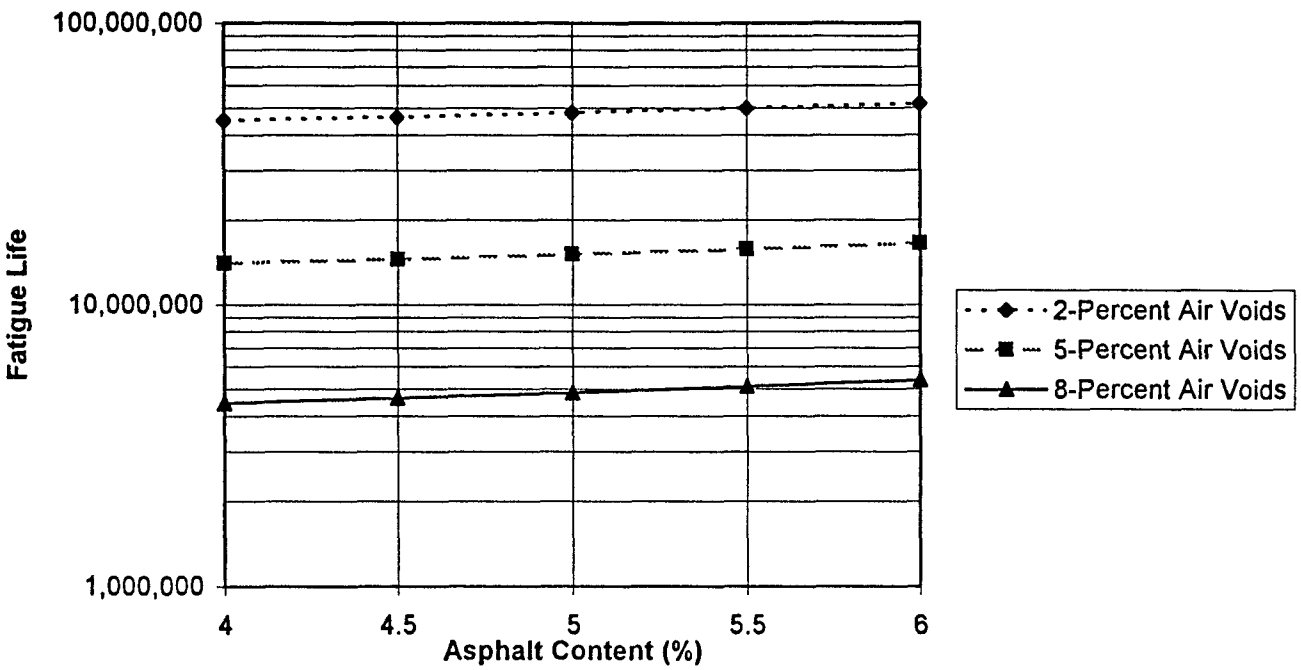

Figure 3.4 Effect of asphalt and air-void contents on simulated, in-situ fatigue life (Class 2 aggregate base, TI of 11, and R-value of 20)

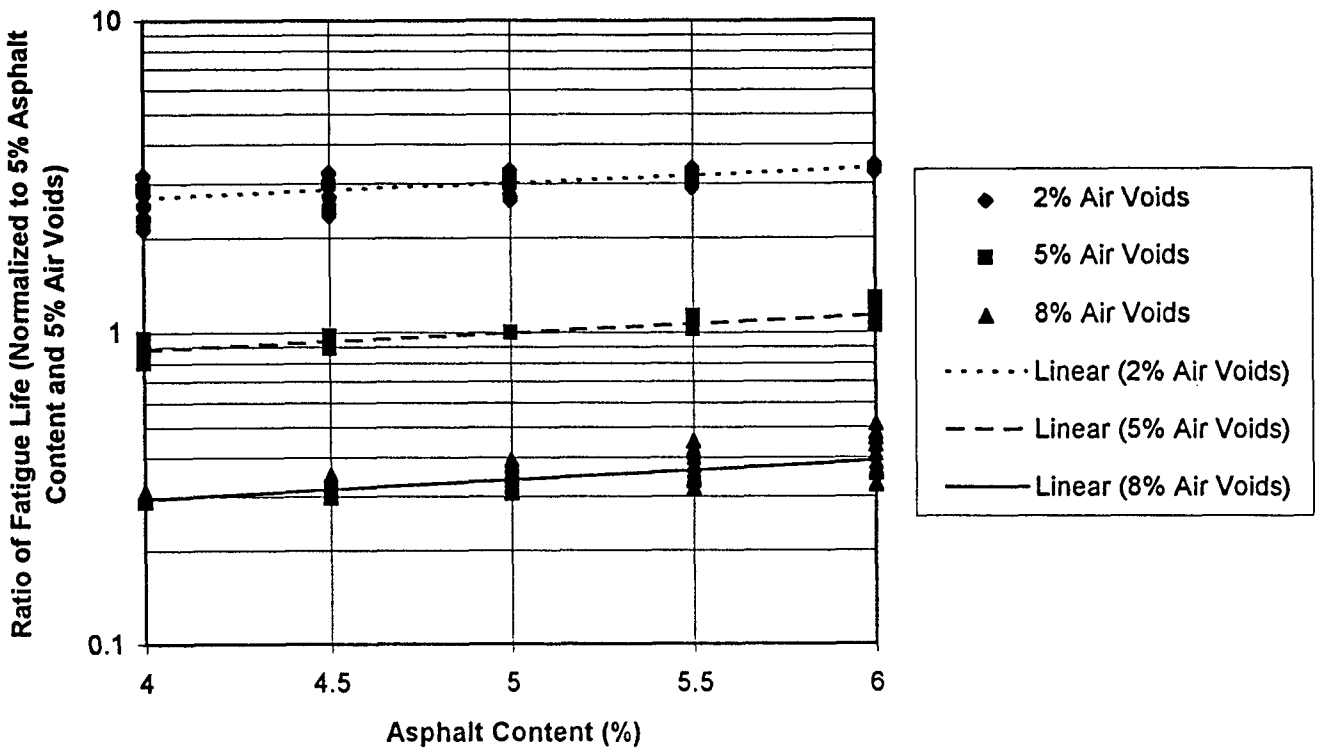

Figure 3.5 Effect of asphalt and air-void contents on simulated, fatigue-life ratio for 270 mix-pavement combinations

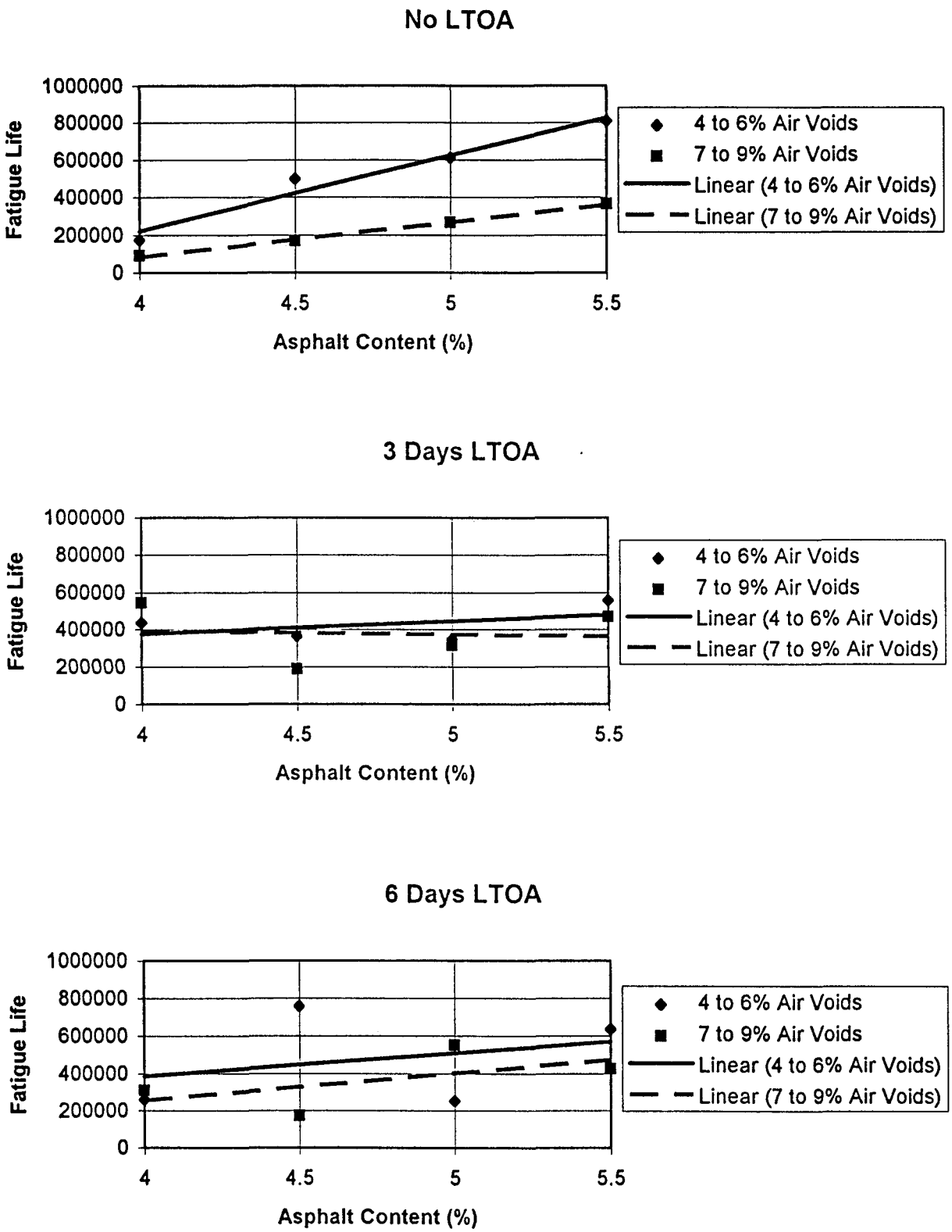

Figure 3.6 Combined effects of asphalt and air-void contents and long-term oven aging on laboratory fatigue life (150 microstrain)

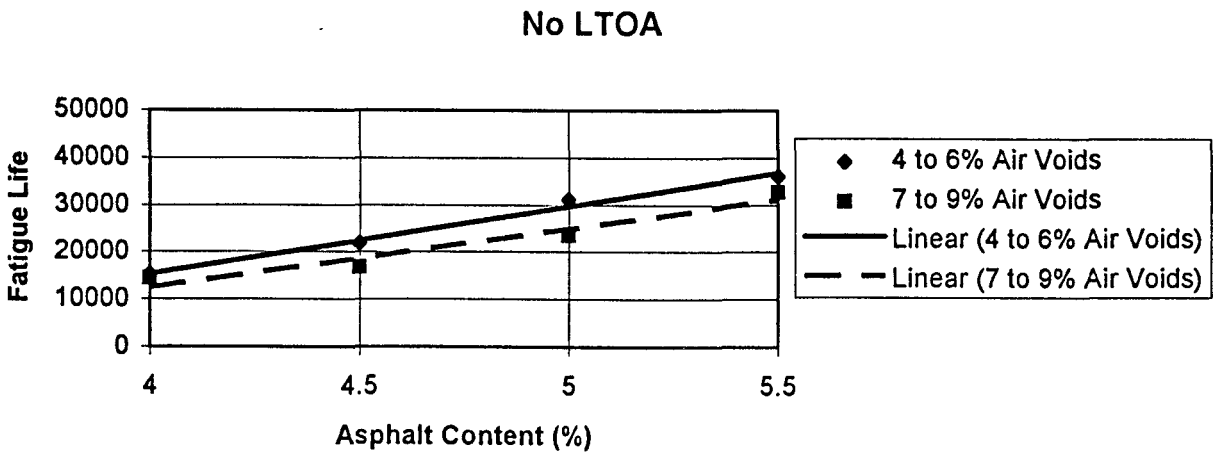

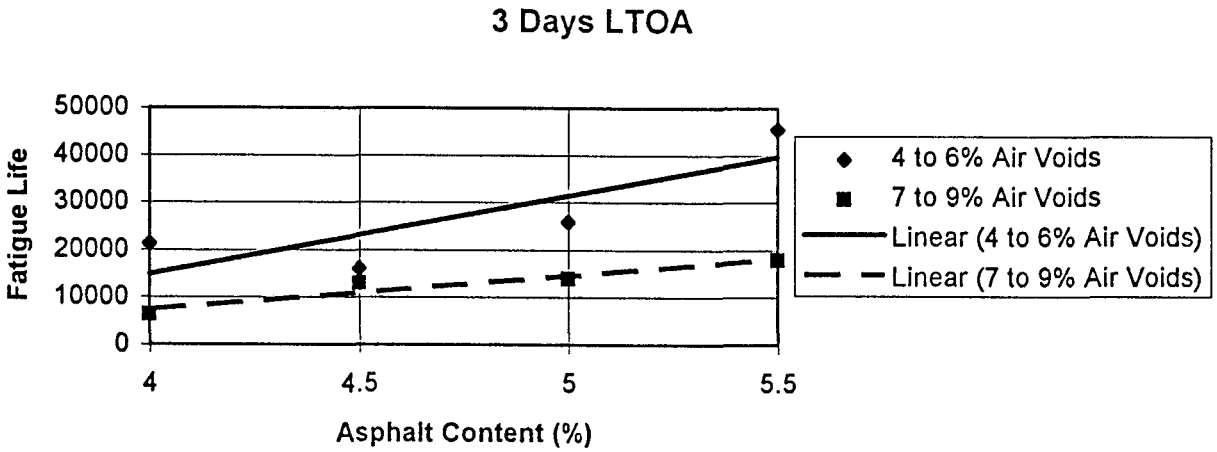

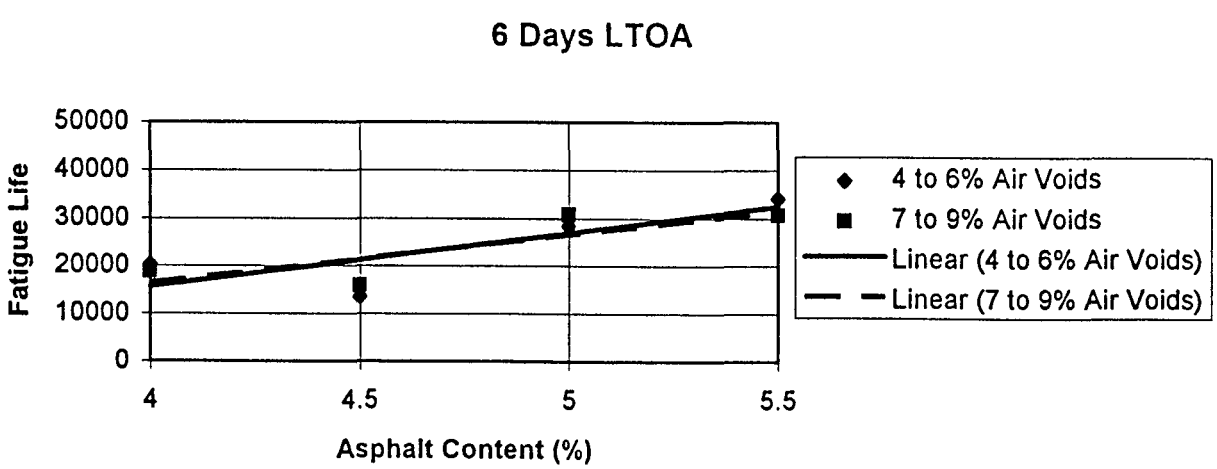

Figure 3.7 Combined effects of asphalt and air-void contents and long-term oven aging on laboratory fatigue life (300 microstrain)

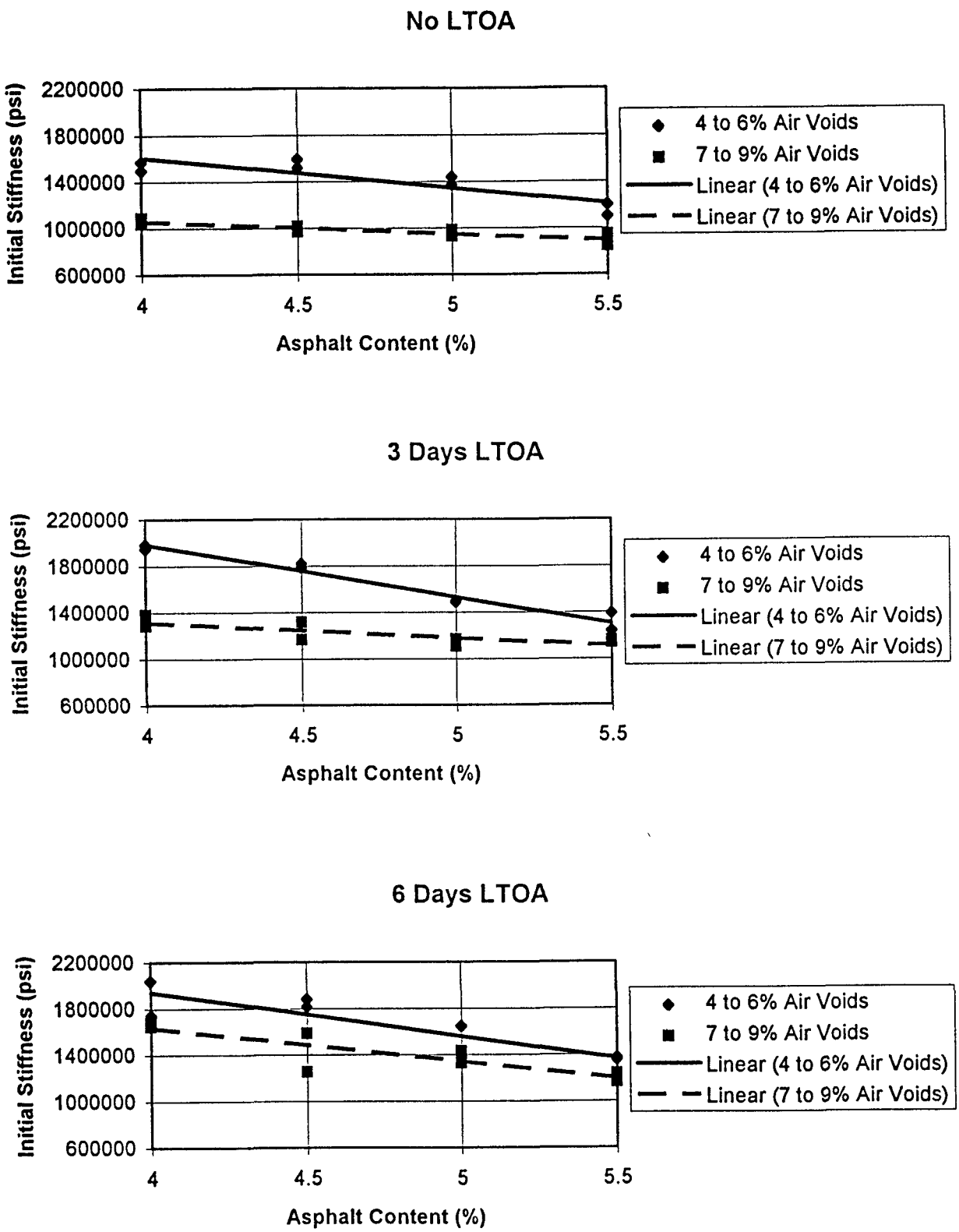

1 psi=6.89 kPa

Figure 3.8 Combined effects of asphalt and air-void contents and long-term oven aging on laboratory initial stiffness

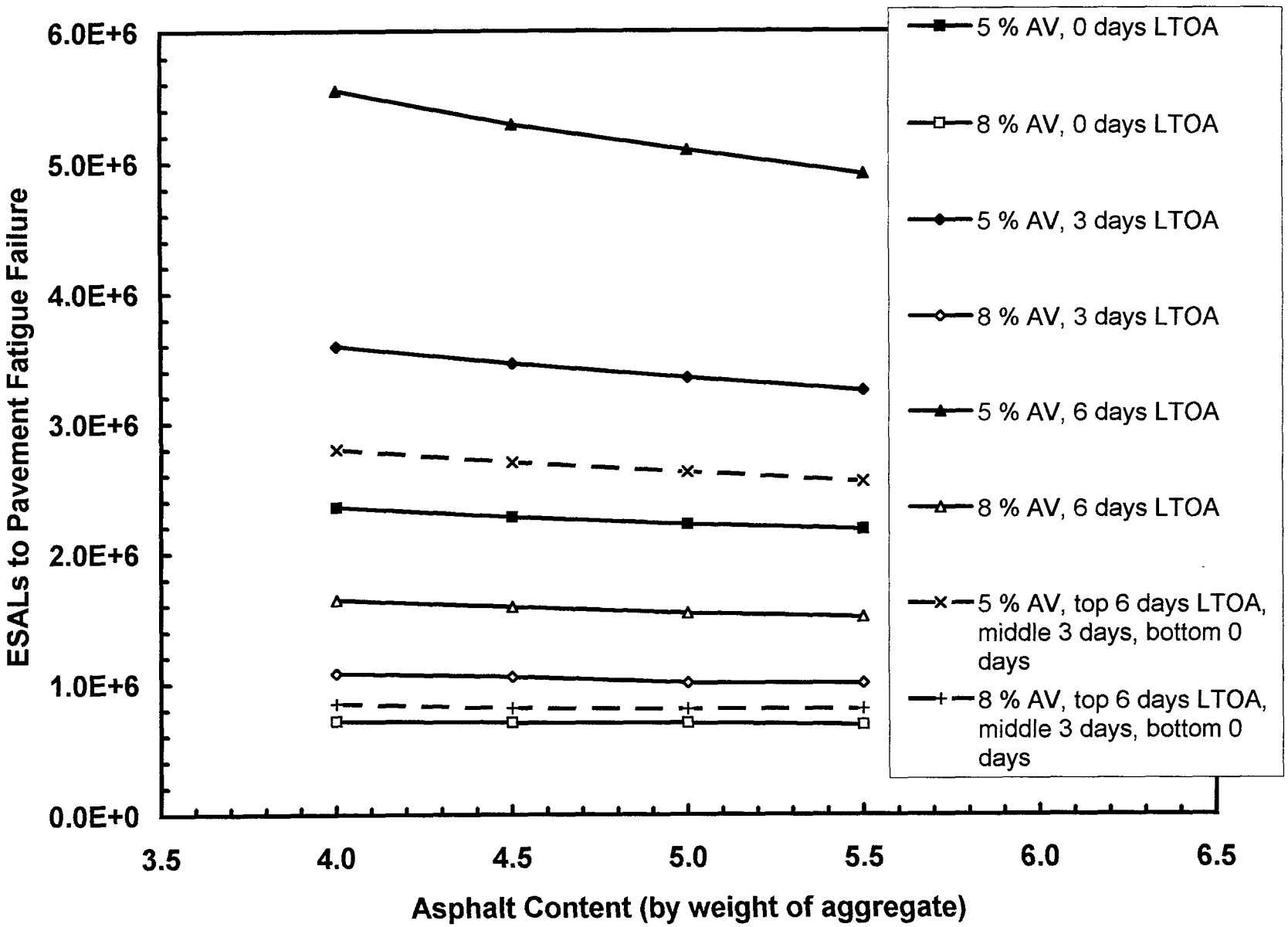

Figure 3.9 Influence of aging (LTOA) on tensile strain on the underside of asphalt bound layers for pavements designed for TI's of 7 and 11

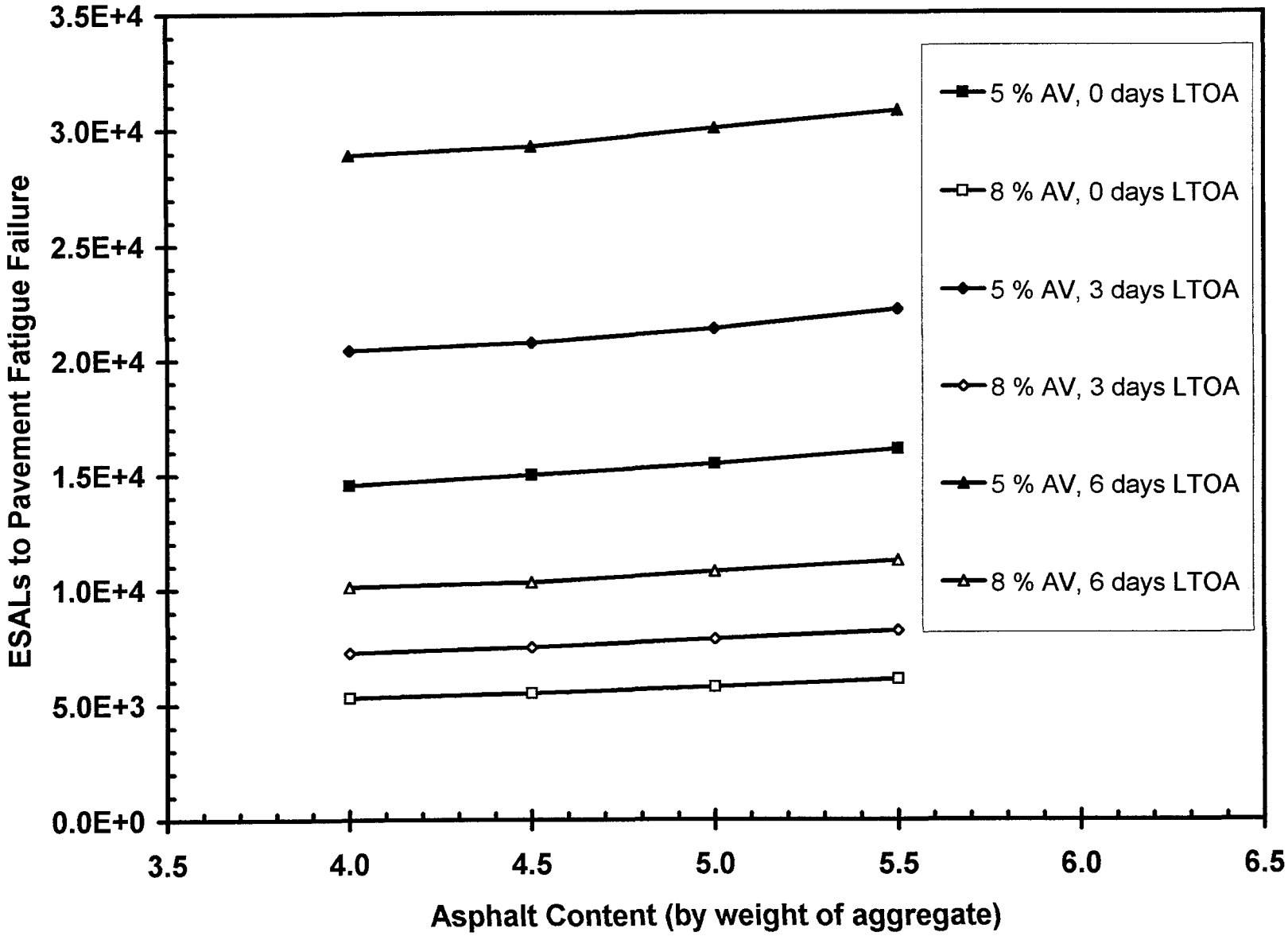

Figure 3.10 Influence of aging (LTOA) on fatigue response of pavements designed for TI's of 7 and 11.

Table 3.1 Summary of test results for primary experiment

Average air-void content (%)	Asphalt content (%)	Average strain (microstrain)	Number of replicates	Average initial stiffness MPa (ksi)	Average fatigue life
2.6	4.0	146	3	9,825 (1,426)	232,500
2.5	4.5	147	4	10,510 (1,525)	376,300
2.2	5.0	148	4	11,800 (1,713)	957,800
1.7	5.5	147	4	9,625 (1,397)	1,162,500
1.2	6.0	147	3	9,970 (1,447)	1,472,100
5.8	4.0	147	3	10,830 (1,572)	175,300
4.6	4.5	148	4	10,980 (1,594)	498,900
5.3	5.0	146	3	9,901 (1,437)	612,600
4.7	5.5	147	3	7,586 (1,101)	810,900
5.8	6.0	152	5	5,967 (866)	423,800
8.7	4.0	147	3	7,489 (1,087)	90,600
7.3	4.5	147	3	7,000 (1,016)	168,400
8.2	5.0	147	3	6,752 (980)	266,200
7.5	5.5	146	3	6,490 (942)	364,600
7.6	6.0	147	4	6,683 (970)	537,100
2.6	4.0	298	3	9,749 (1,415)	17,300
2.5	4.5	296	3	12,590 (1,827)	28,600
2.6	5.0	298	3	11,730 (1,702)	42,900
1.6	5.5	297	3	8,206 (1,191)	77,200
1.2	6.0	297	3	9,419 (1,367)	82,000
5.9	4.0	298	3	10,340 (1,500)	15,300
4.8	4.5	297	3	10,490 (1,523)	21,900
4.9	5.0	295	3	9,460 (1,373)	31,100
4.6	5.5	296	3	8,268 (1,200)	36,200
5.8	6.0	295	3	6,504 (944)	35,100
8.9	4.0	295	3	7,166 (1,040)	14,300
7.4	4.5	295	3	6,676 (969)	16,800
8.6	5.0	296	3	6,408 (930)	23,600
7.0	5.5	298	3	5,795 (841)	32,800
7.6	6.0	295	3	6,098 (885)	35,600

Table 3.2 ANOVA summary for fatigue life and initial flexural stiffness

Factor/interaction	Ln fatigue life	Ln initial stiffness
Air-void content (AV)	H	H
Asphalt content (AC)	H	H
Strain (ε_t)	H	
AV*AC		H
AV*ε		
AC*ε		

Notes:

Description	*Probability*
H = highly significant	less than 0.01
S = significant	0.01 to 0.05
B = barely significant	0.05 to 0.10
Blank = not significant	greater than 0.10

Table 3.3 Pearson correlation matrix

	ln N	ln S_o	VFB	AC	AV	ln ε_t	V_{agg}	V_{asp}
ln N	1.00							
ln S_o	0.15	1.00						
VFB	0.37	0.55	1.00					
AC	0.32	-0.41	0.30	1.00				
AV	-0.31	-0.68	-0.97	-0.09	1.00			
ln ε_t	-0.87	-0.04	-0.03	-0.03	0.02	1.00		
V_{agg}	0.10	0.83	0.68	-0.48	-0.83	-0.01	1.00	
V_{asp}	0.36	-0.26	0.48	0.98	-0.28	-0.02	-0.30	1.00

Notes: ln, logarithm (Naperian base)
N, fatigue life
S_o, initial flexural stiffness (psi)
VFB, voids filled with bitumen (%)
AC, asphalt content (%)
AV, air-void content (%)
ε_t, tensile strain at extreme fiber of beam (in/in)
V_{agg}, volume concentration of aggregate (%)
V_{asp}, volume concentration of asphalt (%)

Table 3.4 Regression models for beam fatigue life (ln N_f) and initial flexural stiffness (ln S_o).

Model number	Model	R^2
	Fatigue life	
1	$\ln N_f = -22.195 - 0.164\ AV + 0.594\ AC - 3.730 \ln \varepsilon_t$	0.916
2	$\ln N_f = -35.812 + 0.164\ V_{agg} + 0.594\ V_{asp} - 3.730 \ln \varepsilon_t$	0.918
3	$\ln N_f = -23.256 + 0.044\ VFB - 3.742 \ln \varepsilon_t$	0.875
4	$\ln N_f = -25.912 - 3.760 \ln \varepsilon_t + 0.623 \ln S_o$	0.767
5	$\ln N_f = -17.470 + 0.053\ VFB - 3.761 \ln \varepsilon_t - 0.726 \ln S_o$	0.885
	Initial flexural stiffness (MPa)	
6	$\ln S_o = 10.726 - 0.076\ AV - 0.171\ AC$	0.685
7	$\ln S_o = 1.901 + 0.086\ V_{agg} - 0.0004\ V_{asp}$	0.682
8	$\ln S_o = 8.189 + 0.012\ VFB$	0.308

where
ln = logarithm, Naperian base,
N_f = mix fatigue life,
AV = air-void content, percent,
AC = asphalt content, percent,
S_o = initial stiffness, MPa,
V_{agg} = volume concentration of aggregate, percent,
V_{asp} = volume concentration of asphalt, percent,
VFB = void filled with bitumen, percent
ε_t = tensile strain at extreme fiber of beam, and

Table 3.5 Evaluation of the VFB fatigue life model (Model 3)

Asphalt content (%)	Air-void content (%)	Voids filled with bitumen (%)	Estimated fatigue life (Model 3 using VFB)	Estimated fatigue life (Model 1 using asphalt and air-void contents)	Percent difference
4.0	7.5	55.0	182,790	132,459	-58
4.5	8.2	55.1	183,313	157,318	-17
5.0	9.0	54.9	182,131	183,786	1
5.5	9.6	55.1	183,882	221,910	17
6.0	10.3	55.1	183,915	263,557	30
4.0	6.2	60.0	227,652	164,148	-39
4.5	6.8	60.0	227,811	198,199	-15
5.0	7.4	60.1	228,989	239,313	4
5.5	8.0	60.0	227,899	288,955	21
6.0	8.6	60.0	227,768	348,895	35
4.0	3.3	74.4	428,889	264,878	-62
4.5	3.6	74.6	432,249	336,054	-29
5.0	3.9	74.8	436,856	426,354	-2
5.5	4.3	74.4	428,963	532,068	19
6.0	4.6	74.5	431,750	675,039	36

Table 3.6 California standard specifications for base materials

Requirement			Class B cement treated base		Class 2 aggregate base	
	sieve size (mm)	(US)	Operating range	Contract compliance	Operating range	Contract compliance
Aggregate gradation (percent passing)	76.2	3 in	100	100		
	63.5	2 1/2 in	90-100	87-100		
	25.4	1 in	---	---	100	100
	19.0	3/4 in	---	---	90-100	87-100
	4.75	No. 4	35-70	28-77	35-60	30-65
	0.60	No. 30	---	---	10-30	5-35
	.075	No. 200	3-20	0-24	2-9	0-12
Resistance (R-value)			60 min before mixing, 80 min after		---	78 min
Sand equivalent			21 min	18 min	25 min	22 min
Durability index					---	35 min

Table 3.7 Characteristics of hypothetical pavement structures

Traffic Index	Subgrade R-value	Layer	Class B cement-treated base					Class B cement-treated base				
			Thickness		Stiffness		Poisson's	Thickness		Stiffness		Poisson's
			mm	in.	MPa	psi	Ratio	mm	in.	MPa	psi	Ratio
7	5	Surface	91.4	3.6	Varies	Varies	0.40	91.4	3.6	Varies	Varies	0.40
		Base	168	6.6	276	40,000	0.30	168	7.2	207	30,000	0.45
		Subbase	259	10.2	138	20,000	0.45	259	10.2	138	20,000	0.45
		Subgrade			26.5	3,850	0.50			26.5	3,850	0.50
	20	Surface	91.4	3.6	Varies	Varies	0.40	91.4	3.6	Varies	Varies	0.40
		Base	168	6.6	276	40,000	0.30	183	7.2	207	30,000	0.45
		Subbase	152	6.0	138	20,000	0.45	152	6.0	138	20,000	0.45
		Subgrade			84.1	12,200	0.50			84.1	12,200	0.50
	40	Surface	91.4	3.6	Varies	Varies	0.40	107	4.2	Varies	Varies	0.40
		Base	183	7.2	276	40,000	0.30	168	6.6	207	30,000	0.45
		Subbase										
		Subgrade			161	23,400	0.50			161	23,400	0.50
11	5	Surface	198	7.8	Varies	Varies	0.40	259	10.2	Varies	Varies	0.40
		Base	198	7.8	220	32,000	0.30	152	6.0	172	25,000	0.45
		Subbase	427	16.8	138	20,000	0.45	335	13.2	138	20,000	0.45
		Subgrade			26.5	3,850	0.50			26.5	3,850	0.50
	20	Surface	213	8.4	Varies	Varies	0.40	244	9.6	Varies	Varies	0.40
		Base	168	6.6	220	32,000	0.30	152	6.0	172	25,000	0.45
		Subbase	259	10.2	138	20,000	0.45	213	8.4	138	20,000	0.45
		Subgrade			84.1	12,200	0.50			84.1	12,200	0.50
	40	Surface	244	9.6	Varies	Varies	0.40	244	9.6	Varies	Varies	0.40
		Base	152	6.0	220	32,000	0.30	152	6.0	172	25,000	0.45
		Subbase										
		Subgrade			161	23,400	0.50			161	23,400	0.50
15	5	Surface	351	13.8	Varies	Varies	0.40	411	16.2	Varies	Varies	0.40
		Base	152	6.0	172	25,000	0.30	152	6.0	138	20,000	0.45
		Subbase	549	21.6	138	20,000	0.45	442	17.4	138	20,000	0.45
		Subgrade			26.5	3,850	0.50			26.5	3,850	0.50
	20	Surface	274	10.8	Varies	Varies	0.40	320	12.6	Varies	Varies	0.40
		Base	259	10.2	220	32,000	0.30	183	7.2	138	20,000	0.45
		Subbase	381	15.0	138	20,000	0.45	381	15.0	138	20,000	0.45
		Subgrade			84.1	12,200	0.50			84.1	12,200	0.50
	40	Surface	366	14.4	Varies	Varies	0.40	335	13.2	Varies	Varies	0.40
		Base	152	6.0	172	25,000	0.30	152	6.0	138	20,000	0.45
		Subbase						107	4.2	138	20,000	0.45
		Subgrade			161	23,400	0.50			161	23,400	0.50

Table 3.8 Summary of test results for long-term aging experiment

Design air-void content (%)	Asphalt content (%)	Days of LTOA	Average strain (microstrain)	Number of replicates	Average initial stiffness MPa (ksi)	Average fatigue life
4 to 6	4.0	0	147	3	10,830 (1,572)	175,300
4 to 6	4.5	0	148	4	10,980 (1,594)	498,900
4 to 6	5.0	0	146	3	9,900 (1,437)	612,600
4 to 6	5.5	0	147	3	7,586 (1,101)	810,900
4 to 6	4.0	3	148	2	13,420 (1,948)	438,500
4 to 6	4.5	3	147	2	12,530 (1,819)	365,500
4 to 6	5.0	3	148	2	10,260 (1,489)	349,600
4 to 6	5.5	3	147	2	9,584 (1,391)	560,400
4 to 6	4.0	6	148	2	14,050 (2,039)	261,000
4 to 6	4.5	6	146	2	12,510 (1,815)	759,700
4 to 6	5.0	6	147	2	9,515 (1,381)	252,600
4 to 6	5.5	6	146	2	9,474 (1,375)	638,600
4 to 6	4.0	0	298	3	10,340 (1,500)	15,300
4 to 6	4.5	0	297	3	10,490 (1,523)	21,900
4 to 6	5.0	0	295	3	9,460 (1,373)	31,100
4 to 6	5.5	0	296	3	8,268 (1,200)	36,200
4 to 6	4.0	3	298	2	13,660 (1,983)	21,300
4 to 6	4.5	3	296	2	12,310 (1,787)	16,200
4 to 6	5.0	3	295	2	10,290 (1,494)	26,000
4 to 6	5.5	3	297	2	8,454 (1,240)	45,500
4 to 6	4.0	6	300	2	12,010 (1,743)	20,300
4 to 6	4.5	6	303	2	12,960 (1,881)	13,700
4 to 6	5.0	6	295	2	11,330 (1,645)	28,400
4 to 6	5.5	6	298	2	9,343 (1,356)	34,100

Table 3.8 Summary of test results for long-term aging experiment (cont'd.)

Design air-void content (%)	Asphalt content (%)	Days of LTOA	Average strain (microstrain)	Number of replicates	Average initial stiffness MPa (ksi)	Average fatigue life
7 to 9	4.0	0	147	3	7,489 (1,087)	90,600
7 to 9	4.5	0	147	3	7,000 (1,016)	168,400
7 to 9	5.0	0	147	3	6,752 (980)	266,200
7 to 9	5.5	0	146	3	6,490 (942)	364,600
7 to 9	4.0	3	148	2	9,515 (1,381)	545,000
7 to 9	4.5	3	146	3	8,048 (1,168)	188,400
7 to 9	5.0	3	148	2	8,034 (1,166)	314,200
7 to 9	5.5	3	147	2	7,827 (1,136)	469,900
7 to 9	4.0	6	147	2	11,660 (1,693)	309,500
7 to 9	4.5	6	147	2	8,640 (1,254)	173,400
7 to 9	5.0	6	147	2	9,866 (1,432)	553,400
7 to 9	5.5	6	146	2	8,509 (1,235)	424,600
7 to 9	4.0	0	295	3	7,166 (1,040)	14,300
7 to 9	4.5	0	295	3	6,676 (969)	16,800
7 to 9	5.0	0	296	3	6,408 (930)	23,600
7 to 9	5.5	0	298	3	5,794 (841)	32,800
7 to 9	4.0	3	299	2	8,881 (1,289)	6,400
7 to 9	4.5	3	297	2	9,067 (1,316)	13,000
7 to 9	5.0	3	300	2	7,613 (1,105)	14,000
7 to 9	5.5	3	297	2	7,986 (1,159)	18,000
7 to 9	4.0	6	299	2	11,350 (1,647)	18,800
7 to 9	4.5	6	295	2	10,940 (1,588)	16,000
7 to 9	5.0	6	298	2	9,136 (1,326)	30,700
7 to 9	5.5	6	295	2	8,006 (1,162)	30,700

Table 3.9 ANOVA for fatigue life and initial flexural stiffness (long-term aging experiment)

Factor/interaction	Ln fatigue life	Ln initial stiffness
Air-void content (AV)	H	H
Asphalt content (AC)	H	H
Strain (ε_t)	H	
LTOA (Days)		H
AV*AC		S
AV*ε_t		
AV*Days		H
AC*ε_t		
AC*Days		
ε_t*Days	B	

Notes:

Description	*Probability*
H = highly significant	less than 0.01
S = significant	0.01 to 0.05
B = barely significant	0.05 to 0.10
Blank = not significant	greater than 0.10

Table 3.10 Pearson correlation matrix (long-term aging experiment)

	ln N	ln S_o	AC	AV	ln ε_t	Days
ln N	1.00					
ln S_o	0.09	1.00				
AC	0.19	-0.43	1.00			
AV	-0.17	-0.62	-0.06	1.00		
ln ε_t	-0.92	-0.03	0.00	-0.01	1.00	
Days	0.04	0.45	0.00	-0.06	0.01	1.00

Table 3.11 Regression models for beam fatigue life (ln N_f) and initial flexural stiffness (ln $S_{o)}$ including long-term oven aging.

Model number	Model	R^2
	Fatigue life	
1	$\ln N_f = -23.52 - 0.152\ AV + 0.489\ AC - 3.942 \ln \varepsilon_t - 0.003 \ln \varepsilon_t * Days$	0.907
2	$\ln N_f = -23.49 - 0.155\ AV + 0.489\ AC - 3.948 \ln \varepsilon_t$	0.906
3	$\ln N_f = -25.28 + 0.048\ VFB - 3.956 \ln \varepsilon_t$	0.893
4	$\ln N_f = -22.99 + 0.052\ VFB - 3.964 \ln \varepsilon_t - 0.288 \ln S_o$	0.895
	Initial flexural stiffness (MPa)	
5	$\ln S_o = 11.72 - 0.262\ AV - 0.411\ AC - 0.023\ Days + 0.031\ AC*AV + 0.010\ AV*Days$	0.824
6	$\ln S_o = 10.57 - 0.091\ AV - 0.205\ AC + 0.041\ Days$	0.781
7	$\ln S_o = 8.135 + 0.014\ VFB + 0.042\ Days$	0.373

where ln = logarithm, Naperian base,
N_f = mix fatigue life,
AV = air-void content, percent,
AC = asphalt content, percent,
Days = days of long-term oven aging
S_o = initial stiffness, MPa,
VFB = void filled with bitumen, percent
ε_t = tensile strain at extreme fiber of beam.

4.0 Mix Design and Analysis System

An important development of the recently completed Strategic Highway Research Program Project A-003A was a mix design and analysis system which explicitly accounts for fatigue distress. The system relies on laboratory, flexural-fatigue testing for mix evaluation and incorporates an analysis system for properly interpreting test results. It recognizes that mix performance in situ depends on critical interactions between mix properties and in-situ conditions, thus providing not only sensitivity to mix behavior but also sensitivity to the in-situ traffic, climatic, and structural environment as well. The mix design and analysis system and its initial calibration have been described in detail elsewhere (Deacon et al., 1994b). The current study has enabled improvements to be made which not only incorporate additional laboratory test results but also better reflect California pavement design experience and climatic conditions. Following a brief overview of the design and analysis system, these refinements are discussed in depth.

4.1 System Description

Mix design typically involves an iterative search for an economical combination of ingredients which meets performance requirements while, at the same time, minimizing the risk of premature failure. Compromise is necessary because the various distress mechanisms--permanent deformation, fatigue, thermal cracking, bleeding, raveling, etc.--often impose

contradictory demands. The following discussion focuses only on fatigue performance. As presented herein, the fatigue design and analysis system assumes that a trial mix has been selected, and it evaluates the likelihood that this mix will satisfactorily resist fatigue cracking in the design pavement under anticipated traffic and temperature conditions.

In essence, a mix is expected to perform satisfactorily if the number of load repetitions sustainable in laboratory testing exceeds the number of load repetitions anticipated in service. To minimize laboratory costs, testing is at an accelerated rate and, for normal asphalts, at a single temperature. Using the UC-Berkeley controlled-strain, flexural-fatigue apparatus, testing can usually be accomplished within a 24- to 48-hour period. The strain at which the number of laboratory repetitions must be estimated is computed using multilayer, elastic theory. For this computation, the strain of interest is the maximum principle tensile strain at the bottom of the asphalt-bound layer in the design pavement. A 40kN (9,000-pound), dual-tire load is applied, and the mix stiffness corresponds to the laboratory test temperature.

Traffic is represented by the number of Equivalent Single Axle Loads (ESALs) in the critical or design lane during the design period. Because these ESALs accumulate within a mixed temperature environment, it is necessary to apply a factor, herein termed the temperature conversion factor, to convert design ESALs to their equivalent at a single temperature, that used in the laboratory testing. Experience has shown that it is also necessary to apply a shift factor, accounting for a host of factors such as traffic wander, crack propagation rate, construction variability, different frequencies of loading, etc., to assure that load repetitions in the field are commensurate with those in the laboratory.

Because of uncertainty or variability in all of the measurements, simulations, and predictions, there is some risk that a mix will fail in service even if its laboratory resistance is

determined, by the aforedescribed process, to exceed the design loading. Fortunately the risk of failure can be limited to a tolerable level by applying a reliability multiplier to the design loading before comparisons are made with the laboratory resistance. The fatigue design and analysis system incorporates risk assessments in this way.

In summary a mix is deemed to be suitable for use in the selected pavement structure to mitigate fatigue cracking (4.1) when:

$$N \geq \frac{ESALs \bullet TCF \bullet M}{SF} \tag{4.1}$$

in which N = the number of laboratory load repetitions to failure under the anticipated in-situ strain level, ESALs = the number of equivalent, 80kN (18,000-pound) single axle loads expected in the design lane during the design period, TCF = the temperature conversion factor, M = the reliability multiplier, and SF = the shift factor. When a mix under consideration doesn't meet this requirement, the designer has a wide range of options including adjusting the mix by adding more asphalt and/or reducing the air voids, using a different asphalt or aggregate, increasing the pavement thickness, and even allowing an increased risk of premature failure.

For especially important and expensive projects, a more comprehensive design process--required for new or unconventional paving materials--may be warranted. As a part of this process, fatigue tests are performed at multiple temperatures [in the range 10-35°C (50-95°F)]. Rather than using temperature conversion factors as in the procedure described above, representative pavement temperatures on a month by month basis should be estimated. With these temperatures and the corresponding traffic distributions, the linear sum of cycle ratios cumulative damage hypothesis is used to evaluate the adequacy of the pavement structure containing the non-conventional mix.

Procedures are available for determining temperature conversion factors, reliability multipliers, and shift factors, and preliminary estimates have been developed (Deacon et al., 1994a and 1994b). Following sections describe additional refinements and changes to more accurately reflect California conditions.

4.2 Temperature Conversion Factor

The temperature conversion factor (TCF) is a multiplicative factor which converts the number of design load repetitions occurring in the mixed temperature environment in situ to its equivalent at a single temperature. The ability to make such a conversion is critically important for routine work, because it reduces the requisite laboratory testing and structural analysis to a single temperature. The temperature conversion factor has been shown to be dependent both on the pavement structure and on the thermal environment (Deacon et al., 1994a). At the same time, it has been hypothesized that it may be relatively unaffected by mixture characteristics, particularly for asphalts of normal temperature sensitivity. It remains for future study to determine the limits within which this hypothesis is valid.

Deacon et al. (1994a) have developed a procedure for calculating TCFs and have applied it to two hypothetical pavement structures located within nine geographic regions of the United States. The desire to more specifically address California climates together with advancements in the computation of pavement temperature profiles led to the additional computations reported herein.

Three California locations, representative of a variety of climatic conditions, were examined including Blue Canyon in Placer County, Daggett Airport in San Bernadino County, and Santa Barbara Airport in Santa Barbara County. At each location, two hypothetical

pavements were examined--the same two used earlier and described in detail by Deacon et al. (1994a)--having 102 mm (4.0 in.) and 203 mm (8.0 in.) surface courses. The asphalt mix was thought to be representative of those used in California, and laboratory stiffnesses and fatigue lives were measured and characterized during the recent SHRP A-003A investigation. Pavement temperature profiles were simulated using the climatic-materials-structural (CMS) pavement analysis model originally developed at the University of Illinois (Dempsey, Herlache, and Patel, 1985, and Herlache, Patel, and Dempsey, 1985) and revised slightly to better accommodate input/output requirements and to replace the method for computing extraterrestrial radiation with a more suitable one.

Pavement temperature simulations spanned 10-year periods for Santa Barbara and Daggett Airports and a 6-year period for Blue Canyon. Table 4.1 presents relevant location information and climatic summaries for the three sites.[7] Important parameters used in the temperature simulations are summarized in Table 4.2. The simulations produced detailed, long-term temperature profiles for each of the two hypothetical pavements mentioned above. Summary results for the 203 mm (8.0 in.) pavement are illustrated in Table 4.3.

Because the laboratory testing of this study was conducted at 19°C, it was necessary to compute TCFs for this temperature. Also determined were the critical temperature (the temperature integer at the mid-point of a 5°C (9°F) temperature range within which the largest amount of damage accumulates) and TCFs to the critical temperature. Results of these computations, summarized in Table 4.4, confirm prior findings that TCFs are both site- as well

[7]Complete weather information for the three sites is included on diskettes obtained from the U.S. Weather Service.

as pavement structure-specific. They also confirm prior findings that critical temperatures are larger for 203 mm (8.0 in.) pavements than for 102 mm (4.0 in.) pavements and, for both thicknesses, are considerably in excess of the test temperature of 19? C. Testing at critical-temperature levels would be advantageous because possible errors due to temperature-sensitivity abnormalities and due to necessary extrapolations are reduced. Nevertheless the convenience of testing at cooler temperatures and uncertainties about the legitimacy of fatigue measurements at higher temperatures have dictated the choice at UC-Berkeley of testing temperatures at or near 20°C.

Because TCFs have been computed for only two surface thicknesses, the precise influence of pavement structure on the TCFs is not now known. To avoid excessively large TCFs that would result from linear extrapolation for thick pavements, the logarithmic relationships depicted in Figure 4.1 are recommended derived by fitting an equation of the following form through the computed values for the 102 mm (4 in.) and 203 mm (8 in.) thick pavements:

$$TCF = a \ \ln(d) + b \tag{4.2}$$

in which d = asphalt concrete thickness in inches. The regression constants, a and b, for the three sites are as follows:

Location	a	b
Santa Barbara	1.754	-1.256
Daggett	2.102	-1.925
Blue Canyon	1.448	-1.125

4.3 Reliability and Variability

Decisions about anticipated mix performance cannot be made with absolute certainty. Although large safety factors can reduce the likelihood of error, their cost consequences can be considerable. Reliability analysis can ensure an acceptable level of risk in mix design without the cost of excessively large safety factors.

Reliability is considered, herein, to be the probability that the mix will provide satisfactory performance throughout the design period. The reliability level for each specific mix design is set by the designer. Larger levels of reliability reduce the chances of accepting deficient mixes: however, the tradeoff is the potentially larger cost associated with reducing the number of acceptable materials or mixes.

Reliability is introduced in the mix design and analysis system by a reliability multiplier, M, which is calculated as follows:

$$M = e^{Z\sqrt{var(\ln N) + var(\ln ESALs)}} \tag{4.3}$$

in which e = the base of natural or Naperian logarithms, Z = a factor depending solely on the design reliability, var(ln N) = the variance of the logarithm of the laboratory fatigue life estimated at the in-situ strain level under the standard, 9,000-pound wheel load, and var(ln ESALs) = the variance of the estimate of the logarithm of the design ESALs. Z is related to design reliability as follows:

Design reliability (percent)	Z
95	1.64
90	1.28
80	0.841
60	0.253
50	0.000

The variability associated with forecasts of design ESALs is unknown. In the absence of better information, var(ln ESALs) has been assumed herein to be 0.300. Because this value has been used in calibrating the mix design model, its use should be continued in the mix design process until a more accurate estimate is made and the model is recalibrated.

The var(ln N) reflects a combination of factors including the inherent variability in fatigue measurements (associated both with specimen preparation as well as testing equipment and procedures), the nature of the laboratory testing program, and the extent of extrapolation necessary for estimating fatigue life (using a least-squares, best-fit line) at the design strain level. It is calculated as follows:

$$var(\ln N) = s^2 \left(1 + \frac{1}{n} + \frac{(X - \bar{x})^2}{q \sum (x_p - \bar{x})^2} \right) \tag{4.4}$$

in which s^2 = the variance in logarithm of fatigue-life measurements, n = number of test specimens, X = ln(in-situ strain) at which ln(N) must be predicted, $\bar{x}$ = average ln(test strain), q = number of replicate specimens at each test strain level, and x_p = ln(strain) at the pth test strain level. For most of the mixes considered herein, six specimens were tested (n = 6) including three (q = 3) at each of two strain levels (x_p = 150 and 300 microstrain).

The replication which was built into the experiment design permits computation of the inherent variance (s^2) in the logarithm of fatigue-life measurements. The experiment design involved 15 different mixes tested at each of two strain levels with nominally three replicates at each of the 30 combinations (a few small-strain tests had four replicates). A total of 96 observations were included in calculating the sample variance using the following relationships:

$$s^2 = \frac{\sum_{k=1}^{d} WSS_k}{n - d} \tag{4.5}$$

and

$$WSS_k = \sum_{i=1}^{n_k} (\ln N_i - \ln N_k)^2 \quad (4.5)$$

in which WSS_k = within sum of squares for factor level combination k (air-void content, asphalt content, and strain level), n = number of observations (96), d = number of factor level combinations (30), ln N_i = logarithm of measured fatigue life for specimen i, **ln N_k** = average logarithm of measured fatigue lives of specimens for factor level k, and n_k = number of replicates at factor level k.

The best estimate of the overall sample variance of the natural logarithm of the fatigue life obtained from this experiment was calculated using the aforedescribed procedure to be 0.220. The sample variance obtained in the SHRP A-003A expanded tested program, using the same testing equipment and procedures, was 0.152. Because of greater replication in the current study (three versus two in A-003A) and smaller strain levels (150 and 300 microstrain versus 400 and 700 microstrain in A-003A), 0.220 seems to be the best possible estimate of s^2 at the current time. It was used in developing the shift factors in the mix design and analysis model and is recommended for use for mix design purposes.

4.4 Shift Factor

As a result of such factors as traffic wander, crack propagation rate, construction variability, different frequencies of loading, etc., highway pavements have been found to sustain from less than 10 to perhaps as many as 100 times the number of load applications that are estimated by procedures similar to those used herein before pavements become seriously distressed. As a result, laboratory estimates of fatigue life can be compared with service estimates of ESALs only after applying a suitable shift factor. Using AASHTO design guidelines

as a basis, SHRP A-003A studies led to the recommendation of shift factors ranging from 10 to 14 depending on the amount of surface cracking considered to be tolerable (Deacon et al., 1994b). A shift factor of 10 means that one application of strain in the laboratory is equivalent to 10 applications of the same strain in situ.

The most accurate way to develop shift factors is probably by observing the fatigue performance of full-scale pavements in test tracks or in accelerated pavement loading experiments. Even without such experimental data, however, first-order approximations of shift factors can be developed based on the pavement performance experience that is captured in specific design procedures. In the current project, results from laboratory fatigue and stiffness testing of the Valley asphalt-Watsonville granite mix are combined with a variety of pavement structures designed by California procedures to produce shift factors suitable for use in mix-design-and-analysis applications.

The mix containing 5-percent asphalt and 8-percent air voids was selected as that typical of mixes for which the California thickness design procedure is most applicable. The performance of this mixture in 18 hypothetical pavement structures, representing three traffic levels, two base types, and three subgrades, has been simulated. Such simulations produce estimates of the laboratory fatigue life (N), and the traffic index determines the traffic loading (ESALs). The mix design and analysis system defines the relationship between N and ESALs for an adequate mixture to be:

$$N = \frac{ESALs \bullet TCF \bullet M}{SF} \tag{4.1}$$

and, as a result, the shift factor (SF) is given by:

$$SF = \frac{ESALs \bullet TCF \bullet M}{N} \tag{4.7}$$

Shift factors were thus determined for each of the 18 hypothetical pavements. In the process, ESALs were estimated from the traffic index by the following relationship:[8]

$$ESALs = 1.2895 \bullet 10^{-2}\, TI^{8.2919} \qquad (4.8)$$

TCFs were computed based on depth of the asphalt concrete layer, and separate computations were performed for three locations, Santa Barbara, Daggett, and Blue Canyon. To compute the reliability multiplier (M), a 90-percent reliability was assumed, and var(ln N) was based on an s^2 of 0.220 and laboratory testing involving three specimens tested at each of two strain levels (150 and 300 microstrain). The fatigue life (N) was computed from in-situ strain simulations under the 40kN (9,000-pound) dual-tire loading.

Results of the shift-factor computations show a dependence of shift factor on both strain level and traffic index (Figure 4.2). The influence of site location seems to be a relatively minor one. Unfortunately the nature of the relationships of Figure 4.2 can not be confirmed from prior work; no prior work has been identified which has investigated variables of possible influence on shift factors. The real difficulty in this analysis, though, is the fact that each pavement represented on Figure 4.2 does not resist fatigue distress equally well. California design relationships do not explicitly treat fatigue distress, and, while it is possible that most designs are at least marginally adequate, some almost certainly are overconservative. Design to accommodate the median condition should lead to a relatively conservative, first-order approximation of shift factors suitable for trial use.

[8]This equation was obtained from the expression: $TI=aESALs^b$ which was developed by regression from the values relating TI and ESALs in the Caltrans Highway Design Manual (a=1.690; b=0.1206).

It seems logical to relate the design shift factor (the number of in-situ load repetitions equivalent to each load application in the laboratory) to the level of pavement strain. The rate of crack propagation, a principal difference between in-situ and laboratory behavior, is affected by strain level: small strains not only increase the number of load repetitions to crack initiation but also slow the rate of crack propagation as well. The opposite is expected for large strains.

Figure 4.3 shows the relationship between the 50th-percentile shift factor and the 50th-percentile pavement microstrain. Each point represents one of the three levels of traffic index. Until such time as more information becomes available, the power relationship is recommended for design purposes because it best represents the available data. Because of its shape at low strain levels, however, extrapolations should not be made beyond the limits of available data. The recommended design relationship is as follows:

$$Design\ \ shift\ \ factor = 2.7639 \bullet 10^{-5}\ \varepsilon^{-1.3586}\quad for\ \ \varepsilon \geq 0.000040 \tag{4.9}$$

in which ε = simulated strain produced by standard wheel load at the underside of the asphalt-concrete layer.

4.5 Summary Perspective

The mix design and analysis system presented herein was originally developed as a part of SHRP Project A-003A. Its most attractive features include the ability to consider not only laboratory measurements but also the anticipated in-situ environment and the ability to make risk assessments about design choices. The current project enabled important refinements to be made, most notably in the procedures for computing pavement temperature profiles, as well as calibrations which reflect uniquely California conditions. Although more refinements will

doubtlessly be necessary in the future, the system is sufficiently mature to warrant its trial use. Experience is necessary to identify its weaknesses and to suggest areas for possible improvement.

Although the shift factors proposed herein represent an effective point of beginning, future adjustments are inevitable. Ultimately, shift factors are expected to depend not only on strain level but also on the extent of permissible cracking and possibly such added factors as the nature and thickness of the structural section, the rate of accumulation of traffic loading, mode of loading, and perhaps mix properties as well.

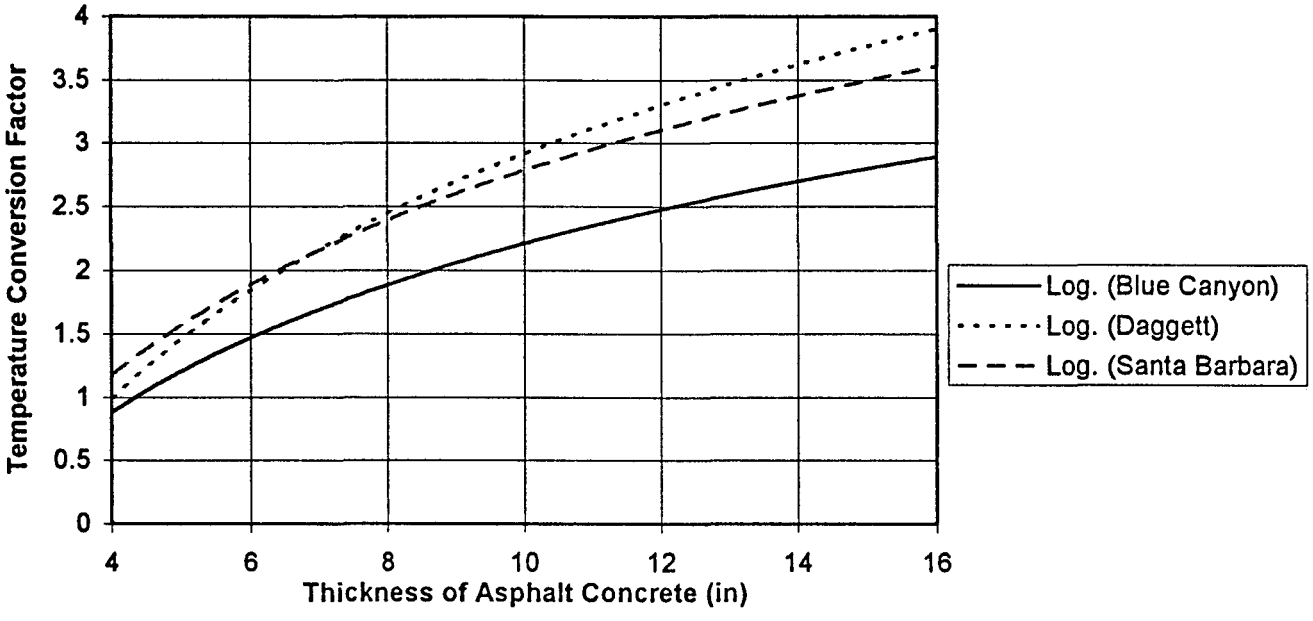

Figure 4.1 Effect of location and surface thickness on temperature conversion factor

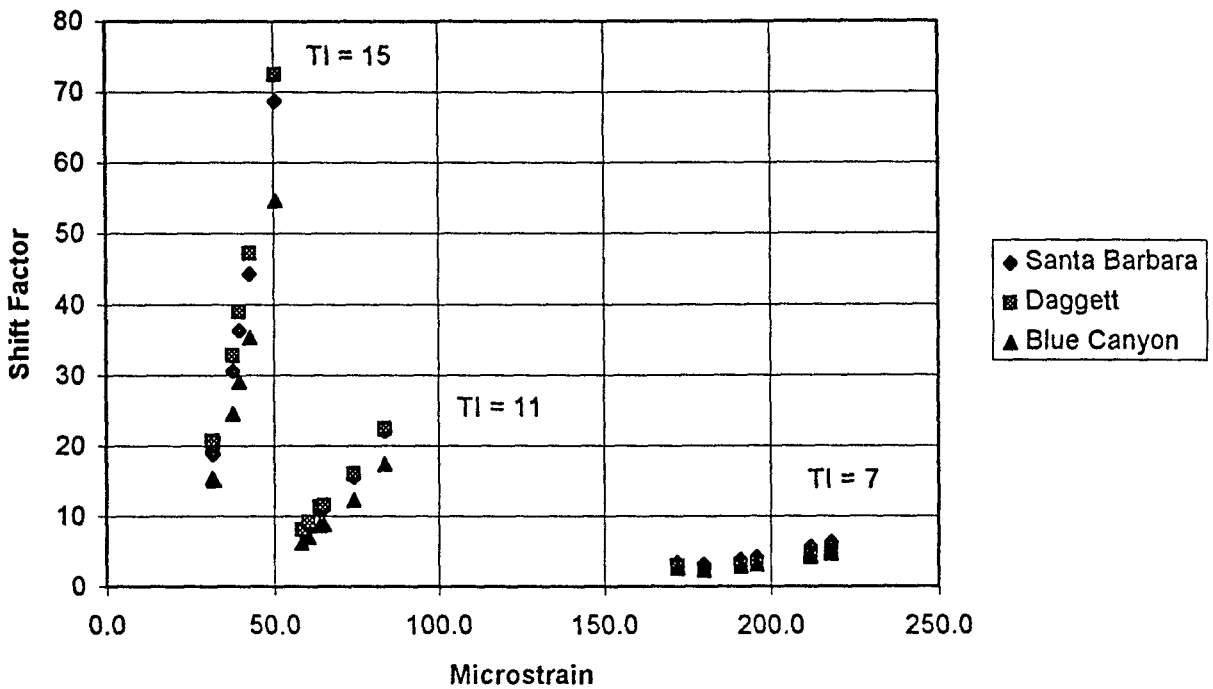

Figure 4.2 Effect of pavement strain and traffic index on shift factor (90-percent reliability)

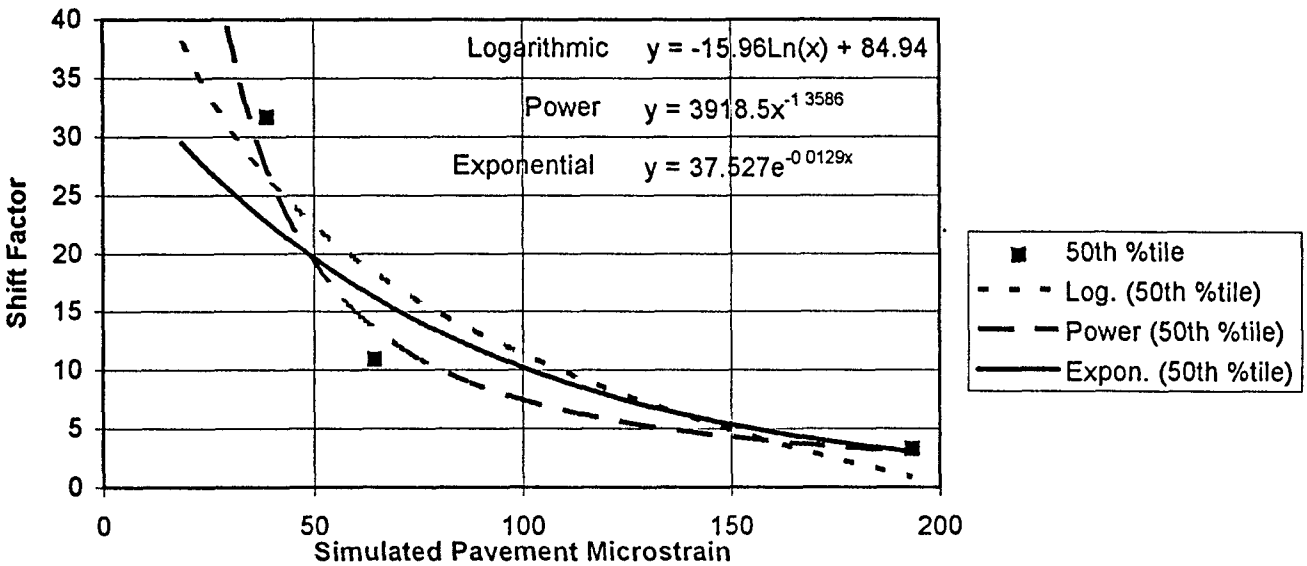

Figure 4.3 Effect of pavement strain on shift factor at 50th-percentile levels

Table 4.1 Location and climatic summary of California sites

Attribute	Site		
	Santa Barbara	Daggett	Blue Canyon
Latitude (°)	34.433	34.867	39.283
Elevation (feet)	3	586	1609
Constant deep ground temperature (F)	62	70	57
Period	1984-1993	1983, 1985-1993	1983-1988
Average minimum daily air temperature (F)	48.8	53.2	43.9
Average maximum daily air temperature (F)	70.7	81.5	58.8
Average daily sunshine (%)	67.9	81.3	65.3
Average daily wind speed (mph)	6.0	11.2	4.3

Note: °C=5/9 (°F-32); 1 mph=1.61 kph

Table 4.2 Selected temperature simulation parameters[9]

Layer	Property	Calibrated Value
Asphalt mixture	Thermal conductivity	0.8 BTU/hr-ft-F (unfrozen, frozen, freezing)
	Heat capacity	0.22 BTU/lb-F (unfrozen and freezing) 1.2 BTU/lb-F (freezing)
	Unit weight	145 pcf
	Water content	2%
Subgrade	Dry density	120 pcf
	Dry heat capacity	0.29 BTU/lb-F
Other	Maximum allowable convection coefficient	3 BTU/hr-ft2-F
	Emissivity factor	0.85
	Absorptivity factor	0.90
	Geiger radiation factor A	0.77
	Geiger radiation factor B	0.28
	Vapor pressure	5 mm mercury
	Cloud base factor for back radiation	0.85

[9]The computer program utilized is based on English units. In addition, the temperature data files used for the temperature simulations are expressed in English units. Hence only these units are reported.

Table 4.3 Simulated temperatures in 202 mm (8 in.) pavement

Depth (inches)	Temperature level (percentile)	Site		
		Santa Barbara	Daggett	Blue Canyon
Surface	Maximum	142.7	151.6	151.5
	98	124.2	138.2	132.6
	95	119.0	131.0	123.2
	90	110.7	120.1	110.6
	50	69.4	75.5	62.9
	10	50.5	47.1	38.5
	5	46.3	42.1	35.0
	2	42.3	37.8	31.6
	Minimum	24.7	19.0	16.7
2	Maximum	127.0	136.6	134.8
	98	111.5	125.6	118.9
	95	107.2	119.8	111.4
	90	100.8	111.2	101.7
	50	71.9	77.6	65.1
	10	53.8	50.5	41.1
	5	50.0	46.0	37.8
	2	46.3	42.2	34.5
	Minimum	34.8	25.7	22.0
4	Maximum	115.4	125.2	122.5
	98	102.6	116.8	109.3
	95	99.2	112.3	103.4
	90	94.4	105.9	96.3
	50	73.6	78.6	66.1
	10	55.9	52.7	42.8
	5	52.5	48.9	39.8
	2	49.1	45.6	36.8
	Minimum	38.3	31.7	26.4
6	Maximum	106.5	116.8	113.6
	98	96.2	110.4	102.4
	95	93.5	107.0	97.9
	90	90.2	102.7	92.9
	50	74.6	79.1	66.6
	10	56.9	54.1	44.0
	5	54.0	51.0	41.3
	2	50.8	48.2	38.6
	Minimum	40.0	36.4	30.2
8	Maximum	99.7	110.9	106.6
	98	91.7	105.9	97.5
	95	89.7	103.4	94.3
	90	87.5	100.7	90.7
	50	75.1	79.2	66.6
	10	57.5	55.0	44.8
	5	54.6	52.5	42.3
	2	51.7	50.1	39.8
	Minimum	41.3	40.2	32.8

Note: °C=5/9 (°F-32)

Table 4.4 Temperature conversion factors and critical temperatures

Thickness of asphalt layer (inches)	Parameter	Site		
		Santa Barbara	Daggett	Blue Canyon
4	TCF (to 19°C)	1.176	0.989	0.883
	Percent of damage in 5°C range about 19°C	16.6	12.8	13.8
	Critical temperature (°C)	27	30	28
	TCF (to critical temperature)	0.655	0.587	0.481
	Percent of damage in 5°C range about critical temperature	34.6	24.4	30.2
8	TCF (to 19°C)	2.392	2.446	1.887
	Percent of damage in 5°C range about 19°C	8.4	5.8	7.3
	Critical temperature (°C)	29	34	30
	TCF (to critical temperature)	0.582	0.546	0.417
	Percent of damage in 5°C range about critical temperature	49.3	32.9	41.4

5.0 Implications for Design and Construction

Explored in this section are possible implications of this project for California design and construction practice. Investigated in order are 1) the consistency over a range in parameters of California structural design practice with respect to fatigue distress; 2) issues related to mix design, construction specifications, and quality assurance; 3) the merits of rich-bottom designs which replace the bottom few inches of the asphalt-concrete surface with a richer and more dense layer; and 4) a mix-design example illustrating use of the UC-Berkeley mix design and analysis system for designing fatigue-resistant mixes.

5.1 Consistency of California Design Practice

Eighteen hypothetical pavements, located in three regions of California and designed using Caltrans procedures, formed the basis for the shift-factor calibrations reported in Section 4.4. The calibration process underscored differences in expected fatigue behavior within a group of pavement sections that had been designed to meet the same specific level of traffic loading by Caltrans procedures. This finding was not unexpected since because the Caltrans design procedure is largely empirical, and no distinction is made among the various forms of pavement distress it considers. At the same time, the UC-Berkeley mix design and analysis system provides the opportunity to examine the consistency of California design practice vis-à-vis the prevention of fatigue distress.

For this analysis, the design reliability was set at 90 percent, and stiffness and laboratory fatigue life were calculated for the Valley asphalt-Watsonville granite mix having 5-percent asphalt and 8-percent air voids. UC-Berkeley ESALs were computed as follows:

$$ESALs = \frac{N \bullet SF}{TCF \bullet M}$$

in which N = the number of laboratory load repetitions to failure under the anticipated in-situ strain level, SF = the shift factor, TCF = the temperature conversion factor, and M = the reliability multiplier. The computation of California design ESALs was based on the traffic index, TI, as follows:

$$ESALs = 1.2895 \bullet 10^{-2}\, TI^{8.2919}$$

Table 5.1 presents results of the calculations. An ESAL ratio much less than one indicates that the UC-Berkeley fatigue life is considerably less than the Caltrans design life and suggests a site-structure combination that appears to be most vulnerable to fatigue distress in situ.

To identify possible patterns of bias, median ESAL ratios were determined for the various levels of each parameter (Table 5.2).[10] Based on this analysis, conditions most vulnerable to fatigue cracking appear to include: 1) designs for a TI of 15, 2) designs incorporating subgrades with R-values of 20, 3) designs for regions of climatic similarity to Santa Barbara, and 4) designs incorporating class B cement-treated base. The relatively low median ratio for R-value 20 subgrades is of particular interest and potential concern. Although the possible significance of these findings is conjectural at the moment, the analysis demonstrates rather conclusively that,

[10]The median ESAL ratio is based on the California design ESALs obtained at a Traffic Index (TI) determined from equation ( ); e.g. for a TI=7, California design ESALs=131,171 (Table 5.1).

even if all Caltrans designs provide adequate fatigue resistance, they vary considerably in the level or extent of that adequacy.

5.2 Mix Design, Construction Specifications, and Quality Assurance

California mix-design and pavement-construction practices have served extremely well for a very long period of time. However, they apparently produce pavement surfaces with relatively small asphalt contents and relatively large air-void contents. Unfortunately, as shown by the test results reported herein, such mixes may have marginal fatigue resistance. Because California design practice doesn't explicitly treat fatigue distress, use of relatively dry, harsh mixes may provide opportunity for the development of premature fatigue cracking. This section briefly focuses on some of the implications of current California design and construction practice.

As explained in Section 1.2.1, field compaction of asphalt concrete is currently specified in terms of relative density, that is, the ratio of in-situ density to the density of laboratory specimens compacted at the design asphalt content. The Triaxial Institute kneading compactor is used for laboratory compaction and typical specifications require a minimum relative compaction of 95 percent. The relative compaction specification allows quite large in-situ air-void contents. For example, even with maximum laboratory compaction (corresponding to the 4.0-percent minimum air-void content allowed by the mix design procedure), the allowable minimum density permits an in-situ air-void content of 8.8 percent. Recent testing at UC-Berkeley of a number of field cores from accepted Caltrans projects reveals air-void contents typically within the range of 6 to 10 percent. Larger values are sometimes obtained when the asphalt content is reduced below that suggested by stabilometer testing.

Stabilometer test results for the Valley asphalt-Watsonville granite mix provide a useful illustration (Figure 5.1). The curves through the data are polynomials established by regression analyses. Two points are significant. First, at the design asphalt content of 4.9 percent (corresponding to a stabilometer value of 35), the air-void content is approximately 5.4 percent. Field compaction meeting the 95-percent relative compaction requirement would produce acceptable mixes with air voids up to about 10 percent, certainly a level sufficiently large for concern about fatigue cracking. Second, these test results demonstrate how, for a given level of compactive effort, the air-void content increases with a decrease in asphalt content. The effect of compaction in the field is similar to that in the laboratory. Thus any reduction in asphalt content, whether by intent or by construction variability, will increase air-void content unless compensated by increasing the compactive effort. Degradation of fatigue performance is the inevitable result.

In addition to mix-design and construction-specification practices, the effect of construction variability is also of interest. To briefly illustrate this effect, attention focused on one of the 18 structures identified in Section 3.0, the pavement section utilizing aggregate base, subjected to a level of traffic represented by a traffic index of 11, and supported on a subgrade having an R-value of 20. Mix-proportion targets were assumed to be 5 percent for both asphalt and air-void contents. In-situ asphalt and air-void contents were assumed to be normally distributed about these targets, and standard deviations were selected to represent ranges reasonably attributable to construction variability. Monte Carlo simulation was used to determine the 10th-percentile fatigue lives resulting from these assumptions.

Without variability, the fatigue life was estimated to be approximately 15,300,000 repetitions (unadjusted by temperature conversion factor, shift factor, etc.). As expected,

construction variability was found to reduce the 10th-percentile life quite significantly for large standard deviations in air-void content (Figure 5.2). Variance in asphalt content was a much less significant factor than variance in air-void content both because asphalt content can be more accurately controlled during construction and because fatigue life is less sensitive to asphalt content than to air-void content.

Conclusions developed from the above discussion and analysis include the following:

1) Specifying in-situ compaction by a relative compaction requirement is an ineffective technique for controlling fatigue distress because it permits relatively large air-void contents that may be detrimental to fatigue performance;
2) In-situ fatigue performance can be quite sensitive to construction variability and, by inference, to the caliber of the quality assurance program; and
3) To minimize the risk of premature failure, mix design should recognize and, if possible, compensate for expected construction practice and conditions such as night and cold weather paving.

These conclusions lead to the following recommendations:

1) Caltrans should consider establishing maximum limits for in-situ air-void contents by changing its construction specifications and/or construction quality assurance procedures;[11]
2) Mix designers should not specify a mix whose fatigue performance could be jeopardized as a result of uncontrollable construction effects. Specifically very

[11]One alternative is to base compaction requirements on a percentage of the actual maximum mix density based on ASTM D) 2041 (the Rice method); for example, many agencies specify a minimum degree of compaction of 92 percent based on ASTM D2041. This results in a maximum air void content of 8 percent at the time of construction.

low design asphalt contents should be avoided or, if that is not possible, layer thickness should be increased as necessary to prevent premature fatigue cracking.

3) Because of the implications of the findings for improved pavement performance, Caltrans should consider further laboratory testing at the Transportation Laboratory and full-scale accelerated pavement testing using the Heavy Vehicle Simulator (HVS) to confirm these findings.

5.3 Rich-Bottom Pavements

From the mix performance evaluation of Section 3.0, it is apparent that decreased air-void content and increased asphalt content result in increased fatigue life. Pavement structural design should take advantage of these properties wherever possible to improve the performance of the pavement. For most pavement structures and typical traffic loads, fatigue cracking is assumed to begin at the bottom of the asphalt concrete layer, where tensile strains are usually largest. Here large asphalt contents and low air-void contents would be most beneficial. The potential for rutting, on the other hand, is usually greatest at the top of the pavement, within 100 mm (4 in.) of its surface (Sousa et al, 1994). Therefore, mixes used near the pavement surface must be more rut resistant, which usually means lower asphalt contents than might be permissible farther from the pavement surface.

As an example of potential improvements in pavement performance that might be obtained by including mix design information in the pavement design process, the fatigue life of pavements with larger asphalt content in the bottom lift was evaluated using the mix fatigue data and pavement structural designs developed as part of this project. The resulting pavement designs were termed "rich-bottom" pavements.

5.3.1 Designs for Rich-Bottom Pavements

The hypothetical pavement structures described earlier served as the basis for evaluating the rich-bottom-pavement concept. However, because they incorporated total asphalt concrete thicknesses less than 150 mm (6 in.), the six structures designed to resist traffic characterized by a traffic index of 7 were not used in the evaluation. Rich-bottom designs were created for the remaining structures by replacing the bottom 50 mm (2 in.) of the asphalt concrete layer with a larger asphalt-content, smaller air-void-content mix of the same thickness. The resulting pavement structural designs are shown in Table 5.3.

Referenced to the original mix, each replacement mix had an asphalt content 0.5 percent larger and an air-void content 3.0 percent smaller. For example, if the original mix had an asphalt content of 5.0 percent and an air-void content of 5.0 percent, the bottom 50 mm of the asphalt concrete layer was changed to have an asphalt content of 5.5 percent and an air-void content of 2.0 percent, while the remainder of the asphalt concrete layer remained unchanged. For this reason, besides being restricted to pavement designs for traffic index 11 and 15, upper layer asphalt contents of 6.0 percent and air-void contents of 2 percent were not included in the analysis.

5.3.2 Predicted Performance of Rich-Bottom Versus Conventional Structures

The same procedure used to calculate fatigue performance for conventional pavement designs was also used for the rich-bottom pavements, except for the following:

1) The fatigue life of both asphalt concrete layers was calculated using the maximum tensile strain at the bottom of each layer, and
2) The smaller of the two calculated fatigue lives was selected as the critical value for the pavement structure.

This analysis also differed from that of Section 3.0 in that measured cell averages were used to represent mix stiffness and fatigue life rather than estimates from the regression models of Table 3.4.

The critical fatigue life in the rich-bottom pavements is plotted versus the fatigue life of the conventional structures in Figures 5.3 and 5.4, for pavement structures designed for traffic indexes of 11 and 15, respectively. The plotted values are based on laboratory measurements of fatigue life, without the application of temperature conversion factors, reliability multipliers, or shift factors. The increased fatigue life of the rich-bottom pavements is readily apparent from these figures. In many cases the increase is quite large, approximating an order-of-magnitude improvement.

These computations not only underscore the possible merit of rich-bottom designs, but they also illustrate the potential for including mix design information in pavement structural design decisions. This potential can be realized by implementation of the A-003A fatigue testing and analysis procedures used for this project. These procedures can provide information necessary to move forward with the concept of decreasing construction air-void contents and increasing asphalt contents near the bottom of thick asphalt concrete layers.

The associated procedures that would provide added potential for increased pavement performance by allowing safe increases in asphalt contents and decreased air-void contents are those developed by SHRP A-003A for evaluating the rutting potential of the mixes. However, at the present time implementation of the SHRP A-003A fatigue procedures with continued use of the Hveem stabilometer to evaluate rutting potential for conventional binder mixes still has the potential to provide significant improvements in California pavement performance.

5.4 Mix-Design Example

Described in this section is an example illustration of the use of the fatigue mix design and analysis system. For this example, a new highway is being constructed, and its pavement must accommodate 9,000,000 ESALs in the design lane during the design period. Climatic conditions at the site are considered to be similar to those at Blue Canyon. Because of the importance of this facility and the difficulty of maintaining traffic operations during resurfacing, a mix-design reliability of 95 percent has been targeted. A trial mix, consisting of Valley asphalt and Watsonville-granite aggregate, has been selected. The asphalt content has been set at 4.5 percent: to reduce the likelihood of rutting distress, it cannot be increased. The in-situ air-void content achieved by normal construction techniques is expected to be 8 percent.

To ascertain whether this mix will provide adequate resistance against fatigue cracking, flexural-beam fatigue tests were performed. Six specimens were tested, three at each of two strain levels. The average initial stiffness was determined to be 6.84 GPa (992,500 psi), and the fatigue life-strain relationship, depicted in Figure 5.5, was quantified by regression analysis. The pavement structural design thicknesses and elastic parameters are as follows:

Layer	Thickness (in)	Modulus (psi)	Poisson's ratio
Surface	9.5	992,500	0.40
Class 2 aggregate base	6.0	25,000	0.45
Subbase	8.4	20,000	0.45
Subgrade		12,200	0.50

The pavement section was selected using NEWCOM 90 for an R value=20 for the subgrade.

Computations, summarized in Table 5.4, revealed that, in this application, the trial mix could withstand approximately 3,000,000 ESALs at 95-percent reliability. Because design ESALs totalled 9,000,000, adjustment was necessary. Although available options included the use of asphalt modifiers and, indeed, the use of entirely different asphalts and aggregates, interest focused on determining the effect of increasing the asphalt-concrete thickness or using a rich-bottom design instead. Examining the effects of less reliable designs was also of interest.

In the rich-bottom design, the bottom two inches of asphalt concrete were replaced with an enriched (5-percent asphalt), well compacted (5-percent air voids) mix. In determining properties of this mix, laboratory test data were assumed to be unavailable. Instead estimates were made based on the regression equations of Section 3.1. Enriching and densifying the mix was estimated to increase its stiffness by a factor of approximately 1.15 and to increase its fatigue life by a factor of approximately 2.18.

Results of the extended analyses are summarized on Figures 5.6 and 5.7. Figure 5.6 shows that the 9.5-inch surface thickness remains inadequate for 9,000,000 ESALs even at reliabilities below 80 percent. To preserve the desired 95-percent reliability, the surface thickness must be increased from 9.5 to 11.5 inches. Another alternative, the rich-bottom design, nicely accommodates approximately 9,000,000 ESALs with the original 9.5-inch surface thickness. Economics, feasibility, and engineering judgement would, of course, dictate the final design choice.

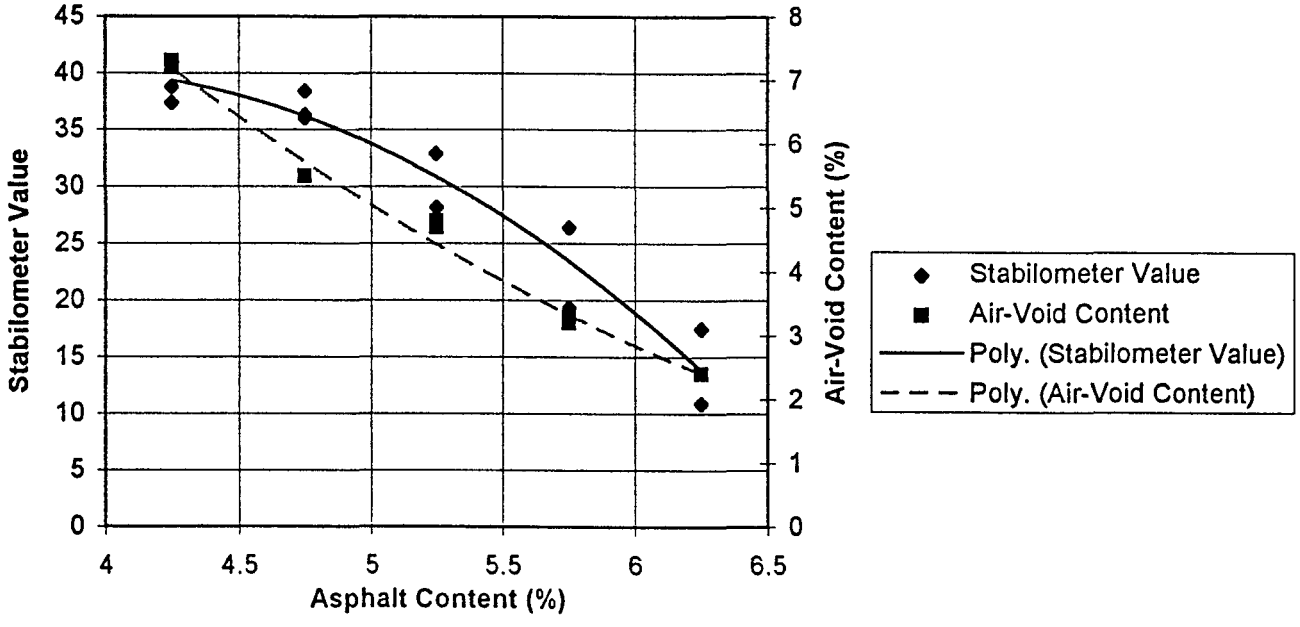

Figure 5.1 Stabilometer test results for the Valley asphalt-Watsonville granite mix

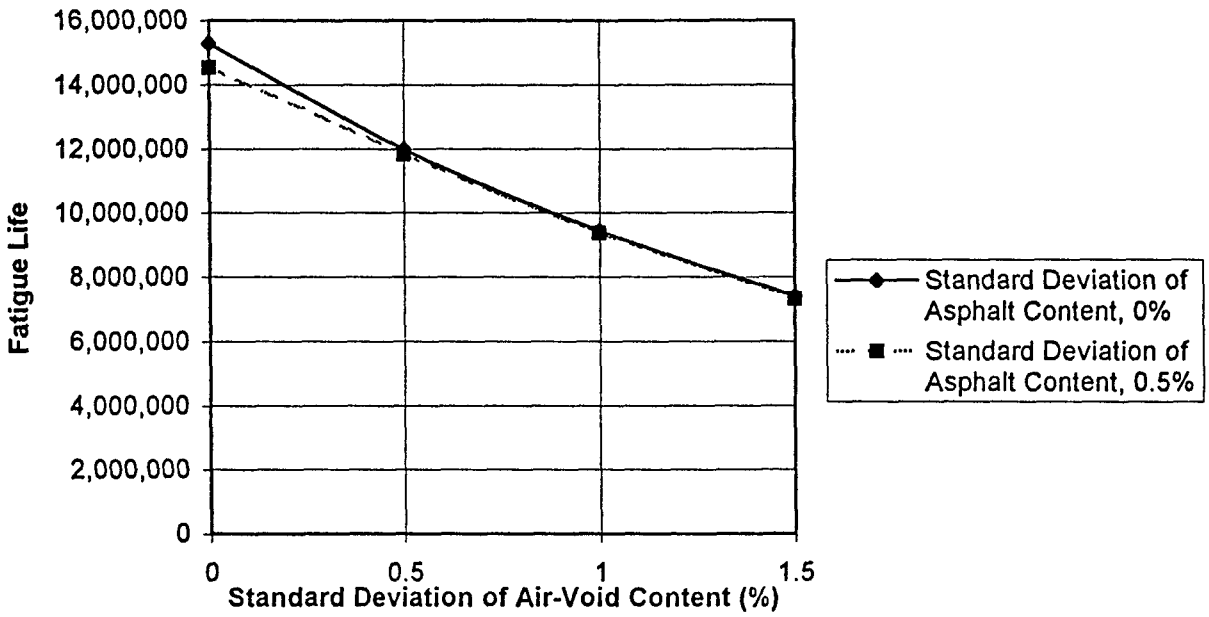

Figure 5.2 Illustrative effect of construction variability on fatigue life

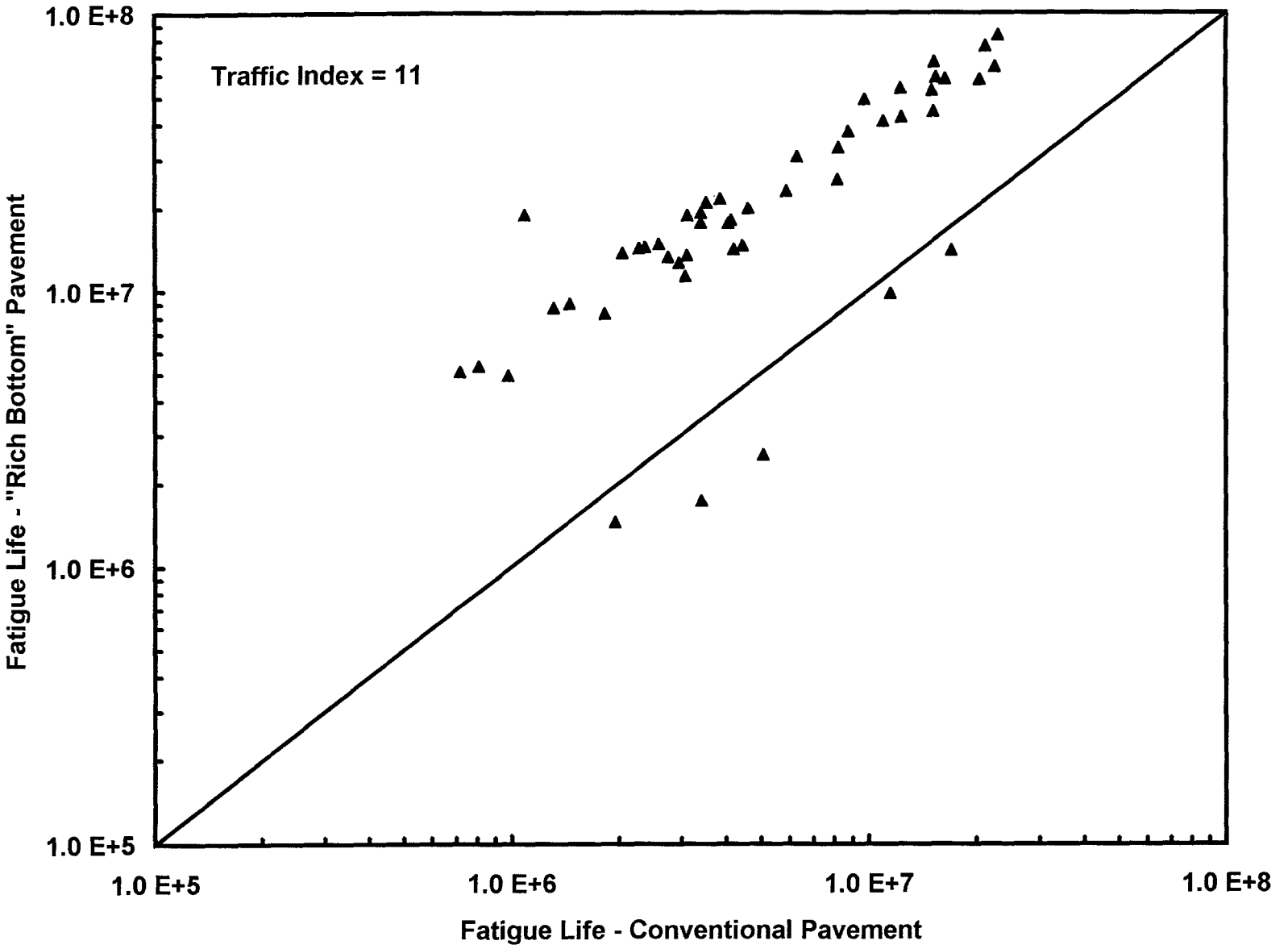

Figure 5.3 Fatigue-life improvement resulting from rich-bottom designs (TI of 11)

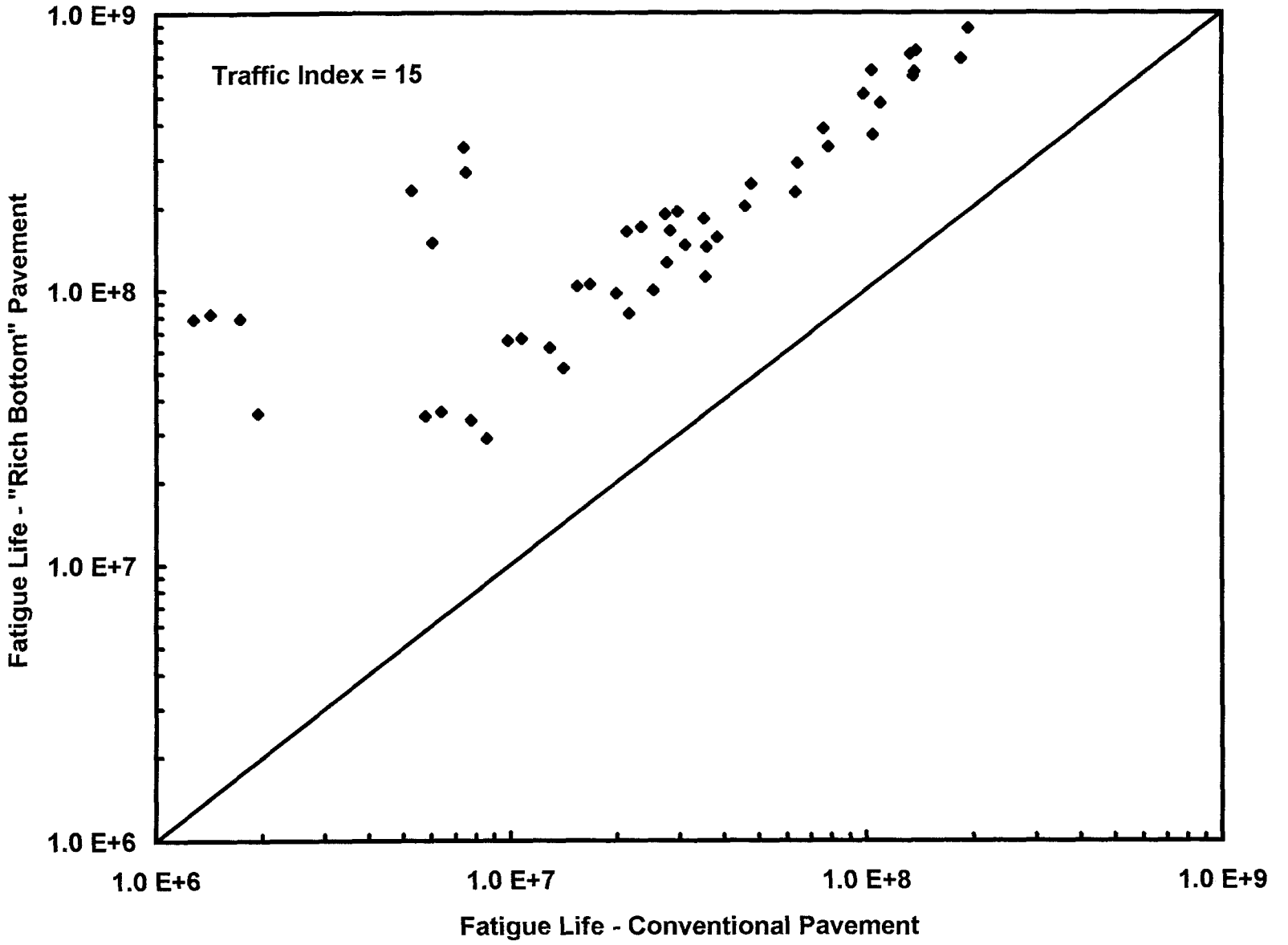

Figure 5.4 Fatigue-life improvement resulting from rich-bottom designs (TI of 15)

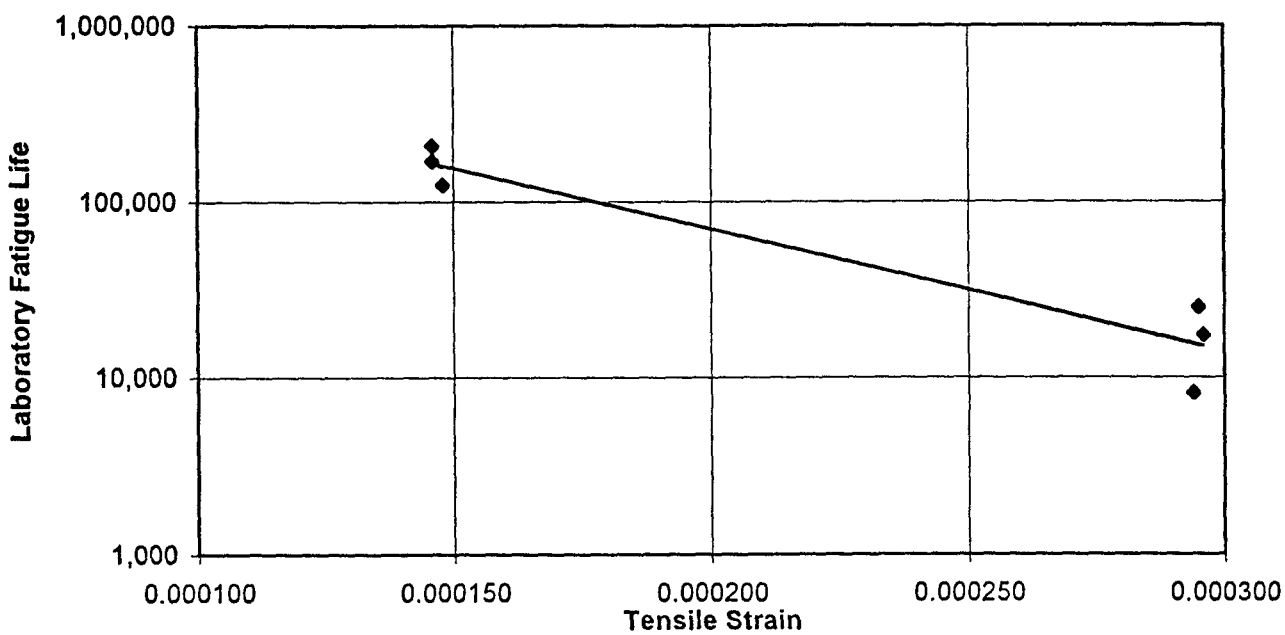

Figure 5.5 Laboratory N-ϵ relationship for mix with 4.5-percent asphalt and 8-percent air voids

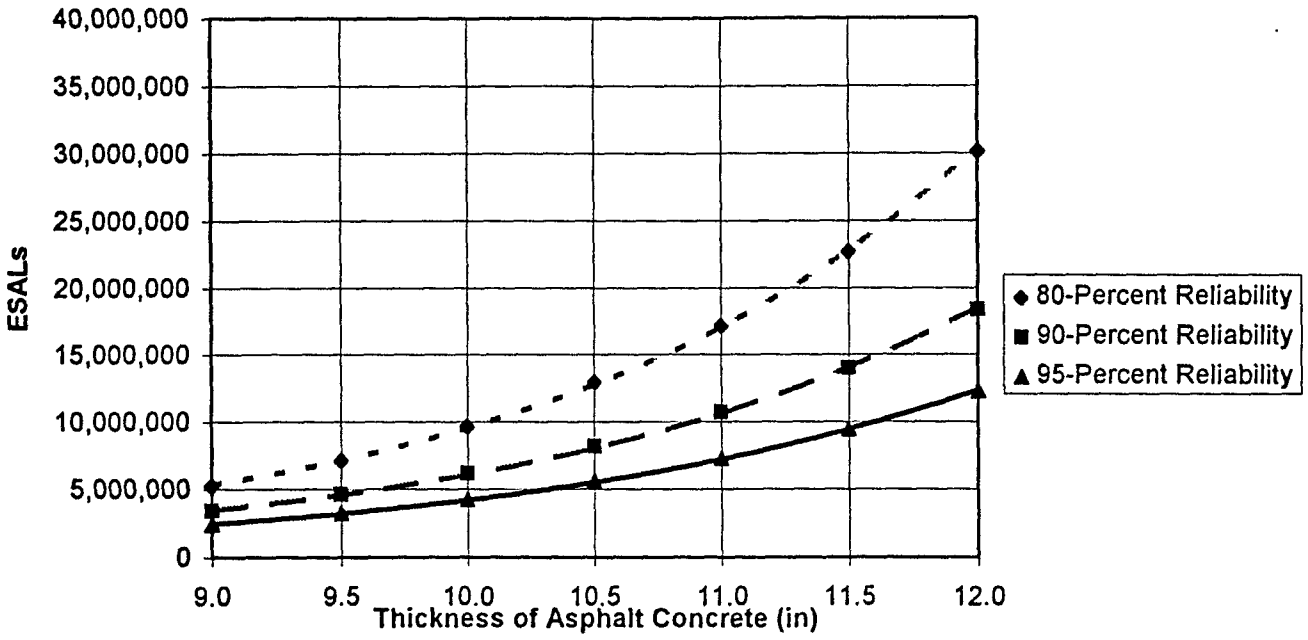

1 in. =25.4 mm

Figure 5.6 Effect of surface thickness and design reliability on in-situ traffic resistance (conventional pavement)

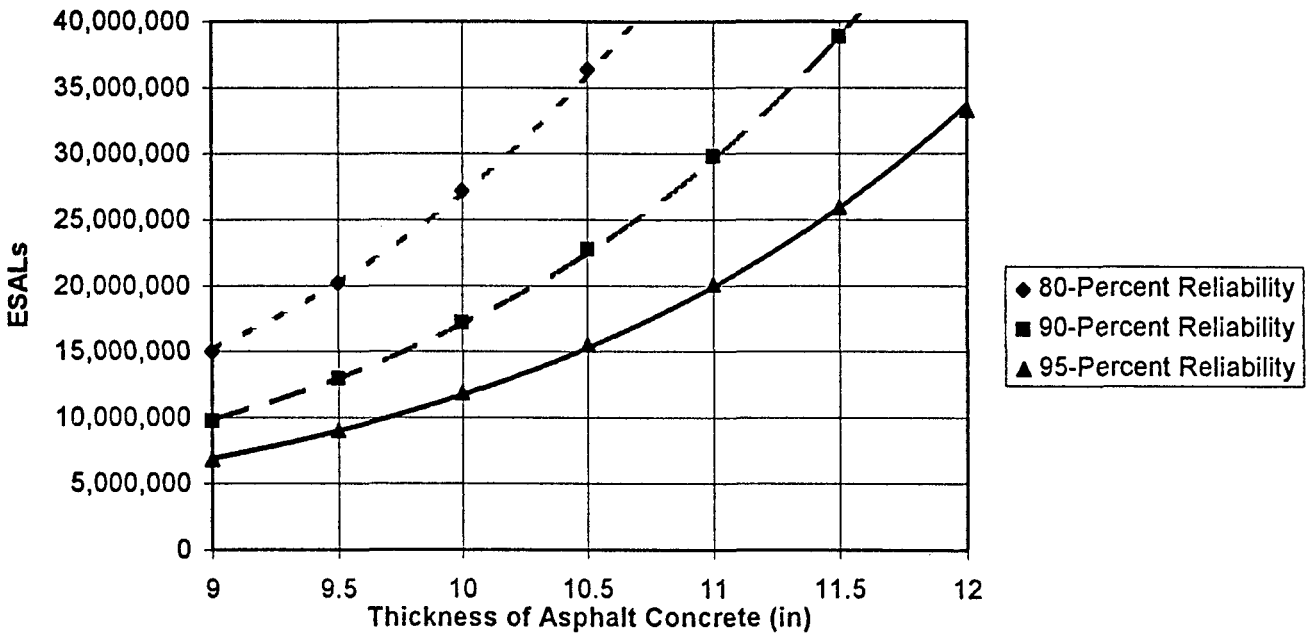

1 in. =25.4 mm

Figure 5.7 Effect of surface thickness and design reliability on in-situ traffic resistance (rich-bottom pavement)

Table 5.1 Comparison of design ESALs (UC-Berkeley fatigue vs. Caltrans)

Traffic index	Base type	Subgrade R-value	Caltrans ESALs	ESAL ratio (UC-Berkeley fatigue system to Caltrans design system)		
				Santa Barbara	Daggett	Blue Canyon
7	ctb	5	131,171	0.72	0.93	0.97
	ctb	20	131,171	0.82	1.05	1.11
	ctb	40	131,171	1.10	1.42	1.49
	ab	5	131,171	0.42	0.54	0.57
	ab	20	131,171	0.48	0.62	0.65
	ab	40	131,171	1.08	1.25	1.43
11	ctb	5	5,565,306	0.43	0.42	0.55
	ctb	20	5,565,306	0.72	0.70	0.91
	ctb	40	5,565,306	2.01	1.92	2.53
	ab	5	5,565,306	1.28	1.22	1.61
	ab	20	5,565,306	1.22	1.17	1.53
	ab	40	5,565,306	1.69	1.62	2.13
15	ctb	5	72,843,811	0.73	0.68	0.91
	ctb	20	72,843,811	0.28	0.26	0.35
	ctb	40	72,843,811	1.89	1.76	2.36
	ab	5	72,843,811	1.89	1.74	2.35
	ab	20	72,843,811	0.54	0.50	0.67
	ab	40	72,843,811	0.92	0.86	1.15

Table 5.2 Effect of study parameters on median ESAL ratio

Parameter	Value	Median ESAL ratio	Parameter	Value	Median ESAL ratio
	7	0.95		Santa Barbara	0.87
	11	1.25		Daggett	0.99
Traffic index	15	0.88	Location	Blue Canyon	1.13
	5	0.82		Aggregate	1.17
	20	0.69	Base type	Cement treated	0.91
Subgrade R-value	40	1.56			

Table 5.3 Characteristics of rich-bottom pavement structures

			Class B cement-treated base					Class 2 aggregate base				
Traffic	Subgrade	Layer	Thickness		Stiffness		Poisson's	Thickness		Stiffness		Poisson's
Index	R-value		mm	in.	MPa	psi	Ratio	mm	in.	MPa	psi	Ratio
11	5	Surface1	147	5.8	Varies	Varies	0.40	208	8.2	Varies	Varies	0.40
		Surface2	50.8	2.0	Varies	Varies	0.40	50.8	2.0	Varies	Varies	0.40
		Base	198	7.8	220	32,000	0.30	152	6.0	172	25,000	0.45
		Subbase	427	16.8	138	20,000	0.45	335	13.2	138	20,000	0.45
		Subgrade			26.5	3,850	0.50			26.5	3,850	0.50
	20	Surface1	163	6.4	Varies	Varies	0.40	193	7.6	Varies	Varies	0.40
		Surface2	50.8	2.0	Varies	Varies	0.40	50.8	2.0	Varies	Varies	0.40
		Base	168	6.6	220	32,000	0.30	152	6.0	172	25,000	0.45
		Subbase	259	10.2	138	20,000	0.45	213	8.4	138	20,000	0.45
		Subgrade			84	12,200	0.50			84	12,200	0.50
	40	Surface1	193	7.6	Varies	Varies	0.40	193	7.6	Varies	Varies	0.40
		Surface2	50.8	2.0	Varies	Varies	0.40	50.8	2.0	Varies	Varies	0.40
		Base	152	6.0	220	32,000	0.30	152	6.0	172	25,000	0.45
		Subbase										
		Subgrade			161	23,400	0.50			161	23,400	0.50
15	5	Surface1	300	11.8	Varies	Varies	0.40	361	14.2	Varies	Varies	0.40
		Surface2	50.8	2.0	Varies	Varies	0.40	50.8	2.0	Varies	Varies	0.40
		Base	152	6.0	172	25,000	0.30	152	6.0	138	20,000	0.45
		Subbase	549	21.6	138	20,000	0.45	442	17.4	138	20,000	0.45
		Subgrade			26.5	3,850	0.50			26.5	3,850	0.50
	20	Surface1	224	8.8	Varies	Varies	0.40	269	10.6	Varies	Varies	0.40
		Surface2	50.8	2.0	Varies	Varies	0.40	50.8	2.0	Varies	Varies	0.40
		Base	259	10.2	220	32,000	0.30	183	7.2	138	20,000	0.45
		Subbase	381	15.0	138	20,000	0.45	381	15.0	138	20,000	0.45
		Subgrade			84	12,200	0.50			84	12,200	0.50
	40	Surface1	315	12.4	Varies	Varies	0.40	284	11.2	Varies	Varies	0.40
		Surface2	50.8	2.0	Varies	Varies	0.40	50.8	2.0	Varies	Varies	0.40
		Base	152	6.0	172	25,000	0.30	152	6.0	138	20,000	0.45
		Subbase						107	4.2	138	20,000	0.45
		Subgrade			161	23,400	0.50			161	23,400	0.50

Table 5.4 Summary of parameter calculations in mix-design example.

Parameter	Source	Notes
ESALs	$\frac{N \bullet SF}{TCF \bullet M}$	
N	$1.364 \bullet 10^{-8} e^{-3.412\varepsilon}$	Calibration from laboratory testing
ε	**ELSYM5**	
SF	$2.7639 \bullet 10^{-5} \varepsilon^{-1.3586}$	
TCF	$1.448 \ln(d) - 1.125$	Blue Canyon calibration, d = thickness of asphalt concrete in inches
M	$e^{Z\sqrt{var(\ln N) + 0.3}}$	Z = 0.841, 1.28, and 1.64 for reliabilities of 80, 90, and 95 percent, respectively
var(ln N)	$0.220\left(1 + \frac{1}{n} + \frac{(X - \bar{x})^2}{q\sum(x_p - \bar{x})^2}\right)$	n = 6, q = 3, x_1 = ln(0.000150), x_2 = ln(0.000300)

6.0 Summary, Conclusions, and Recommendations

This project has examined the influence of mix proportions, specifically asphalt and air-void contents, on fatigue behavior both in the laboratory and in situ. It has refined and recalibrated a mix design and analysis system capable of quickly and easily determining the likely fatigue endurance of design mixes in specific pavement structures, at specific locations, and under anticipated traffic loading. Finally, it has explored ways for improving the fatigue performance of asphalt concrete pavements in California. Specific findings and recommendations are as follows:

1. For controlled-strain testing, an increase in asphalt content results in an increase in laboratory fatigue life and a decrease in mix stiffness.
2. For controlled-strain testing, an increase in air-void content results in a decrease in laboratory fatigue life and a decrease in mix stiffness.
3. For the materials tested, the effects of asphalt and air-void contents on laboratory fatigue performance can be modeled as follows:

$$N = 2.2953*10^{-10}\, e^{0.594AC-0.164AV}\varepsilon_t^{-3.730} \qquad (R^2=0.916) \quad (3.3)$$

and

$$S_o\ (\text{MPa}) = 4.5524*10^{5}\, e^{-0.171AC-0.076AV} \qquad (R^2=0.685) \quad (3.4)$$

Main effects in these models are statistically significant at a level of significance in excess of 99 percent. Interactive effects of the independent variables are not included in the models because they are not statistically significant.

4. Voids filled with bitumen apparently captures some, but not all, of the effects of asphalt and air-void contents on fatigue life. An increase in voids filled with bitumen results in an increase in laboratory fatigue life which can be modelled as follows:

$$N=7.9442*10^{-11}\ e^{0.044VFB}\varepsilon_t^{-3.742} \qquad (R^2=0.875) \quad (3.5)$$

The advantage of including voids filled with bitumen in comprehensive fatigue models is that, unlike asphalt and air-void contents, voids filled with bitumen is not highly correlated with flexural stiffness. Because of this relatively weak correlation, both variables can be simultaneously incorporated into fatigue models as indicated below:

$$N=2.5875*10^{-8}\ e^{0.053VFB}S_o^{-0.726}\varepsilon_t^{-3.761} \qquad (R^2=0.885) \quad (3.6)$$

Such a model is one of the more promising types for generally describing the effects on fatigue life of a wide range of mixture characteristics, including not only asphalt and air-void contents but also asphalt type and possibly aggregate type and gradation as well. At the same time, users of such models must recognize the imprecision with which they capture mix-proportion effects and must not use them for detailed mix-design purposes.

5. Because asphalt and air-void contents affect not only fatigue life but also mixture stiffness, simulation is required to estimate their effects on in-situ pavement performance. Simulation of the performance of a variety of pavement structures (compatible with current California design practice) and a variety of traffic loads demonstrates that fatigue performance is maximized by providing the maximum feasible asphalt content and the minimum feasible air-void content.

6. The basic effects of asphalt and air-void contents on laboratory fatigue life and stiffness are not affected by long-term aging. Nevertheless, long-term aging increases mix stiffness but has little, if any, effect on laboratory fatigue life. Limited in-situ simulations

suggest that long-term aging may benefit pavement fatigue performance slightly but only as a result of increases in mix stiffness. Conditioning laboratory fatigue specimens by long-term oven aging does not appear to be necessary for purposes of mix design and analysis. These findings of the effects of long-term aging are tentative pending completion of testing and analysis--currently underway--of a second, more aging-susceptible mix.

7. For given mixture constituents, maximum asphalt content and minimum air-void content are limited not only by economics but also by other distress mechanisms, specifically pavement rutting, instability, and bleeding. Fatigue analysis is necessary to assure that the mixture will perform satisfactorily at these limits or, if not, to design a better performing alternative. Flexural beam testing and related analysis provide a powerful, easy-to-use, and efficient tool for evaluating fatigue life and stiffness.
8. Another important consideration in mixture design is construction control. With respect to fatigue performance, accurate control of air-void content is more important than accurate control of asphalt content. For example, a mixture targeted at 5-percent asphalt and 5-percent air voids will suffer a 30-percent reduction in fatigue life if the air-void content exceeds its target by 1 percent but only a 12-percent reduction if the asphalt content is shy of its target by 1 percent. Complicating this matter, however, is the likelihood that smaller-than-specified asphalt contents will result in increased air-void contents.

The findings and developments of this project offer considerable potential for enhancing the fatigue performance of California pavements. Specific recommendations include the following:

1. For mixes for new and overlay pavement designs:

a. Use the mix design and analysis system on a trial basis;

b. Avoid specifying very low design asphalt contents or, if that is not possible, compensate by increasing layer thickness as necessary to prevent premature fatigue cracking;

c. Evaluate the current structural design system to identify any conditions for which typical California mixes might be particularly susceptible to fatigue distress; and

d. Explore means for more closely integrating the processes of mix design with those of structural design.

2. Relative to construction:

a. Consider establishing maximum limits for in-situ air-void contents by changing construction specifications and/or construction quality assurance procedures;

b. Consider construction and evaluation of one or more experimental rich-bottom pavement sections. The use of accelerated pavement testing with the Heavy Vehicle Simulator provides an excellent opportunity to evaluate this recommendation.

7.0 References

Bell, C. and D. Sosnovske (1994), "Aging: Binder Validation," Strategic Highway Research Program Report No. SHRP-A-384, National Research Council, Washington, D.C.

Bell, C., A. Wieder, and M. Fellin (1994), "Laboratory Aging of Asphalt-Aggregate Mixtures: Field Validation," Strategic Highway Research Program Report No. SHRP-A-390, National Research Council, Washington, D.C.

California Department of Transportation (1994), Standard Specifications, Sacramento, California.

Christenson, D. and D. Anderson (1992), "Interpretation of Dynamic Mechanical Analysis Test Data for Paving Grade Asphalt Cements," Journal of the Association of Asphalt Paving Technologists, Volume 61, pp. 67-116.

Deacon, J. (1965), "Fatigue of Asphalt Concrete," Graduate Report, Institute of Transportation and Traffic Engineering, University of California, Berkeley.

Deacon, J., J. Coplantz, A. Tayebali, and C. Monismith (1994a), "Temperature Considerations in Asphalt-Aggregate Mixture Analysis and Design," Transportation Research Record 1454, Transportation Research Board, pp. 97-112.

Deacon, J., A. Tayebali, J. Coplantz, F. Finn, and C. Monismith (1994b), "Fatigue Response of Asphalt-Aggregate Mixes, Part III - Mix Design and Analysis," Strategic Highway Research Program Report No. SHRP-A-404, National Research Council, Washington, D.C.

Del Valle, H. (1985), "Procedure - Bulk Specific Gravity of Compacted Bituminous Mixtures Using Parafilm-Coated Specimens," Chevron Research Company, Richmond, California.

Dell, P.S., Discussion of paper by Lister and Powell in Proceedings The Association of Asphalt Paving Technologists, Vol. 44, 1975, pp. 111-114.

Dempsey, B., W. Herlache, and A. Patel (1985), "Volume 3. Environmental Effects on Pavements - Theory Manual," FHWA/RD-84/115, University of Illinois at Urbana-Champaign.

Epps, J. (1969), "Influence of Mixture Variables on the Flexural and Tensile Properties of Asphalt Concrete," Graduate Report, Institute of Transportation and Traffic Engineering, University of California, Berkeley.

Folliard, K. and D. Trejo (1991), "An Experimental Study of the SHRP Aggregates," CE 299 report prepared for Prof. Carl Monismith, Department of Civil Engineering, University of California, Berkeley.

Harvey, J. (1991), "University of California - Berkeley SHRP A-003A Asphalt Concrete Specimen Preparation Manual, Version 3.0," SHRP Technical Memorandum No. TM-UCB-A-003A-91-2, Berkeley.

Harvey, J. (1992), "Mix Design Compaction Procedures for Hot-Mix Asphalt Concrete and Rubber-Modified Asphalt Concrete Mixtures," Doctoral Thesis, Graduate Division, University of California at Berkeley.

Harvey, J. and C. Monismith (1994), "Effects of Laboratory Asphalt Concrete Specimen Preparation Variables on Fatigue and Permanent Deformation Test Results Using SHRP A-003A Testing Equipment," Transportation Research Record 1417, Transportation Research Board, pp 38-48.

Harvey, J., C. Monismith, and J. Sousa (1994), "A Comparison of Field and Laboratory Compacted Asphalt-Rubber, SMA, Recycled and Conventional Asphalt Concrete Mixes Using SHRP A-003A Equipment," Journal of the Association of Asphalt Paving Technologists, vol 63, pp 511-560.

Harvey, J., T. Mills, C. Scheffy, J. Sousa, and C. Monismith (1994), "An Evaluation of Several Asphalt Concrete Specimen Air-Void Content Measurement Techniques," Journal of Testing and Evaluation, JTEVA, Vol. 22, No. 5, September, pp. 424-430.

Herlache, W., A. Patel, and B. Dempsey (1985), "The Climatic-Materials-Structural Pavement Analysis Program User's Manual," FHWA/RD-86/085, University of Illinois at Urbana-Champaign.

Kallas, B.F. and J.F. Shook (1977)
San Diego County Experimental Base Project - Final Report
Research Report 77-1 (RR-77-1), The Asphalt Institute, College Park, Maryland.

Lister, N.W. and W.D. Powell, AThe Compaction of Bituminous Base and Base Coarse Materials and its Relation to Pavement Performance,@ Proceedings, The Association of Asphalt Paving Technologists, Vol. 44, 1975, pp. 75-118.

Lytton, R., D. Pufahl, C. Michalak, H. Liang, and B. Dempsey (1990), "An Integrated Model of the Climatic Effects in Pavements," FHWA-RD-90-33, Federal Highway Administration, Washington, D.C.

McGennis, R., R. Anderson, T Kennedy, and M. Solaimanian (1994), "SUPERPAVE™ Asphalt Mixture Design and Analysis," National Asphalt Training Center Demonstration Project 101, Federal Highway Administration Office of Technology Applications, Washington, D.C. and the Asphalt Institute, Lexington, Kentucky.

Paangchit, P., R.G. Hicks, J.E. Wilson, and C.A. Bell, Impact of Variation in Material Properties on Asphalt Pavement Life, Final Report, FHWA-OR-82-3 to Oregon DOT; Oregon State University, Corvallis, OR, May 1982, 152 pp.

Shatnawi, S., M. Nagarajaiah, and J. Harvey (1995), "Moisture Sensitivity Evaluation of Binder-Aggregate Mixtures," Paper presented and accepted for publication by the Transportation Research Board, Washington, D.C.

Sousa, J. B., J. A. Deacon, S. Weissman, J. T. Harvey, C. L. Monismith, R. B. Leahy, G. Paulsen, J. S. Coplantz. *Permanent Deformation Response of Asphalt-Aggregate Mixes*, Report No. SHRP-A-414. Strategic Highway Research Program, National Research Council, Washington, D.C., 1994.

Tayebali, A., J. Deacon, J. Coplantz, F. Finn, and C. Monismith (1994a), "Fatigue Response of Asphalt-Aggregate Mixes, Part II - Extended Test Program," Strategic Highway Research Program Report No. SHRP-A-404, National Research Council, Washington, D.C.

Tayebali, A., J. Deacon, J. Coplantz, J. Harvey, and C. Monismith (1994b), "Fatigue Response of Asphalt-Aggregate Mixes, Part I - Test Method Selection, " Strategic Highway Research Program Report No. SHRP-A-404, National Research Council, Washington, D.C.

Tayebali, A., J. Deacon, J. Coplantz, J. Harvey, and C. Monismith (1994c), "Mixture and Mode of Loading Effects on Fatigue Response of Asphalt-Aggregate Mixtures," Journal of the Association of Asphalt Paving Technologists, Volume 63, pp. 118-151.

Tsai, B. and A. Tayebali (1992), "Computer Software for Fatigue Test Data Analysis for SHRP Project A-003A," Prepared for SHRP Project A-003A, Institute of Transportation Studies, University of California, Berkeley.

Appendix A - Method of Test for Flexural Fatigue

Standard Method of Test for

Determining the Fatigue Life of Compacted Bituminous Mixtures Subjected to Repeated Flexural Bending

SHRP Designation: M-009[1]

1. SCOPE

1.1 This method determines the fatigue life and fatigue energy of a bituminous mixture beam specimen subjected to repeated flexural bending until failure. The failure point is defined as the load cycle at which the specimen exhibits a 50% reduction in stiffness relative to the initial stiffness.

1.2 The values stated in SI units are to be regarded as the standard.

1.3 *This standard may involve hazardous materials, operations and equipment. This standard does not purport to address all of the safety problems associated with its use. It is the responsibility of the user of this standard to establish appropriate safety and health practices and determine the applicability of regulatory limitations prior to use.*

2. APPARATUS

2.1 *Test System*—The test system shall be capable of providing repeated sinusoidal loading at a frequency of between 5 and 10 Hz. The specimen shall be subjected to 4-point bending with free rotation and horizontal translation at all load and reaction points. Figure 1 illustrates the loading conditions. The specimen shall be forced back to its original position (i.e., zero deflection) at the end of each load pulse. The test system or surrounding environment shall maintain the specimen at 20°C during testing.

The test system shall be a closed-loop, computer-controlled system that, during each load cycle, measures the deflection of the beam specimen, computes the strain in the specimen, and adjusts the load such that the specimen experiences a constant level of strain on each load cycle. The test system should record load cycles, the applied load and beam deflection, and compute the maximum tensile stress, maximum tensile strain, phase angle, stiffness, dissipated energy, and cumulative dissipated energy at load cycle intervals specified by the user.

---

[1]This standard is based on SHRP Product 1019.

As a minimum, the test system should meet the following requirements:

Load Measurement and Control

Range: ± 4.5 kN
Resolution: 0.002 kN
Accuracy: ±0.004 kN

Displacement Measurement and Control

Range: ± 5.0 mm
Resolution: 0.00254 mm
Accuracy: ± 0.005 mm

Frequency Measurement and Control

Range: 5 to 10 Hz
Resolution: 0.005 Hz
Accuracy: 0.01 Hz

Temperature Measurement and Control

Resolution: 0.25°C
Accuracy: ± 0.5°C

2.2 *Miscellaneous Apparatus:*

- epoxy for attaching nut to specimen
- screw, nut, block assembly for referencing LVDT to neutral axis of specimen
- jig for setting proper clamp spacing

3. TEST SPECIMENS

3.1 *Compacted Bituminous Concrete Specimens*—Specimens shall be sawn on all sides with a diamond blade from a slab or beam of bituminous mixture prepared by kneading compaction or rolling wheel compaction. Specimens shall be 381 ± 6.35 mm in length, 50.8 ± 6.35 mm in height and 63.5 ± 6.35 mm in width.

3.2 *Measurement of Specimen Size*—Measure the height and width of the specimen at three different points along the middle 90 mm of the specimen length. Report measurements to the nearest 0.025 mm. Average the three measurements for each dimension and report the averages to the nearest 0.25 mm.

3.3 *Epoxy Nut to Neutral Axis of Specimen*—Figure 2 illustrates a nut epoxied to the neutral axis of the specimen. Locate the center of a specimen side. Apply epoxy in a circle around this center point and place the nut on the epoxy such that the center of the nut is over the center point. Avoid applying epoxy such that it fills the center of the nut. Allow the epoxy to harden before moving the specimen.

4. TEST PROCEDURE

4.1 *Stabilize Specimen to Test Temperature*—If the ambient temperature is not 20°C, place the specimen in an environment which is at 20 ± 1°C for 2 hours to ensure the specimen is at the test temperature prior to beginning the test.

4.2 *Specimen Setup*—Refer to figures 3 and 4.

The clamps should be open to allow the specimen to be slid into position. The jig is used to ensure proper horizontal spacing of the clamps: 119 mm center-to-center. Once the specimen and clamps are in the proper positions, close the outside clamps by applying sufficient pressure to hold the specimen in place. Next, close the inside clamps by applying sufficient pressure to hold the specimen in place.

Figure 4 illustrates the connection of the screw/nut/block assembly and the LVDT such that beam deflections at the neutral axis will be measured. Attach the LVDT block to the specimen by screwing the screw into the nut epoxied to the specimen. The LVDT probe should rest on top of the block and the LVDT should be positioned and secured within its clamp so its reading is as close to zero as possible.

4.3 *Test Parameter Selection*—The operator selects the following test parameters and enters them into the automated test program: deflection level, loading frequency and load cycle intervals at which test results are recorded and computed by the computer. The deflection level depends on the strain level desired. The loading frequency should be between 5 and 10 Hz. The selection of load cycle intervals at which test results are computed and recorded is limited by the amount of memory available for storing data.

4.4 *Estimation of Initial Stiffness*—Apply 50 load cycles at a constant strain of 100–300 micro-in/in. Determine the specimen stiffness at the 50th load cycle. This stiffness is an estimate of the initial stiffness which will be used as a reference for determining specimen failure.

4.5 *Selection of Strain Level*—The selected deflection level should correspond to a strain level such that the specimen will undergo a minimum of 10,000 load cycles before its stiffness is reduced to 50% or less of the initial stiffness. A stiffness reduction of 50% or more represents specimen failure. A minimum of 10,000 load cycles ensures the specimen does not decrease in stiffness too rapidly.

4.6 *Testing*—After selecting the appropriate test parameters, begin the test. Monitor and record (*if not automated*) the test results at the selected load cycle intervals to ensure the

system is operating properly. When the specimen has experienced greater than 50% reduction in stiffness, stop the test.

5. CALCULATIONS

5.1 The following calculations shall be performed at the operator-specified load cycle intervals:

5.1.1 *Maximum Tensile Stress (kN)*

$$\sigma_t = \frac{300aP}{wh^2} \tag{1}$$

where

a = $L/3$
L = the beam span, typically 356 mm
P = the load in kilonewtons
w = the beam width in millimeters
h = the beam height in millimeters

5.1.2 *Maximum Tensile Strain (mm/mm)*

$$\epsilon_t = (12\delta h)/(3L^2 - 4a^2) \tag{2}$$

where

δ = maximum deflection at center of beam, in mm
L = length of beam between outside clamps, 356 mm

5.1.3 *Flexural Stiffness (kPa)*

$$S = \sigma_t/\epsilon_t \tag{3}$$

5.1.4 *Phase Angle (deg)*

$$\phi = 360fs \tag{4}$$

where

f = load frequency, in Hz
s = time lag between P_{max} and δ_{max}, in seconds

5.1.5 *Dissipated Energy (kPa) per cycle*

$$D = \pi\sigma_t\epsilon_t\sin(\phi) \tag{5}$$

5.1.6 *Cumulative Dissipated Energy (kPa)*

$$\sum_{i=1}^{i=n} D_i \tag{6}$$

where

D_i = D for the i^{th} load cycle

NOTE 1.—If data acquisition is automated, dissipated energy (D) cannot be calculated for *every* load cycle, due to memory limitations of the computer system. Therefore, dissipated energy must be plotted against load cycles for the particular load cycles at which data was collected (i.e., the load cycles selected by the operator) up to the load cycle of interest. The area under the curve represents the cumulative dissipated energy. See figure 5 for a typical dissipated energy versus load cycle plot.

5.1.7 *Initial Stiffness (kPa)*—The initial stiffness is determined by plotting stiffness (S) against load cycles (N) and best-fitting the data to an exponential function of the form

$$S = Ae^{bN} \tag{7}$$

where

e = natural logarithm to the base e
A = constant
b = constant

Figure 6 presents a typical plot of stiffness versus load cycles. The constant A represents the initial stiffness.

5.1.8 *Cycles to Failure*—Failure is defined as the point at which the specimen stiffness is reduced to 50% of the initial stiffness. The load cycle at which failure occurs is computed by solving for N from equation 7, or simply

$$N_{f,50} = [\ln(S_{f,50}/A)]/b \tag{8}$$

where

$S_{f,50}$ = stiffness, 50% of initial stiffness, in kPa
$S_{f,50}/A$ = 0.5, by definition

5.1.9 *Cumulative Dissipated Energy to Failure (kPa)*

$$\sum_{i=1}^{i=N_{f,50}} D_i \tag{9}$$

NOTE 2.—It is not necessary to measure the dissipated energy for *every* load cycle; the computer program used to control the fatigue test will systematically determine the dissipated energy at specified load cycles during the test. The total dissipated energy to failure will be summarized as part of the computer output.

6. REPORT

6.1 The test report shall include the following information:

6.1.1 *Bituminous Mixture Description*—bitumen type, bitumen content, aggregate gradation, and air void percentage.

6.1.2 *Specimen Length*—millimeters, to four significant figures

6.1.3 *Specimen Height*—millimeters, average as per section 3.2, to three significant figures

6.1.4 *Specimen Width*—millimeters, average as per section 3.2, to three significant figures

6.1.5 *Test Temperature*—average during test, to the nearest 1.0°C

6.1.6 *Test Results*—table listing the following results (to three significant figures) for each load cycle interval selected by the operator:

Load Cycle	Applied Load	Beam Deflection	Tensile Stress	Tensile Strain	Flexural Stiffness	Phase Angle	Cumulative Dissipated Energy	Dissipated Energy
	kN	mm	kPa	mm/mm	kPa	deg	kPa	kPa

6.1.7 *Plot of Stiffness versus Load Cycles*—refer to figure 6 for typical plot

6.1.8 *Initial Flexural Stiffness*—kPa, to three significant figures

6.1.9 *Cycles to Failure*

6.1.10 *Cumulative Dissipated Energy to Failure*—kPa, to three significant figures

6.1.11 *Plot of Dissipated Energy versus Load Cycles*—refer to figure 5 for typical plot

7. PRECISION

7.1 A precision statement has not yet been developed for this test method.

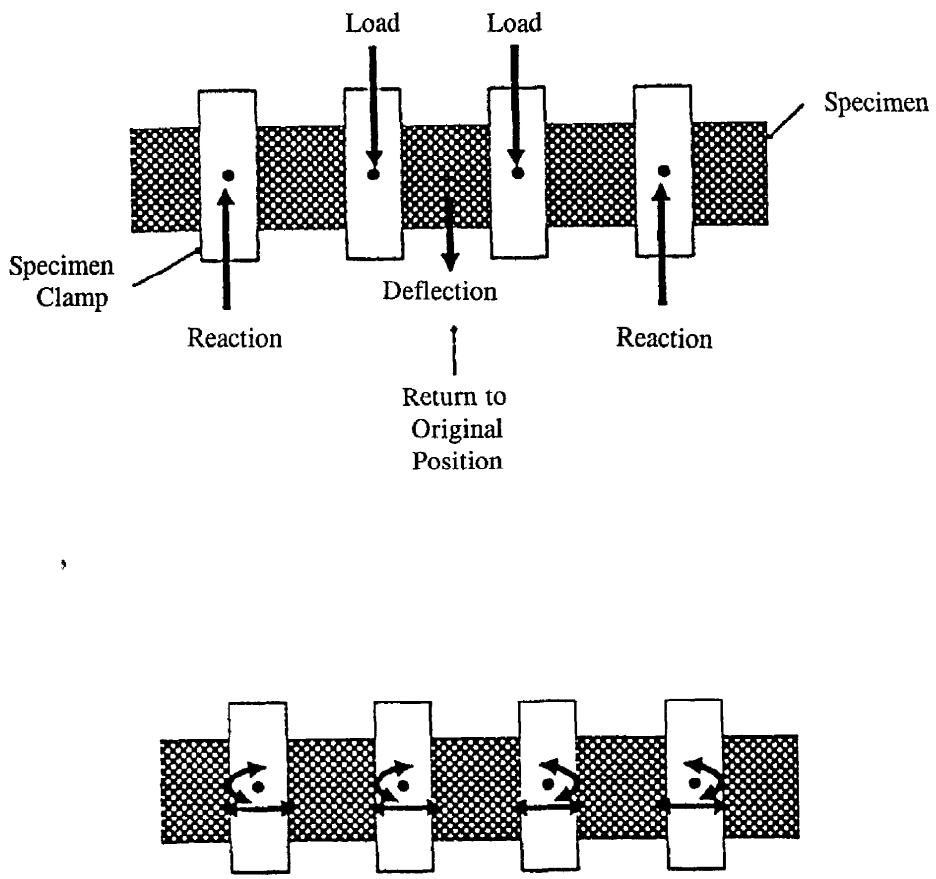

Figure 1. Load and Freedom Characteristics of Fatigue Test Apparatus

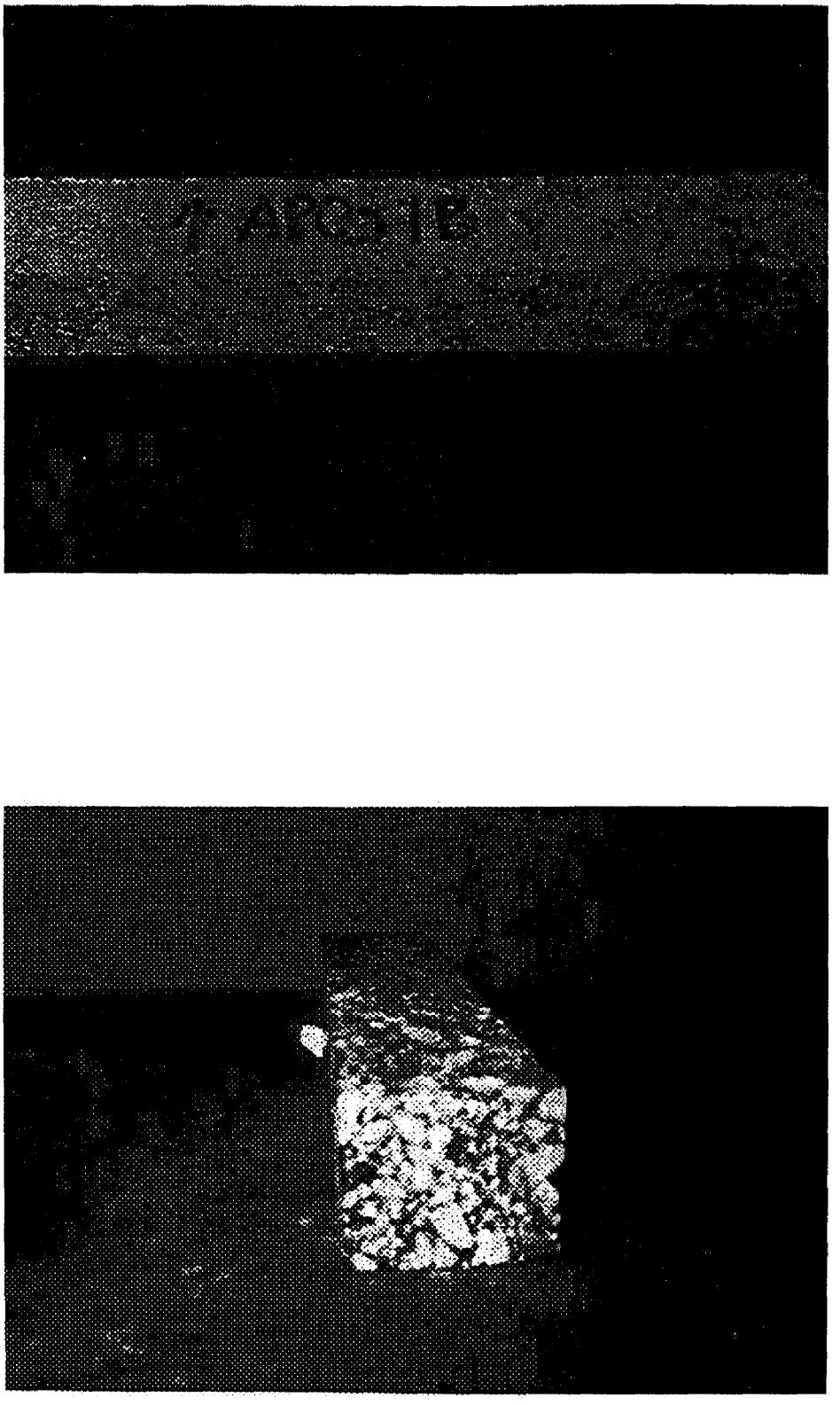

Figure 2. Nut Epoxied to Neutral Axis of Specimen and LVDT Block Attached

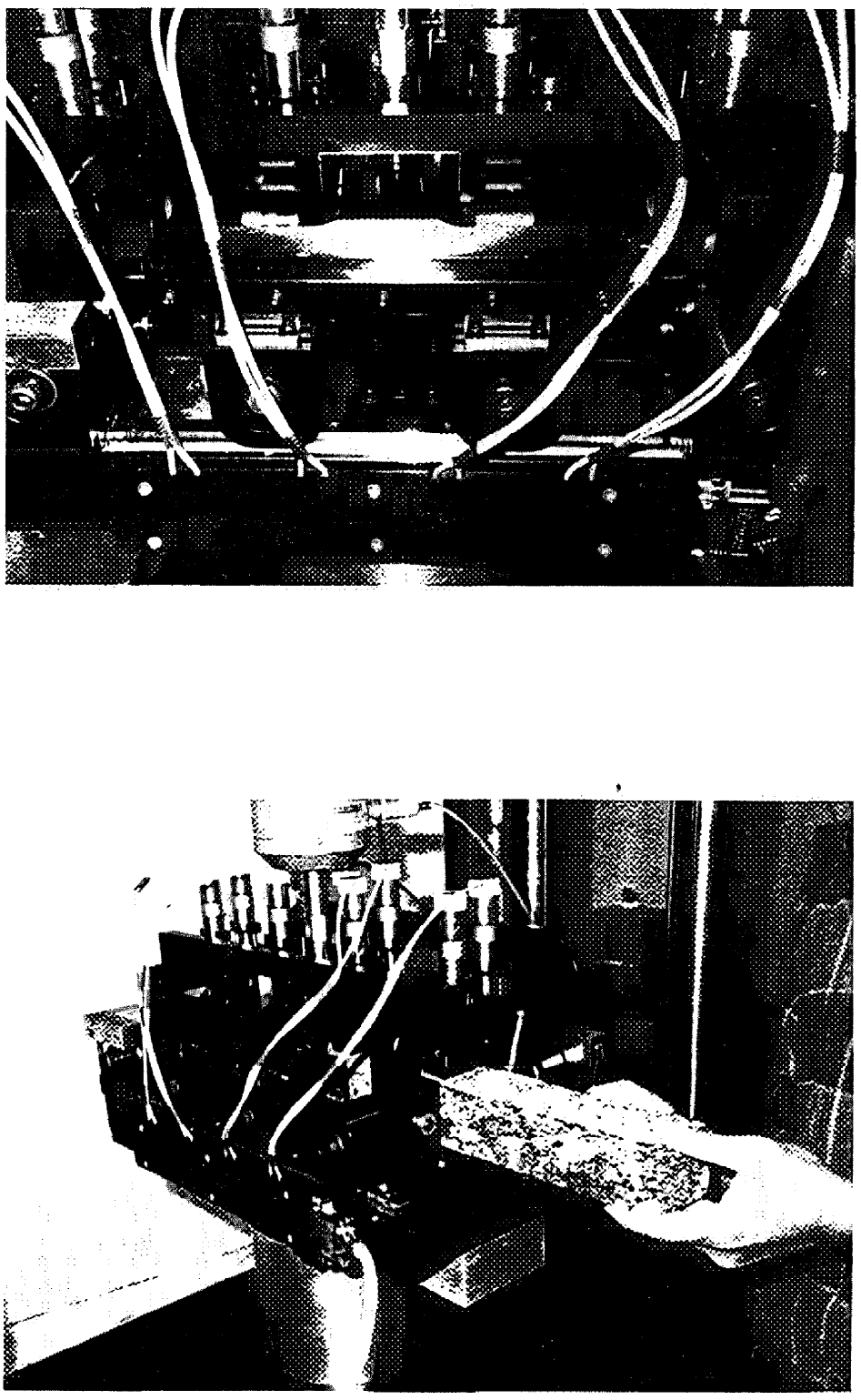

Figure 3. Inserting Specimen into Device

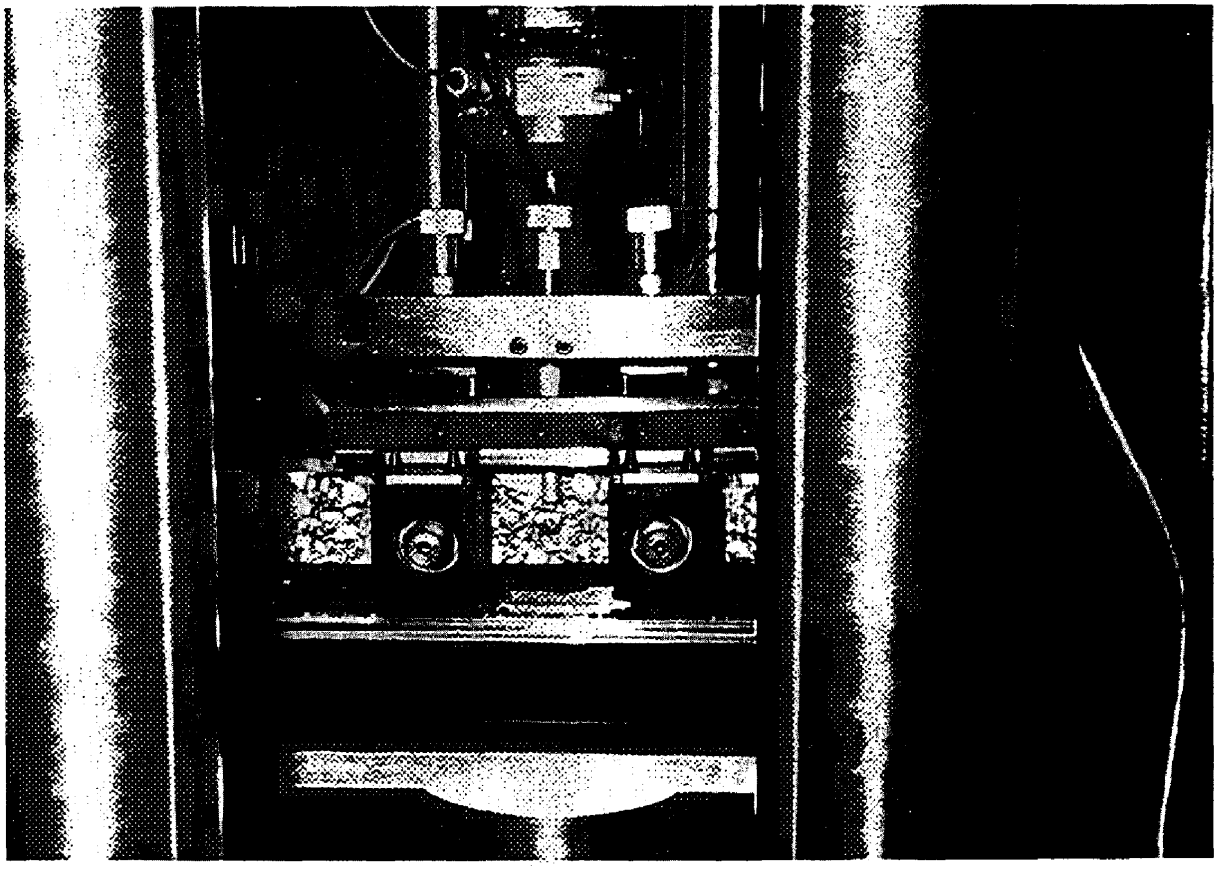

Figure 4. Nut/Block/Screw/LVDT Connection

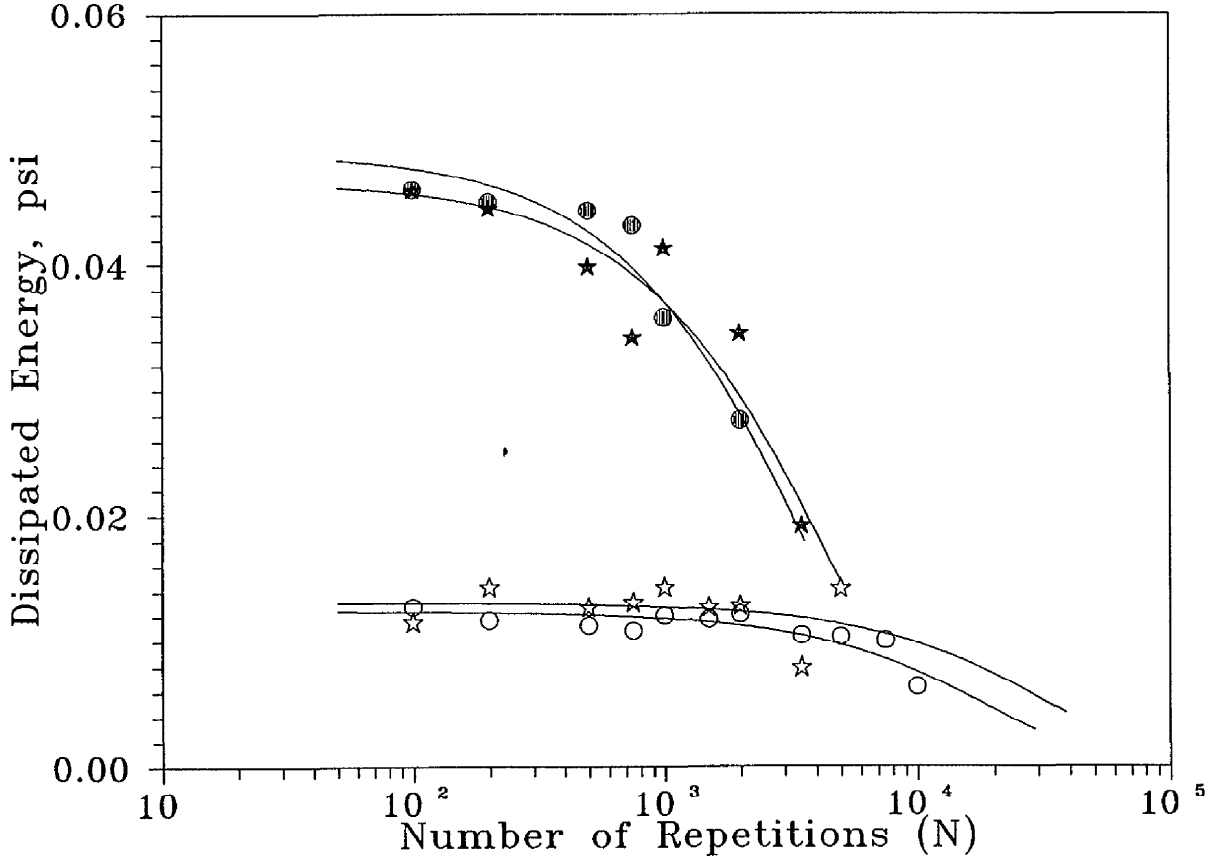

Figure 5. Dissipated Energy versus Load Cycles (Repetitions)

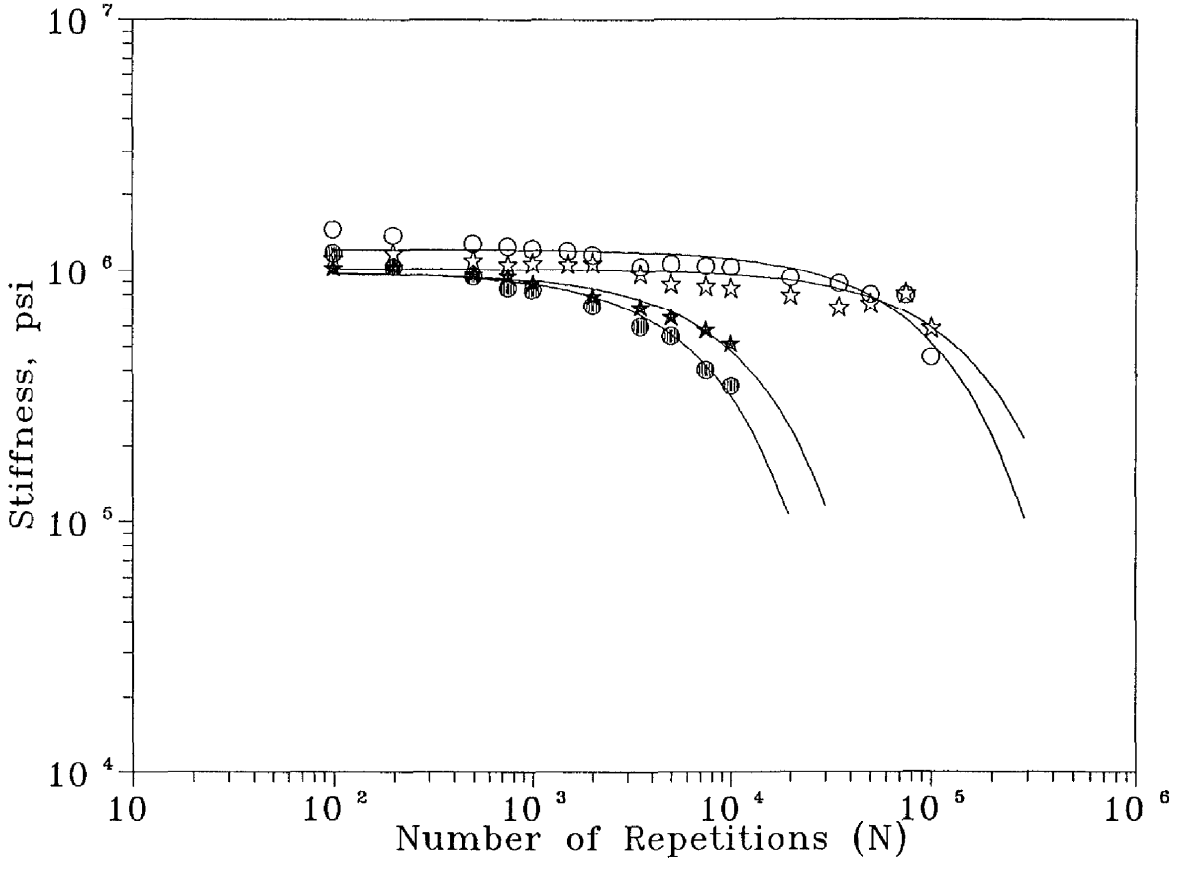

Figure 6. Stiffness versus Load Cycles (Repetitions)